

แบบจำลองคณิตศาสตร์ของการเคลื่อนที่ความชื้นในถุ้งน้ำตาลีใหญ่
เนื่องจากการเปลี่ยนแปลงของอุณหภูมิในรูปวัฏจักร



นายชลาวุธ สุวรรณไตรย์

วิทยานิพนธ์นี้เป็นส่วนหนึ่งของการศึกษาตามหลักสูตรปริญญาวิศวกรรมศาสตรมหาบัณฑิต

สาขาวิชาวิศวกรรมเคมี

มหาวิทยาลัยเทคโนโลยีสุรนารี

ปีการศึกษา 2555

**MATHEMATICAL MODELING OF MOISTURE
MIGRATION IN A BIG BAG OF SUGAR DUE TO
CYCLIC TEMPERATURE CHANGES**

Chalawut Suwannatrai



**A Thesis Submitted in Partial Fulfillment of the Requirements for the
Degree of Master of Engineering in Chemical Engineering
Suranaree University of Technology**

Academic Year 2012

**MATHEMATICAL MODELING OF MOISTURE MIGRATION IN
A BIG BAG OF SUGAR DUE TO CYCLIC TEMPERATURE
CHANGES**

Suranaree University of Technology has approved this thesis submitted in partial fulfillment of the requirement for a Master's Degree.

Thesis Examining Committee

(Asst. Prof. Dr. Boris Golman)

Chairperson

(Dr. Terasut Sookkumnerd)

Member (Thesis Advisor)

(Dr. Supunnee Junpirom)

Member

(Prof. Dr. Sukit Limpijumnong)

Vice Rector for Academic Affairs

(Assoc. Prof. Flt. Lt. Dr. Kontorn Chamniprasart)

Dean of Institute of Engineering

ชลาธร สุวรรณไตรย์ : แบบจำลองคณิตศาสตร์ของการเคลื่อนที่ความชื้นในถุงน้ำตาลใหญ่
เนื่องจากการเปลี่ยนแปลงของอุณหภูมิในรูปแบบวัฏจักร (MATHEMATICAL
MODELING OF MOISTURE MIGRATION IN A BIG BAG OF SUGAR DUE TO
CYCLIC TEMPERATURE CHANGES) อาจารย์ที่ปรึกษา : อาจารย์ ดร.ธีระสุด
สุขกำเนิด, 114 หน้า

สาเหตุของการจับตัวเป็นก้อนของน้ำตาลในถุงใหญ่ คือ การถ่ายเทความชื้นเนื่องจากการเปลี่ยนแปลงของอุณหภูมิจัดเก็บหรือขนส่ง ผลกระทบนี้เหนี่ยวนำไปสู่การเพิ่มขึ้น/ลดลงของความชื้นสัมพัทธ์ของอากาศภายในถุงน้ำตาลใหญ่ ด้วยเหตุนี้การเชื่อมกันระหว่างเม็ดน้ำตาลที่เป็นของเหลว (Liquid bridging) และของแข็ง (Solid bridging) จะถูกทำให้เกิดขึ้นเมื่อความชื้นสัมพัทธ์บริเวณนั้นเพิ่มขึ้นและลดลง หลังจากการเกิดขึ้นของการเชื่อมกันระหว่างเม็ดน้ำตาลที่เป็นของเหลวและของแข็งหลายครั้ง การจับตัวเป็นก้อนจะเกิดขึ้นในที่สุด ดังนั้นปัจจัยสำคัญของการจับตัวเป็นก้อนคือ ความชื้นเริ่มต้นของน้ำตาลในถุงขนาดใหญ่และการเปลี่ยนแปลงของอุณหภูมิระหว่างการขนส่ง ฉะนั้นเป้าหมายของงานวิจัยนี้คือการศึกษากายการถ่ายเทความชื้นภายในถุงน้ำตาลขนาดใหญ่ โดยการศึกษาผลกระทบของปริมาณความชื้นเริ่มต้นภายใต้การเปลี่ยนแปลงอุณหภูมิที่เป็นวัฏจักรและคำนึงถึงผลของฮิสเทอรีซิสของการดูดซับและคายด้วย (Hysteresis of adsorption and desorption) เพื่อให้เห็นบริบทเป้าหมายแบบจำลองทางคณิตศาสตร์พิสูจน์มาจากการอนุรักษ์ของมวลและพลังงานได้ถูกพัฒนาขึ้นและแก้หาคำตอบได้โดยวิธีคำนวณเชิงตัวเลขแบบเส้น (Numerical Method of Lines) และจากนั้นจะถูกตรวจสอบความถูกต้องกับข้อมูลการทดลองในงานวิจัยรายงานก่อนหน้านี้

ผลของการแก้หาคำตอบโดยวิธีคำนวณเชิงตัวเลขแสดงให้เห็นว่าปริมาณความชื้นเริ่มต้นสูง (0.040%) อาจมีความเสี่ยงที่จะทำให้เกิดการจับตัวเป็นก้อนของน้ำตาล และฮิสเทอรีซิสของการดูดซับและคายไม่ได้มีความสำคัญในการทำนายการโยกย้ายความชื้น ผลที่ได้นี้มีประโยชน์มากสำหรับการศึกษาในอนาคตของการจับตัวเป็นก้อนของน้ำตาล

สาขาวิชา วิศวกรรมเคมี

ปีการศึกษา 2555

ลายมือชื่อนักศึกษา _____

ลายมือชื่ออาจารย์ที่ปรึกษา _____

CHALAWUT SUWANNATRAI : MATHEMATICAL MODELING OF
MOISTURE MIGRATION IN A BIG BAG OF SUGAR DUE TO CYCLIC
TEMPERATURE CHANGES. THESIS ADVISOR : TERASUT
SOOKKUMNERD, Ph.D., 114 PP.

MOISTURE MIGRATION/ CYCLIC TEMPERATURE CHANGES/ SUGAR/
MATHEMATICAL MODELING/ HEAT AND MASS BALANCES

The cause of caking of sugar in a big bag is the moisture migration due to the fluctuation of storage/shipping temperature; this effect leads to the variation of local relative humidity in the big bag. Consequently, the liquid and solid bridges are formed when the local humidity increases and decreases, respectively. After the periodically liquid and solid bridges happen, caking occurs at last. The important factors of caking are the initial moisture content of sugar in the big bag and the temperature changes during transportation. Therefore, the goal of this research is to investigate the moisture migration in the big bag by studying effect of the initial moisture content under the cyclic fluctuation of temperature and also included the hysteresis of adsorption-desorption effect. For this propose, the mathematical model is derived from the conservation of mass and energy. This model is solved by numerical method of lines and is then validated with experimental data reported in the literature.

The numerical results of mathematical model developed in this thesis show that the high initial moisture content (0.040%) is definitely riskier to induce the occurrence of caking phenomenon and the hysteresis of adsorption desorption has no

significant effects on the prediction of the moisture migration. These reported results are very helpful for study the caking in the future.



School of Chemical Engineering

Academic Year 2012

Student's Signature_____

Advisor's Signature_____

ACKNOWLEDGEMENTS

I would like to express my sincere gratitude to my advisor Dr. Terasut Sookkumnerd for the continuous support of my research, his patience, motivation, enthusiasm, and immense knowledge. His guidance helped me in all the time of research and writing this thesis.

I would like to thank my thesis committee; Assist. Prof. Dr. Boris Golman and Dr. Sunpunnee Junpirom. for their insightful comments, hard questions and encouragement. Also, I would like to thank all of the lectures at School of Chemical Engineering, Suranaree University of Technology, whom led me to the world of Chemical Engineering.

I would like to thank my family; my parents Padungchit and Sinthanee, for giving birth to me.

Finally, I would like to thank all graduate students in School of Chemical Engineering; especially, Natthaya Punsuwan for giving me lends her personal computer, Chaturaporn and Nikom for making good atmosphere during working.

Chalawut Suwannatrai

TABLE OF CONTENTS

	Page
ABSTRACT (THAI)	I
ABSTRACT (ENGLISH)	II
ACKNOWLEDGEMENTS.....	IV
TABLE OF CONTENTS.....	V
LIST OF TABLES.....	IX
LIST OF FIGURES	X
SYMBOLS AND ABBREVIATIONS.....	XV
CHAPTER	
I INTRODUCTION.....	1
1.1 Rational of the Study.....	1
1.2 Research Objective.....	3
1.3 Scope and Limitation.....	4
1.4 Expected Results	4
II THEORY AND LITERATURE REVIEW.....	5
2.1 Sugar.....	5
2.1.1 Type of Moisture in Sugar Crystal	5
2.1.2 Moisture Content Analysis	6
2.2 Sorption Isotherm of Sugar	7

TABLE OF CONTENTS (Continued)

	Page
2.2.1 Sorption Isotherm Equation of Sugar	10
2.2.2 Scanning Curve	13
2.3 Caking Phenomenon of Sugar and Moisture Migration.....	16
2.4 Mathematical Modeling of Moisture Migration.....	18
2.5 Mathematical Techniques Involved in this Work	25
2.5.1 Nonlinear Least Square Method.....	25
2.5.2 Numerical Method of Lines.....	26
III RESEARCH METHODOLOGY.....	28
3.1 Derivation of Mathematical Model	28
3.1.1 Conceptual Model	28
3.1.2 System	29
3.1.3 Assumptions	30
3.1.4 Mathematical Model.....	30
3.1.5 Initial and Boundary Conditions	32
3.1.6 Constitutive Equations.....	36
3.2 Sorption Isotherm Equation.....	37
3.3 Numerical Solution.....	42
3.3.1 Transforming the Modeling Equation to $M(t, y) y' = f$ form.....	42

TABLE OF CONTENTS (Continued)

		Page
	3.3.2 Discretizing the Derivative Terms.....	45
	3.3.3 Determining the Number of Node.....	47
	3.4 Model Validation.....	48
	3.5 Conditions of Model Prediction	49
	3.6 Sensitivity Analysis.....	51
IV	RESULTS AND DISCUSSIONS	52
	4.1 Result of Sorption Isotherm Fitting.....	52
	4.2 Result of Determining the Number of Node	54
	4.3 Result of Model Validation	57
	4.4 Model prediction results	59
	4.4.1 Short Term View.....	59
	4.4.2 Long term View.....	65
	4.4.3 Hysteresis	71
	4.5 Sensitivity Analysis Result.....	78
V	CONCLUSIONS.....	80
	5.1 Sorption Isotherm Fitting	80
	5.2 Model Validation.....	80
	5.3 Model Prediction	80
	5.3.1 Effect of Initial Condition	80

TABLE OF CONTENTS (Continued)

	Page
5.3.2 Effect of Sorption Isotherm.....	81
5.3.3 Sensitivity Analysis.....	81
VI RECOMMENDATIONS	82
6.1 Mathematical Model.....	82
6.2 Environmental Condition during Transport	82
6.3 Sorption Isotherm	82
REFERENCES.....	83
APPENDICES	
APPENDIX A DETAILED DERIVATION OF MATHEMATICAL MODELS.....	88
APPENDIX B DETAILED TRANSFORMED EQUATIONS.....	92
APPENDIX C <i>lsqnonlin</i> AND <i>ode15s</i> PROGRAMS IN MATLAB®	99
APPENDIX D TEMPERATURE, ABSOLUTE HUMIDITY, AND MOISTURE CONTENT PROFILES FOR SHORT TERM VIEW.....	106
APPENDIX E SORPTION ISOTHERM OF SUGAR GRAIN FROM GAB-T MODEL.....	111
BIOGRAPHY	114

LIST OF TABLES

Table		Page
2.1	Finite difference formula	27
3.1	Material properties	36
3.2	The moisture content data of adsorption and desorption isotherm from Figure 2.7	37
3.3	The approximation of derivative terms in mathematical model	46
3.4	The discretion of derivative terms in boundary condition	47
3.5	Conditions of this study	50
3.6	The values used to analyze the sensitivity	51
4.1	Parameters of sorption isotherm in GAB-T equation	51

LIST OF FIGUERS

Figure		Page
2.1	Type of moisture content (Rodgers and Lewis, 1963)	6
2.2	The residual moisture content of sugar measured by the oven and the Karl-Fisher method (Rastikian et al. 1991)	7
2.3	General shape of adsorption isotherms of (1) crystalline sucrose, (2) amorphous sucrose, and (3) saturated solution (Mathlouhi and Rogé, 2003).....	8
2.4	Water vapor sorption isotherms as a function of crystal size distribution (Mathlouhi and Rogé, 2003)	9
2.5	Water vapor adsorption isotherm of sucrose crystallized in presence of cations (Mathlouhi and Rogé, 2003)	9
2.6	Sorption isotherm of sucrose at 22 and 35°C (Rastikain et al, 1998)	10
2.7	Moisture sorption isotherm curves for sucrose at 10, 20, and 40°C obtained by the IGAsorp (Leaper et al, 2002)	11
2.8	Isotherm for sucrose at 20°C. Fitted GAB model prediction line is shown. (♦) Iglesias and Chirife (1982), (▲,Δ) Roth (1976), (■) Bakhit and Schmidt (1993), (—) GAB model $r = 0.989$ (Billing and Paterson, 2008).....	12

LIST OF FIGURES (Continued)

Figure	Page
2.9	Diagram of scanning curve proposed by Salin (2011), Clouties and Fortin (1994), Peralta (1995), Frandsen (2007) and Time (1998, 2002) 14
2.10	Diagram of adsorption scanning curve (Frandsen 2007, Salin 2011) 15
2.11	Diagram of desorption scanning curve (Frandsen 2007, Salin 2011) 15
2.12	Block diagram of relationship between moisture migration and caking (Leaper et al, 2002) 17
2.13	Moisture movement induced by an applied temperature gradient (Bronlund, 1997)..... 17
3.1	The big bag of sugar 29
3.2	Schematic diagram of system for shell balance..... 31
3.3	Flowchart for searching the lowest sum of squares error by decreasing evenly 0.1 of previous value 41
3.4	The results of temperature distribution by experimental data of Leaper et al (2001) and Wang and coworkers' numerical results (2004)..... 48
3.5	Fluctuation of temperature in cyclic form 50
4.1	Comparison sorption isotherm of sucrose, including experimental data by Leaper et al.(2002), empirical equation by Leaper et al.(2002), and GAB-T equation 53

LIST OF FIGURES (Continued)

Figure	Page
4.2	The comparison of temperature profiles in a big bag of each different number of node when $M_0=0.068\%$ and $T_0=18^\circ\text{C}$ and keeping $T_{\text{out}}=40^\circ\text{C}$ 55
4.3	Comparison temperature profiles of between experimental data (Leaper et al., 2001), Wang et al. (2004)'s results, and numerical results at 18°C of initial temperature and increasing the outside temperature to 40°C 58
4.4	Schematic diagram of moisture migration for high initial moisture content using adsorption isotherm in period of 0 -12 hrs. 60
4.5	Schematic diagram of moisture migration for high initial moisture content using adsorption isotherm in period of 15 -24 hrs. 60
4.6	Schematic diagram of moisture migration for high initial moisture content using adsorption isotherm in period of 27 -36 hrs. 61
4.7	Schematic diagram of moisture migration for low initial moisture content using adsorption isotherm in period of 0 -12 hrs. 62
4.8	Schematic diagram of moisture migration for high initial moisture content using adsorption isotherm in period of 15 -24 hrs. 63
4.9	Schematic diagram of moisture migration for high initial moisture content using adsorption isotherm in period of 27 -36 hrs. 63

LIST OF FIGURES (Continued)

Figure	Page
4.10	Numerical result throughout 720 hrs for <i>high</i> initial moisture content with <i>adsorption isotherm</i> 66
4.11	Numerical result throughout 720 hrs for <i>low</i> initial moisture content with <i>adsorption isotherm</i> 67
4.12	Numerical result throughout 720 hrs for <i>high</i> initial moisture content with <i>desorption isotherm</i> 68
4.13	Numerical result throughout 720 hrs for <i>low</i> initial moisture content with <i>desorption isotherm</i> 69
4.14	The temperature profile at different node which calculated using <i>hysteresis</i> Isotherm for <i>low</i> initial moisture content..... 72
4.15	The absolute humidity profile of each node which calculated using <i>hysteresis</i> Isotherm for <i>low</i> initial moisture content..... 73
4.16	The moisture content profile of each node which calculated using <i>hysteresis</i> Isotherm for <i>low</i> initial moisture content..... 77
4.17	The temperature profile at different node which calculated using <i>hysteresis</i> Isotherm for <i>high</i> initial moisture content 75
4.18	The moisture content profile of each node which calculated using <i>hysteresis</i> Isotherm for <i>high</i> initial moisture content 76

LIST OF FIGURES (Continued)

Figure	Page
4.19	The moisture content profile of each node which calculated using <i>hysteresis</i> Isotherm for <i>high</i> initial moisture content77
4.20	The profiles of temperature and moisture content from sensitivity analysis consisting of effects heat conductivity of sugar (a), porosity of bed (b), and heat conductivity of air (c); the red, blue, and pink lines represent position at $r=0.0$, 0.238 , and 0.476 meters, respectively, while the solid lines, dash lines, and short-long dash lines represent the results of deviation each parameter of 0% , -10% , and $+10\%$, respectively 79

SYMBOLS AND ABBREVIATIONS

a	=	fitted parameter of sorption isotherm
a_w	=	water activity
$a_{w,eq}$	=	water activity at equilibrium
A	=	cross sectional area, m^2
b	=	fitted parameter of sorption isotherm
c	=	fitted parameter of sorption isotherm
C	=	Guggenheim constant
C'_0	=	parameter in GAB-T model
C_{pa}	=	heat capacity of dry air, $J\ kg^{-1}\ K^{-1}$
$C_{p,PE}$	=	heat capacity of PE bag, $J\ kg^{-1}\ K^{-1}$
C_{ps}	=	heat capacity of solid, $J\ kg^{-1}\ K^{-1}$
C_{pv}	=	heat capacity of vapor, $J\ kg^{-1}\ K^{-1}$
C_{pw}	=	heat capacity of water, $J\ kg^{-1}\ K^{-1}$
C_{pg}	=	heat capacity of gas phase, $kJ\ kg^{-1}\ K^{-1}$
C_{pp}	=	heat capacity of particle, $kJ\ kg^{-1}\ K^{-1}$
$C_{p,l,e}$	=	heat capacity of liquid of external domain, $kJ\ kg^{-1}\ K^{-1}$
D_a	=	diffusivity of vapor in day air, $m^2\ s^{-1}$
D_{eff}	=	effective diffusivity, $m^2\ s^{-1}$

SYMBOLS AND ABBREVIATIONS (Continued)

$D_{e,eff}$	=	effective diffusion coefficient of external domain, $m^2 s^{-1}$
ERH	=	equilibrium relative humidity, %
F	=	set of nonlinear equation
g	=	acceleration of gravity, $m s^{-2}$
H	=	total enthalpy, $J m^{-3}$
H_l	=	heat of condensation of pure water, $J K^{-1} mol^{-1}$
H_m	=	total heat of sorption the first layer, $J K^{-1} mol^{-1}$
H_q	=	total heat of sorption the multilayer molecules, $J K^{-1} mol^{-1}$
h	=	heat transfer coefficient, $W m^{-2} K^{-1}$
h_e	=	heat source term external domain, $J m^3 s$
h_i	=	heat source term internal domain, $J m^3 s$
h_g	=	enthalpy of gas, $J kg^{-1}$
h_s	=	enthalpy of sugar, $J kg^{-1}$
h_v	=	enthalpy of vapor, $J kg^{-1}$
h_{fg}	=	latent heat of water, $J kg^{-1}$
J	=	jacobian
k	=	constant correcting properties of multilayer molecules
k'	=	parameter in GAB-T model
k_a	=	thermal conductivity of gas phase, $W m^{-1} K^{-1}$

SYMBOLS AND ABBREVIATIONS (Continued)

k_{eff}	=	effective thermal conductivity, $W m^{-1} K^{-1}$
$k_{e,eff}$	=	effective thermal conductivity of external domain, $W m^{-1} K^{-1}$
k_{PE}	=	thermal conductivity of PE, $W m^{-1} K^{-1}$
k_s	=	thermal conductivity of solid phases, $W m^{-1} K^{-1}$
K_β	=	permeability of liquid phase in the potash bed, m^2
l	=	thickness, m
L	=	length of the surface of heat transfer, m
L_h	=	latent heat of water vaporization, $kJ kg^{-1}$
\dot{m}	=	rate of phase change, $kg m^3 s^{-1}$
\dot{m}_e	=	mass source term of external domain, $kg m^3 s^{-1}$
M	=	moisture content in solid phase, kg of water/ kg dry solid
M_{eq}	=	moisture content in solid phase at equilibrium, kg of water/ kg dry solid
M_0	=	moisture content in solid phase at initial condition, kg of water/ kg dry solid
	=	monolayer water content
M'_0	=	parameter in GAB-T model
MC	=	moisture content, g/100g
Nu	=	nuselt number
Pr	=	prandtl number
P_{sat}	=	vapor pressure of water at saturated, mm.Hg

SYMBOLS AND ABBREVIATIONS (Continued)

$\langle P_c \rangle$	=	volume average pore or capillary pressure, Pa
\dot{Q}	=	heat flow rate, W
R	=	gas constant, J K ⁻¹ mol ⁻¹
RH	=	relative humidity, %
Ra	=	rayleigh number
S	=	saturation
r	=	radius, m
SS_{err}	=	sum of squares error
T	=	temperature, °C
$T_{outside}$	=	temperature around bag surface, °C
T_j^i	=	temperature at node position i and time step j , °C
$T_{g,e}$	=	temperature of gas phase of external domain, °C
T_i	=	temperature of internal domain, °C
X_i^{cal}	=	moisture content from calculation at i from adsorption or desorption
X_i^{exp}	=	experiment data of moisture content at i from adsorption or desorption
t	=	time, s
W	=	total moisture in bed, kg of water/m ³
x	=	bed position, m
Y	=	absolute humidity in gas phase, kg of water/ kg dry air

SYMBOLS AND ABBREVIATIONS (Continued)

Y	=	dimensionless representing amount of moisture in gas phase
Y_{eq}	=	absolute humidity in gas phase at equilibrium, kg of water/ kg dry air
Y_0	=	absolute humidity in gas phase at initial condition, kg of water/ kg dry air
Y_j^i	=	absolute humidity at node position i and time step j , kg of water/ kg dry air

Greek symbols

ε	=	porosity of bed
ε_γ	=	the volume fraction of gas
ε_β	=	the volume fraction of liquid
ε_σ	=	volume fraction of solid
$\varepsilon_{g,e}$	=	porosity of gas phase of external domain
$\varepsilon_{l,i}$	=	porosity of liquid phase of internal domain
$\varepsilon_{l,e}$	=	porosity of liquid phase of external domain
ε_p	=	porosity of particle
$\rho_{v,e}$	=	density of vapor of external domain
ρ_{da}	=	density of dry air, kg m ⁻³
ρ_{PE}	=	density of PE bag, kg m ⁻³
ρ_s	=	density of sugar, kg m ⁻³

SYMBOLS AND ABBREVIATIONS (Continued)

ρ_v	=	density of vapor, kg m^{-3}
ρ_β	=	the density of water, kg m^{-3}
β	=	volumetric coefficient of expansion, K^{-1}
	=	parameter in GAB-T model
	=	set of parameters
ν	=	kinematic viscosity, $\text{m}^2 \text{s}^{-1}$
α	=	thermal diffusivity, $\text{m}^2 \text{s}^{-1}$
	=	parameter in GAB-T model
	=	parameter in sorption equation
γ	=	parameter in GAB-T model
γ_1	=	parameter in sorption equation
γ_2	=	parameter in sorption equation
γ_3	=	parameter in sorption equation
η_β	=	viscosity of water-salt solution in the potash bed, N s m^{-2}
u_D	=	darcy velocity, m s^{-1}

CHAPTER I

INTRODUCTION

1.1 Rational of the Study

Thailand exports 6.71 million tons of sugar and has become the world's second-biggest exporter of sugar in 2011 (Business Recorder, 2012). Because of transportation cost, the exported sugar is generally shipped by sea in which the temperature can extremely fluctuate and the transportation also takes a long time. As a result, some sugar in containers or big bags often forms agglomerated particles and lumps, called caking, during transportation, especially for sugar having high moisture content. This phenomenon degrades the quality of sugar and the caked sugar is often rejected from customer. In general, the caking often occurs in powder and particle materials such as soils, fertilizers, pharmaceuticals, foods, plastics, etc, and the other materials that have hygroscopic properties.

The cause of caking is the periodically liquid and solid bridging that occur during adsorption and desorption phenomena. Since the equilibrium of moisture between solid and gas phases is disturbed by changing temperature, the relative humidity is altered; thus, the moisture gradient in gas phase arises and moisture then move away from the hot region into the cool region by diffusion through air spaces. Consequently, moisture would adsorb on sugar at the high relative humidity region and desorb on sugar at the low relative humidity region.

In the past, there are many researchers studied moisture migration in order to understand and prevent the caking phenomenon of sugar grain by both experiment and mathematical model.

Excell and Stone (1989) measured the temperature, relative humidity, and moisture inside a container during transportation and they observed that the wet sugar often occurred on floor near the door due to moisture moving away from the centre of a container; thus, this area near the door was very risky for the caking to occur.

Leaper et al. (2002) simulated and measured the moisture migration inside a caking box. They also presented the experimental data and empirical equation of sorption isotherm which was used incorporated in mathematical models in the subsequent communication (Wang et al., 2004, Christakis et al., 2006).

Wang et al. (2004) simulated the moisture migration inside a sugar bag when the outside temperature changes in cyclic form with only one condition of initial condition and used the finite-volume method to solve the mathematical models. They found that moisture migration was highest within 0.2 meters from the interface.

Christakis et al. (2006) simulated the moisture migration inside a small cylinder in which the top side was exposed to the air at constant temperature and fluctuated relative humidity. They also calculated the tensile strength from moisture migration data and compared with experimental data.

Billing and Paterson (2008) simulated and measured the moisture migration in a packed bed when applied a temperature difference across edge sides.

However, mathematical modeling, all of previous work above, has something missing that could be improved for better understanding of the moisture migration in the real situation. For example, Wang et al. (2004) and Christakis et al. (2006) used

the total moisture equation defined by Leaper et al. (2002) that was not suitable (because they defined that the total moisture equation of any nodes at in-equilibrium is equal to the total moisture equation of that node at equilibrium, it is not correct since moisture must also transfer between nodes), Billing and Paterson (2008) did not consider the effect of temperature in sorption isotherm equation even though Leaper et al.(2002) shown the sorption isotherm of sugar depending on temperature. Therefore, this thesis work will work on improving the simulation of moisture migration by relaxing the above assumptions.

1.2 Research Objective

The main objective of this thesis work is to study the moisture migration in a big bag of sugar during transportation by using the mathematical model, which focused on the effects of initial moisture content and sorption isotherms; the initial moisture content is a factor which can be controlled by using conditioning silo. Therefore, if the condition of initial moisture content that leads to occur the caking is known, one can prevent it by controlling the moisture content of sugar leaving the conditioning silo not over that condition. In sorption isotherms, it has already known from the literature reported by Leaper et al. (2002) that the sorption isotherm of sugar is a function of temperature and it also contains the hysteresis effect; hence, considering these effects in this thesis may lead us to the better understanding of the caking phenomenon.

1.3 Scope and Limitation

In order to accomplish the objective above, the mathematical model is derived from the conservation of mass and energy in one-dimensional, r-direction of cylindrical coordinate, and validated with other results reported in literature at the same condition (Leaper et al., 2001). Then, the mathematical model is used to predict the phenomenon in the shipping condition. The properties and parameters of corresponding correlations are taken from the previous literatures. Additionally, the new sorption isotherm equations are performed with a function of temperature by GAB-T model which would be used to fit the both of adsorption and desorption data. Moreover, the hysteresis effect is also included in the model.

1.4 Expected Results

- 1) The results of thesis would help us better understand the moisture migration phenomenon of sugar grain in a big bag and could be extended to other particles (i.e., fertilizers, pharmaceuticals, foods) and other systems (i.e., 2D, 3D).
- 2) The result of this thesis work would roughly identify the condition that induces to occur the caking. This is the important information and helpful for the prevention of caking of sugar grain during transportation.
- 3) The study of this work would be the platform for study the caking in the future.

CHAPTER II

LITERATURE REVIEW AND THEORY

This chapter describes published research papers which have been done and some theories that would be useful in studying moisture migration of sugar grain in a big bag. The chapter is arranged into the topics of sugar, water sorption isotherm of sugar, caking phenomenon of sugar and moisture migration, mathematical modeling of moisture migration, and mathematical methods involved in analysis of moisture migration.

2.1 Sugar

Sugar is one of hygroscopic substances which readily absorb moisture when it is exposed to atmosphere, particularly at the high humidity, since there are H-bonds in both the molecules of sucrose and water that attract each other.

2.1.1 Type of Moisture in Sugar Crystal

The moisture in sugar crystal after crystallization and drying process can be classified into three types (Rodgers and Lewis, 1963);

2.1.1.1 *Surface or free moisture* is the moisture on the surface of sugar, which can be dried out by a rotary dryer. If this moisture is removed quickly, it will become bound moisture or amorphous sugar on the surface of sugar crystal.

2.1.1.2 *Bound moisture* is the moisture under the surface of sugar crystal. It has an effect on the stability of sugar crystal during storage or transportation.

2.1.1.3 *Inherent moisture* is the moisture or mother liquor trapped in the core of sugar crystal during the crystallization.

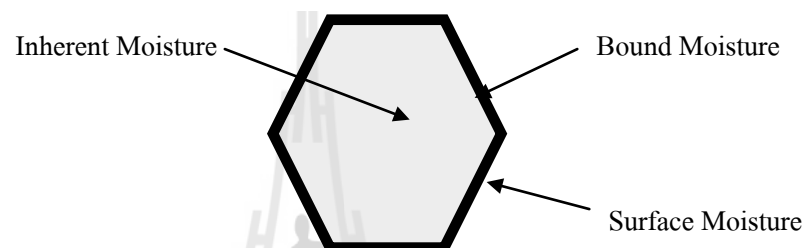


Figure 2.1 Type of moisture content (Rodgers and Lewis, 1963).

2.1.2 Moisture Content Analysis

The moisture content in sugar grain can be analyzed by two different methods mostly used in sugar process (Rastikian et al., 1991);

- i) A conventional gravimetric method by taking a small sample to oven at 105°C and 3 hours.
- ii) A Karl-Fisher method by performing with a coulometric titrator which uses Hydranal to be a typical composite reagent (Scholz, 1984).

The Karl-Fisher method can analyze all types of moisture in the sugar grain; free moisture, bound moisture, and inherent moisture. However, the conventional gravimetric method cannot analyze the inherent moisture. Nonetheless, those two methods give the similar results when measuring moisture content is in

ranging from 0.2 to 1.0% which can be used to study sufficiently a kinetic of sugar during drying. After drying, the Karl-Fisher method should be used to analyze the moisture because it is reliable than the conventional gravimetric method at very low moisture content.

Figure 2.2 shows the comparison of residual moisture that was analyzed by the oven and Karl-Fisher method at below 0.1% of moisture content. It obviously shows that the result measured by Karl-Fisher is always higher than the one measured by conventional gravimetric method.

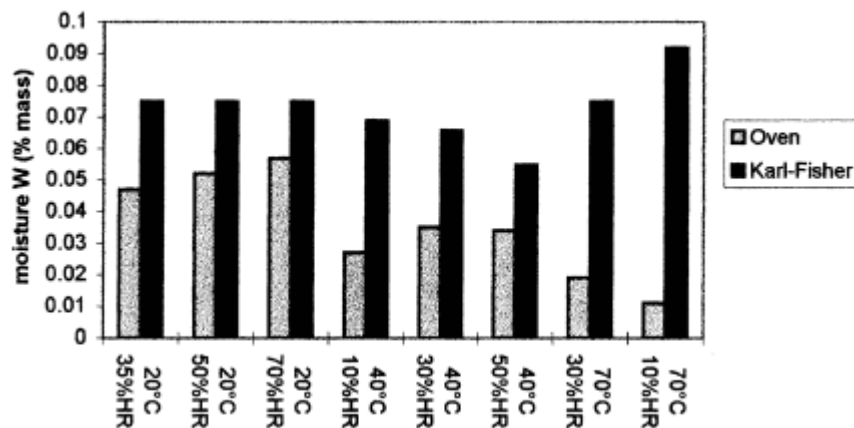


Figure 2.2 The residual moisture content of sugar measured by the oven and the Karl-Fisher method (Rastikian et al. 1991).

2.2 Sorption Isotherm of Sugar

The relationship of moisture content in solid and in gas phases at equilibrium at constant temperature is known as “sorption isotherm”. It can be used in sugar grains to approximately identify a condition that will tend to occur caking. It is also

used incorporating along with mathematical model for prediction the onset of caking, which is more precise than merely used sorption isotherm.

The shape of sorption isotherm is important and depends on a nature of powder or particle. In the case of sugar grains, the shape of sorption isotherm depends on the amount of amorphous, crystal size distribution, and amount of impurities as shown in Figure 2.3 to 2.5 (Mathlouhi and Rogé, 2003).

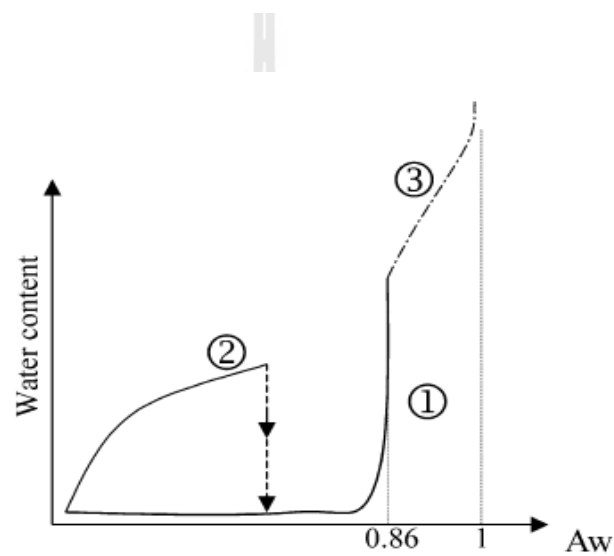


Figure 2.3 General shape of adsorption isotherms of (1) crystalline sucrose, (2) amorphous sucrose, and (3) saturated solution (Mathlouhi and Rogé, 2003).

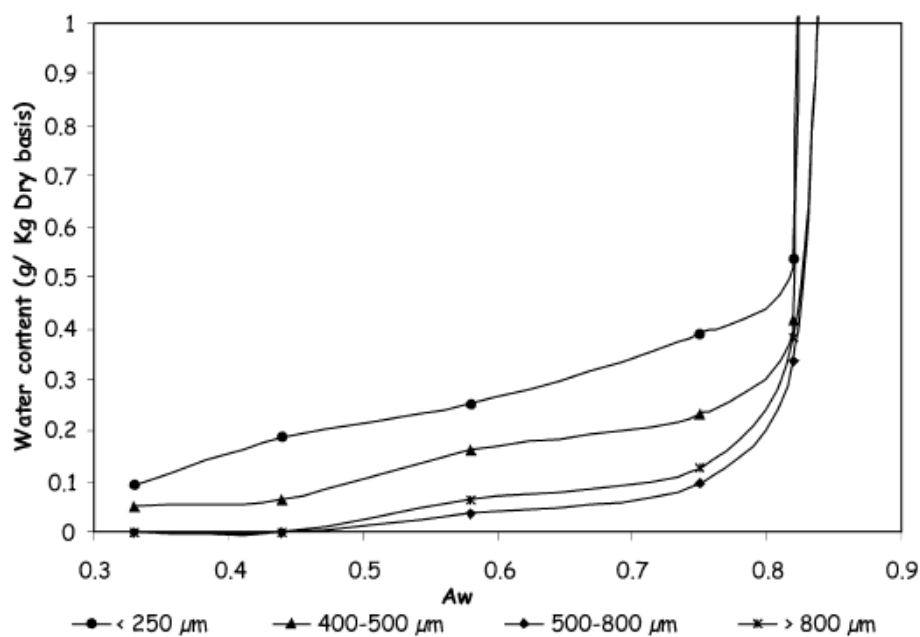


Figure 2.4 Water vapor sorption isotherms as a function of crystal size distribution (Mathlouhi and Rogé, 2003).

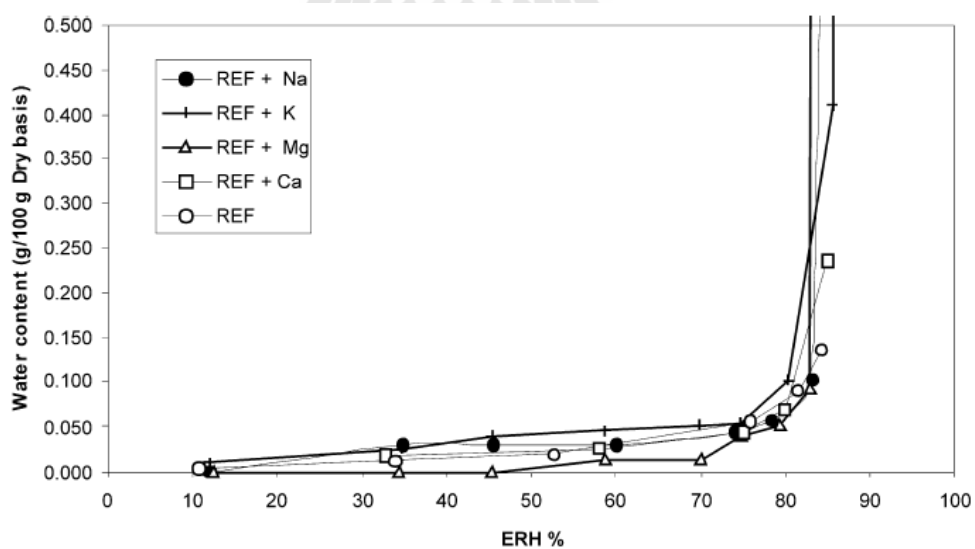


Figure 2.5 Water vapor adsorption isotherm of sucrose crystallized in presence of cations (Mathlouhi and Rogé, 2003).

2.2.1 Sorption Isotherm Equation of Sugar

The sorption isotherm can be correlated with equations by fitting the equations with the experimental data. Several sorption isotherm equations were fitted with the experimental data in the previous research articles.

Rastikain et al. (1998) performed the sorption isotherm of sucrose at 22 and 35°C as shown in Figure 2.6 and correlated the results by Equation (2.1)

$$ERH = 82.5 \left(1 - \exp \left(38.485 - 2683 \times M + 60949 \times M^2 - 481480 \times M^3 \right) \right) \quad (2.1)$$

where ERH is the equilibrium relative humidity in %, M is moisture content of sugar in kg water per kg dry sugar.

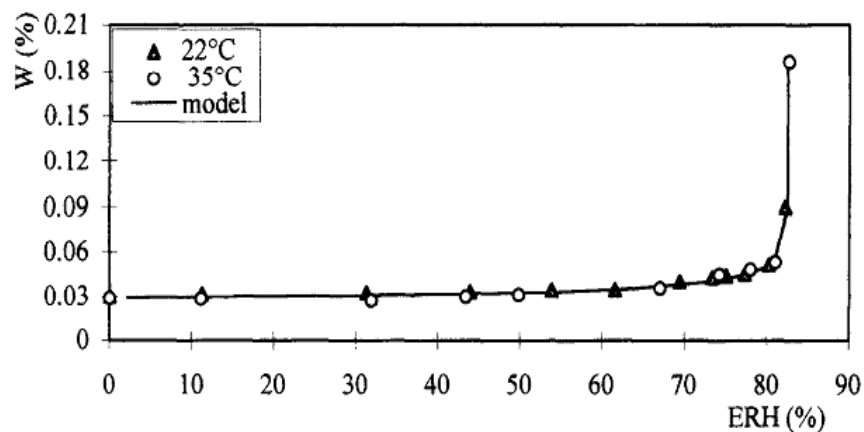


Figure 2.6 Sorption isotherm of sucrose at 22 and 35°C (Rastikain et al, 1998).

Leaper et al. (2002) fitted equation of sorption isotherm from the experimental data sorption isotherm that reported by Iglesias et al. (1982) which was determined by using IGA-sorpt as shown in Figure 2.7. It clearly shows that the effect of temperature was important in the temperature ranges of 10 to 40 as well as the

presence of hysteresis. However, the effect of temperature was only considered in their equation as illustrated by Equation (2.2). Wang et al. (2004) and Christakis et al. (2006) have used this equation to explain the moisture migration in sugar.

$$M_{eq} = \left(\gamma_1 + \gamma_2 a_{w,eq}^{\gamma_3} \right) \left(\frac{T}{20} \right)^\alpha \quad (2.2)$$

where M_{eq} is the equilibrium solid moisture content in %, $a_{w,eq}$ is the equilibrium relative humidity in %, and $\gamma_1, \gamma_2, \gamma_3, \alpha$ are the fitted parameters that equal to 0.03, 0.075, 2, 0.6, respectively.

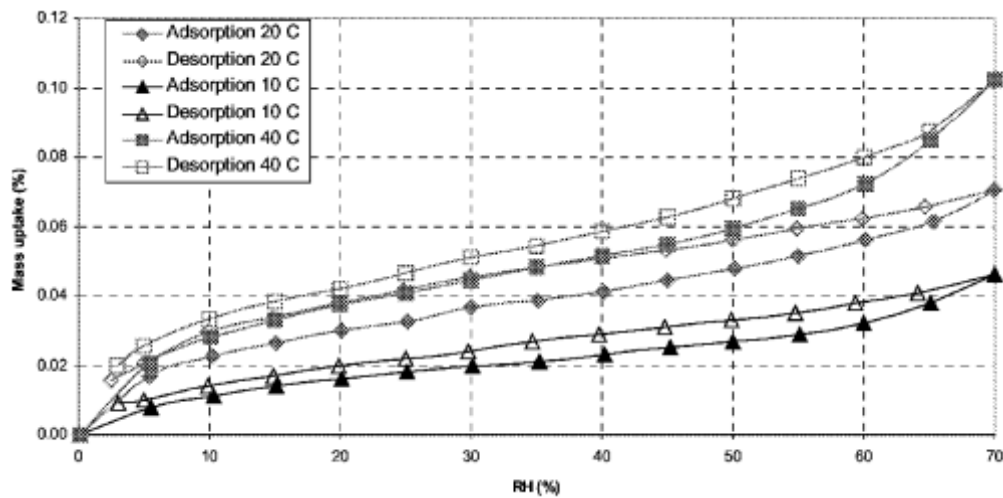


Figure 2.7 Moisture sorption isotherm curves for sucrose at 10, 20, and 40°C obtained by the IGAsorp (Leaper et al, 2002).

Billing and Paterson (2008) proposed a sorption isotherm model for using in their work by using the GAB equation to fit the experimental data at 20°C.

$$MC = \frac{a \cdot b \cdot c \cdot a_w}{(1 - b \cdot a_w)(1 + (c - 1) \cdot b \cdot a_w)} \quad (2.3)$$

where MC is moisture content in g/100g, a_w is water activity, and a , b , c are fitted constants that equal to -0.0125, -29.0078, 1.037366, respectively.

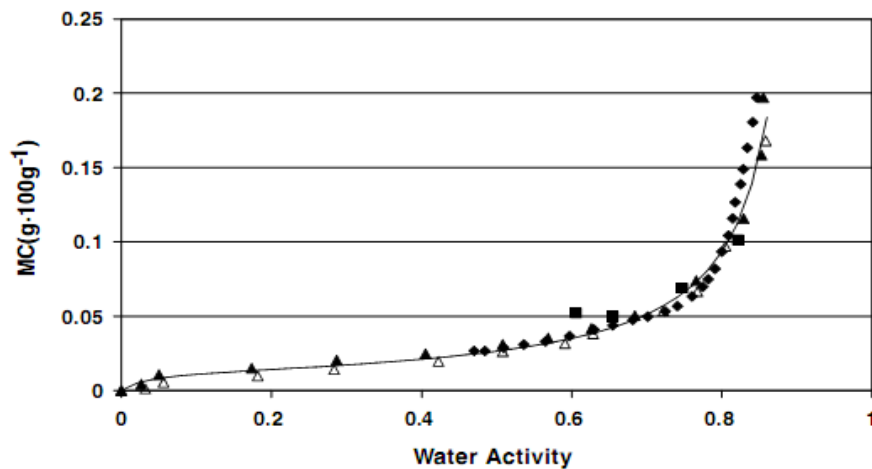


Figure 2.8 Isotherm for sucrose at 20°C. Fitted GAB model prediction line is shown.

(◆) Iglesias and Chirife (1982), (▲,Δ) Roth (1976), (■) Bakhit and Schmidt (1993), (—) GAB model $r = 0.989$ (Billing and Paterson, 2008).

In addition, the Guggenheim-Anderson-DeBoer or GAB equation as used in Billing and Paterson (2008) can also be used in modeling of water sorption in food materials (Lievonen and Roos, 2002 and van der Berg and Bruin, 1881). The GAB equation can be extended to consider the effect of temperature (Lievonen and Roos, 2002 and Weisser, 1985) and it is thus called as GAB-T equation which can be illustrated as Equations (2.4) to (2.7). The real advantage of this model is providing a

good fitted experimental data in ranging 0.0-0.90 of water activity as well as explaining the effect of temperature on water sorption isotherm.

$$\frac{M_{eq}}{M_0} = \frac{Cka_{w,eq}}{(1-ka_{w,eq})(1-ka_{w,eq} + Cka_{w,eq})} \quad (2.4)$$

$$M_0(T) = M'_0 e^{\frac{\Delta H}{RT}} \quad (2.5)$$

$$C(T) = C' e^{\frac{H_l - H_m}{RT}} \quad (2.6)$$

$$k(T) = k' e^{\frac{H_l - H_q}{RT}} \quad (2.7)$$

where M_{eq} is moisture content in solid phase in %, $a_{w,eq}$ is water activity, M_0 is the monolayer water content, C is the Guggenheim constant, and k is the constant correcting properties of multilayer molecules with respect to bulk liquid, the constants M'_0 , C' , k' and terms inside exponent were obtained by nonlinear regression analysis.

2.2.2 Scanning Curve

As seen in Figure 2.7, there is the presence of hysteresis in the sorption isotherm of sugar. Hence, in order to reflect the realistic situation, this effect should be taken into consideration in the mathematical model.

The scanning curve help us choose a path involving shifting from adsorption curve into the desorption curve and vice versa when air temperature and humidity surrounding of sugar changes. There are many approaches that reported in

previous literatures. For examples, it has been suggested that the shifting between adsorption and desorption curves by using a nearly horizontal straight line (Salin 2011, Clouties and Fortin 1994, Peralta 1995, Frandsen 2007) as shown by the sequence of A-B-C-D in Figure 2.9. However, Time (1998, 2002) suggested that the horizontal straight line should have a little slope as the straight line below BC line. Figure 2.10 and 2.11 also show the examples of scanning curve, which were produced from calculating the equation that was fitted from experimental data with no physical background (Salin 2011, Frandsen 2007, Frandsen and Damkilde 2000).

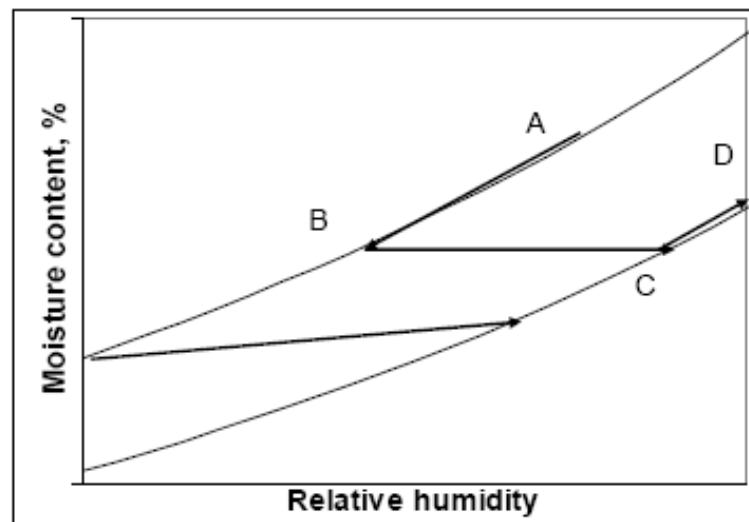


Figure 2.9 Diagram of scanning curve proposed by Salin (2011), Clouties and Fortin (1994), Peralta (1995), Frandsen (2007) and Time (1998, 2002).

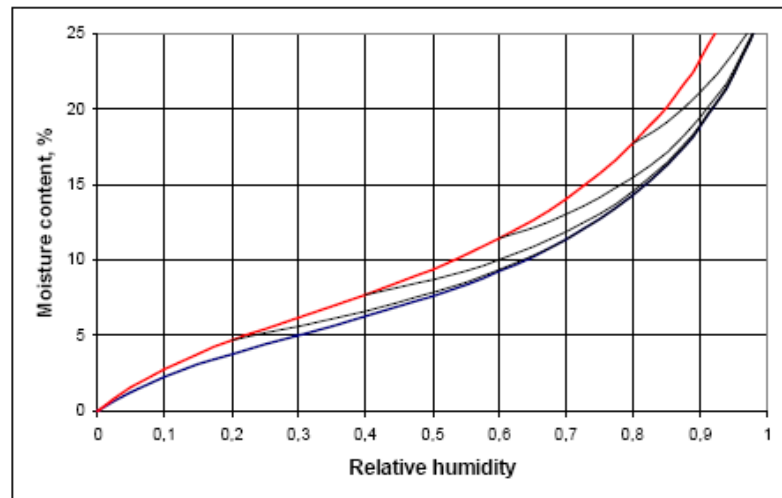


Figure 2.10 Diagram of adsorption scanning curve (Frandsen 2007, Salin 2011).

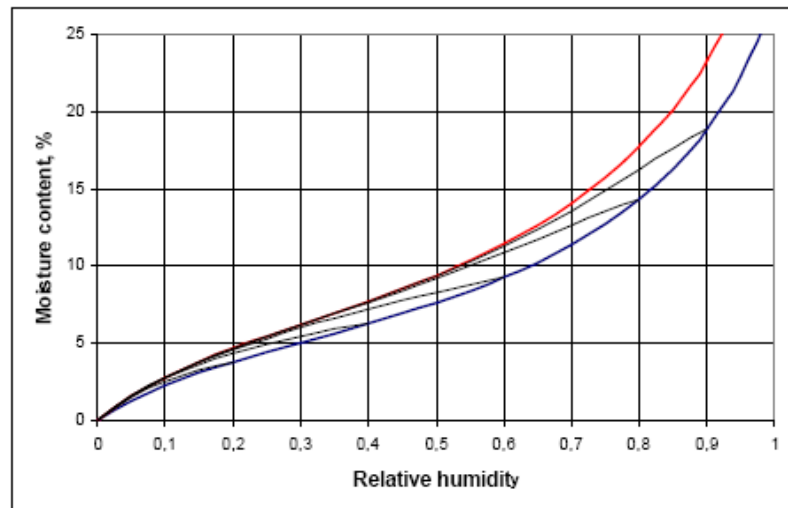


Figure 2.11 Diagram of desorption scanning curve (Frandsen 2007, Salin 2011).

2.3 Caking Phenomenon of Sugar and Moisture Migration

Caking is a phenomenon which changes a free-flowing particle into lumped material by agglomerating with neighboring particles. This phenomenon will take place when the liquid bridging was formed and then transformed into solid bridging.

In the case of sugar, as presented in previous works, the formation of liquid bridging comes from either the releasing of residual moisture in sugar grain into outside (Rastikian and Capart, 1998) or the adsorption moisture on surface sugar grain (Leaper et al., 2002, Wang et al., 2004, Christakis et al., 2006, Billings and Peterson, 2008). Both ways will make the surface of sugar grains dissolving with high concentration of sugar solution and being sticky. Hence, the liquid bridging will be formed. Moreover, the liquid bridging can also be occurred by melting of surface sugar grain if ambient temperature is higher than the temperature of glass transition which depends on the amount of amorphous state in sugar grain. However, this condition would most happen during drying. The solid bridging would then be formed after the recrystallization of liquid bridging when the excess moisture in liquid bridging was dried out or desorbed into air.

In the recent years, many researchers have focused on how the liquid bridging and solid bridging occur. The interested topic is the “moisture migration” in a bulk sugar or big bag because this is the beginning point of investigating the formation of caking. Leaper et al. (2002) obviously shows the relationship of the effect moisture migration to occurrence liquid/solid bridging and caking occur at last as shown in Figure 2.12.

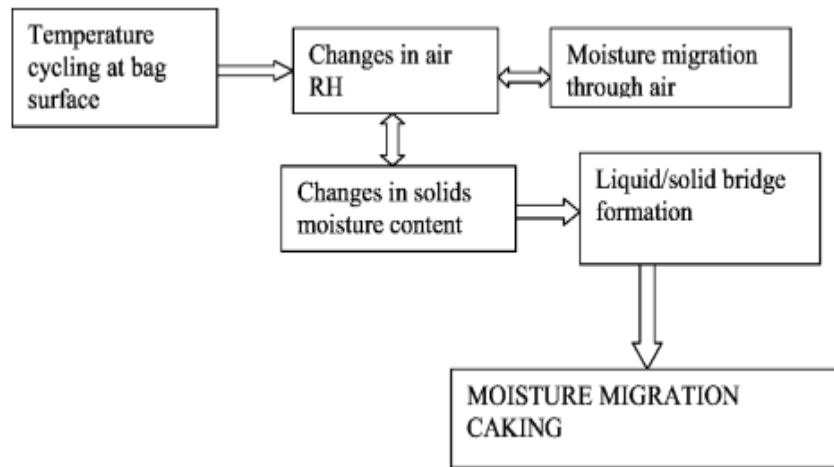


Figure 2.12 Block diagram of relationship between moisture migration and caking (Leaper et al, 2002).

Moisture migration in a bulk sugar will occur when the equilibrium moisture in sugar and air was disturbed by temperature changes. It can be explained as Figure 2.13 by Bronlund and Peterson (2008).

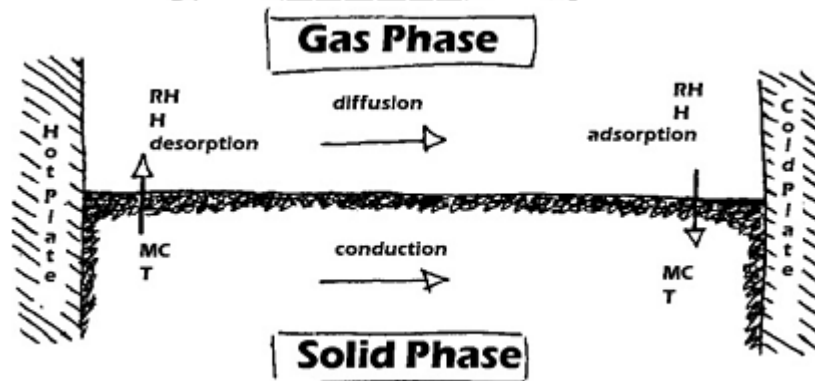


Figure 2.13 Moisture movement induced by an applied temperature gradient (Bronlund, 1997).

Figure 2.13 shows the diagram of a packed bed where the both sides of the bed are the plates which introduce temperature difference; the solid phase is sugar grain, and the gas phase is the void of bed. When the temperature difference is applied; first, heat conduction transfers from the hot side to the cold side. Simultaneously, the gas phase at the cold region is at a high relative humidity and then adsorbed on the surface of sugar grain while the gas phase at the hot region is at a low relative humidity and is desorbed to the gas phase. Consequently, the moisture gradient would rise and moisture would migrate from the hot region to the cold region at last. This process (moisture migration) would continue until both thermal and moisture reach to the final equilibrium.

2.4 Mathematical Modeling of Moisture Migration

In the recent years, many researchers have known the instigator of the caking that is “moisture migration” which is the consequence of either temperature cyclic or relative humidity cyclic.

Leaper et al. (2002) studied the moisture migration in a big bag when the outside temperature changes one cycle by simplified mathematical model. Equations (2.8) and (2.9) are the finite difference of heat transport equation which only considered the heat conduction of solid phase and Equation (2.10) is the finite difference of mass transport equation by moisture diffusion.

$$\dot{Q} = k_s A \frac{T_i^{j-1} - T_{i-1}^{j-1}}{l} \quad (2.8)$$

$$T_i^j = \frac{\dot{Q}_t}{MC_{ps}} + T_i^{j-1} \quad (2.9)$$

where T_i^j is the temperature at node position i and time step j , \dot{Q} is the heat flow rate through an area A of the thickness l between the two points at j , the mass and heat capacity of this segment is M and C_{ps} respectively.

$$Y_i^j = D_a A \frac{Y_i^{j-1} - Y_{i-1}^{j-1}}{l} + Y_{i-1}^j \quad (2.10)$$

where Y is an absolute humidity and D_a is the diffusion coefficient. Additionally, the caking box had been performed to use to verify the mathematical model. They found that their model can be used to predict the moisture migration in the big bag.

Wang et al. (2004) studied the moisture migration in a big bag similar to Leaper et al. (2002) but they assumed a length of the big bag to be infinite and the heat and moisture only transfer in r-direction. The interesting of this work that is considering the outside temperature around the big bag, which will disturb the equilibrium of moisture and leads moisture migration, is the temperature cyclic in square wave form oscillating between 40 and 10°C.

They represented the equations of conservation of energy and mass as Equations (2.11) and (2.12), respectively.

$$(1 - \varepsilon) \rho_s C_{ps} \frac{\partial T}{\partial t} = \frac{1}{r} \frac{\partial}{\partial r} \left(k_s r \frac{\partial T}{\partial r} \right) + L_h (1 - \varepsilon) \rho_s \frac{\partial M}{\partial t} \quad (2.11)$$

where C_{ps} and k_s are the specific heat capacity and thermal conductivity for granulated sugar, respectively. L_h is the latent heat of water vaporization, ε is the fraction of the total volume of the package occupied by air, and M is the moisture content of the solid.

$$\frac{\partial Y}{\partial t} = \frac{1}{r} \frac{\partial}{\partial r} \left(D_{eff} r \frac{\partial Y}{\partial r} \right) - \frac{(1-\varepsilon) \rho_s}{\varepsilon \rho_a} \frac{\partial M}{\partial t} \quad (2.12)$$

where D_{eff} is the effective diffusion coefficient for water vapor in air. Y is dimensionless and represents the mass of water vapor in the air around the solid particles.

Their mathematical model was solved by PHYSICA solver which based on overrelaxed Jacobi (JOR) and overrelaxed Gauss-Seidel (SOR) techniques. This solver was used to solve the system nonlinear equation which comes from the discretizing mathematical models by using the finite-volume method.

They found that the moisture adsorption and desorption processes most occurred at around the region of 0.2 meters from interface. As a result of this, the moisture content change in the big bag core was less than at the region near interface. Additionally, the moisture migration can be reduced by either decreasing the oscillating temperature amplitudes and the oscillating temperature average or increasing the thickness of the big bag or changing the big bag material that has a low thermal conductivity.

Christakis et al. (2006) investigated the moisture migration similar to the Wang et al. (2004) work but changed the big bag to be an insulated cylinder (cylindrical tensile test cell) with exposed the top to the relative humidity cycles. The

significance of this work is that the mathematical modeling of moisture migration was linked into the mathematical modeling of tensile strength. The numerical results agreed with very well with the experimental ones. The mathematical model in this work is also similar to the one proposed in Wang et al. (2002) but changed the coordinate from the r-direction to be z-direction as shown in Equations (2.13) and (2.14). Furthermore, they used the same method as in Wang et al. (2002) to solve their model equations.

$$(1-\varepsilon)\rho_s C_{ps} \frac{\partial T}{\partial t} = \frac{\partial}{\partial x} \left(k_s \frac{\partial T}{\partial x} \right) + L_h (1-\varepsilon) \rho_s \frac{\partial M}{\partial t} \quad (2.13)$$

$$\frac{\partial Y}{\partial t} = \frac{\partial}{\partial x} \left(D_a \frac{\partial Y}{\partial x} \right) - \frac{(1-\varepsilon)\rho_s}{\varepsilon\rho_a} \frac{\partial M}{\partial t} \quad (2.14)$$

Bronlund and Paterson (2008) investigated the moisture migration of the crystalline lactose powders in a packed bed when applied a temperature difference on both sides of the packed bed both by experiment and numerical analysis. The purpose of this work is to determine how much the temperature gradients were needed to induce moisture movement in a packed bed and to monitor the redistribution of moisture after disturbing by introducing temperature gradients. The results of the model agreed well with experimental data. The mathematical model of this work is of very interest because they used the assumption of local equilibriums of thermal and moisture, which allows us to overcome the problem of scattered and unreliable the mass transfer coefficient. Additionally, they considered and put the effect of heat conduction of air and enthalpy of moisture diffusion into the heat transport equation, which have been neglected in most previous works.

The following are the heat and moisture transport equations that only considers in x-direction (Note that it is equivalent to z-direction of Cartesian coordinate);

$$\frac{\partial H}{\partial t} = D_{eff} \frac{\partial^2 (h_v Y \rho_a)}{\partial x^2} + k_{eff} \frac{\partial T}{\partial x^2} \quad (2.15)$$

$$H = h_g \varepsilon \rho_a + h_s (1 - \varepsilon) \rho_s \quad (2.16)$$

where H is the total enthalpy in porous bed, D_{eff} is the effective diffusivity, Y is the absolute humidity, θ is the temperature. ρ_a and ρ_s are the density of dry air and solid, respectively. h_v , h_g , and h_s are enthalpy of water vapor, gas phase, solid phase, respectively.

$$\frac{\partial W}{\partial t} = D_{eff} \frac{\partial^2 (Y \rho_a)}{\partial x^2} \quad (2.17)$$

$$W = \varepsilon Y \rho_a + (1 - \varepsilon) M \rho_s \quad (2.18)$$

where W is the moisture concentration in porous, M is moisture content in solid phase.

Their mathematical model was solved in a Borland C++ program by using an explicit finite difference schemes.

Billings and Peterson (2008) worked on the similar problem as the work of Bround and Paterson (2008), but they used sucrose instead of crystalline lactose powders. They produced a graph that indicated the effects of initial moisture content

and temperature difference that probably lead to occur the caking by setting the criteria not exceed 80%RH.

In additional, the study of moisture migration using mathematical model has also been found in studying the caking of potash and urea by Chen and Wang (2006) and Nie et al. (2008) respectively, besides of sugar and lactose powder that have been published.

Chen and Wang (2006) investigated the moisture migration in a packed bed of potash by experiment and simulation. In the mathematical model, they only considered moisture transport, excluding the heat transport because this system was isothermal. Equations (2.19) and (2.20) are the moisture transport equations by vapor diffusion and transferring between gas phase and liquid phase, respectively. They also added the moisture transport by capillarity and gravity as Equation (2.21), which based on Whitaker's theory (Whitaker, 1980), since the potash has been ability to absorb the large amount of moisture. The mathematical models were solved by iteration method; firstly the modeling equations were discretized to be the set of nonlinear equations by using control volume method (Patankar, 1980) before taking the iterative procedure.

$$\frac{\partial(\varepsilon_v \rho_v)}{\partial t} - \dot{m} = \frac{\partial}{\partial x} \left(D_{eff} \frac{\partial \rho_v}{\partial x} \right) \quad (2.19)$$

$$\frac{\partial \varepsilon_\beta}{\partial t} + \frac{\dot{m}}{\rho_\beta} = 0 \quad (2.20)$$

$$\frac{\partial S}{\partial t} = \frac{1}{n_\beta (1 - \varepsilon_\sigma)} \frac{\partial}{\partial x} \left[K_\beta \left(-\frac{\partial \langle P_c \rangle}{\partial S} \frac{\partial S}{\partial x} + \rho_\beta g \right) - \frac{\dot{m}}{\varepsilon \rho_\beta} \right] \quad (2.21)$$

where ρ_v is density of vapor, ε_γ is the volume fraction of gas, \dot{m} is the rate of phase change, D_{eff} is the effective diffusion coefficient, ε_β is the volume fraction of liquid, ρ_β is the density of water, S is the saturation, η_β is the viscosity of water-salt solution in the potash bed, ε_σ is the volume fraction of solid, K_β is the permeability of liquid phase in the potash bed, $\langle P_c \rangle$ is the volume average pore or capillary pressure, g is the gravitational acceleration, ε is the porosity.

Nie et al. (2008) studied moisture migration in a packed bed of urea when air flows uniformly through the bed. The highlight of this work that is they considered the moisture migration along the height of bed and the inside of urea particle because some moisture can absorb into internal particle of urea, which is different from potash that moisture only coats outer surface.

The mass balance equation for water vapor transport in the interstitial air;

$$\frac{\partial(\varepsilon_{g,e}\rho_{v,e})}{\partial t} + \frac{\partial(u_D\rho_{v,e})}{\partial x} = \frac{\partial}{\partial x}\left(D_{e,eff}\frac{\partial\rho_{v,e}}{\partial x}\right) + \dot{m}_e \quad (2.22)$$

where $\varepsilon_{g,e}$ is the porosity of gas phase, $\rho_{v,e}$ is the density of vapor, u_D is the Darcy velocity, $D_{e,eff}$ is the effective diffusion coefficient, \dot{m}_e is the mass source term, t is time, x is bed position. Note that any variables having been subscripted with i and e , these refer to the internal and external domains.

The mass balance equation for water vapor diffusion in the urea particle;

$$\frac{\partial(\varepsilon_{g,i}\rho_{v,i})}{\partial t} = \frac{1}{r^2}\frac{\partial}{\partial r}\left(r^2D_{i,eff}\frac{\partial\rho_{v,i}}{\partial r}\right) - \dot{m}_i \quad (2.23)$$

where r is radial position inside a particle.

The energy equation in the interstitial air;

$$\frac{\partial \left[\varepsilon_{g,e} (\rho C_p)_g T_{g,e} \right]}{\partial t} + \frac{\partial \left[u_D (\rho C_p)_g T_{g,e} \right]}{\partial x} = \frac{\partial}{\partial x} \left(k_{e,eff} \frac{\partial T_{g,e}}{\partial x} \right) + h_e \quad (2.24)$$

where ρ is density, C_p is specify heat capacity, T is temperature, $k_{e,eff}$ is effective thermal conductivity, h_e is heat source term. Note that any variables having been subscripted with g , this refers to the gas phase.

The energy equation in the urea particle in axial direction;

$$\frac{\partial \left\{ \left[\varepsilon_p (\rho C_p)_p + (\varepsilon_{l,i} \varepsilon_p + \varepsilon_{l,e}) (\rho C_p)_{l,e} \right] T_i \right\}}{\partial t} = \frac{\partial}{\partial x} \left(k_{i,eff} \frac{\partial T_i}{\partial x} \right) - \dot{h}_e + \dot{h}_i \quad (2.25)$$

Note that any variables having been subscripted with p and l , these refer to the particle and liquid phases.

All equations above were discretized by finite volume method (Patankar, 1980). Those equations were then transformed to the set of nonlinear equation system and were solved by the iterative technique.

2.5 Mathematical Techniques Involved in this Work

2.5.1 Nonlinear Least Square Method

The nonlinear least square method (Björck, 1996) is a technique to determine parameters of nonlinear equations or models in order to interpret a set of data by minimizing the summation of the square of error.

The summation square error of error is defined;

$$SS_{err} = \sum_{i=1}^m (y_i - f(x_i, \beta))^2 \quad (2.26)$$

where SS_{err} is the sum of squares error, $(x_1, y_1), (x_2, y_2), \dots, (x_m, y_m)$ is the set of data m points, $\beta = (\beta_1, \beta_2, \dots, \beta_n)$ is the set of parameter with n parameters and $m \geq n$, $f(\)$ is any equation or model that need to find the parameters.

The summation square of error is minimized by taking derivative with respect to each parameter and setting them equal to zero. As a result, we will obtain the system of nonlinear equation which can be rearranged as illustrated in Equation (2.27).

$$J \Delta \beta = -F \quad (2.27)$$

where J is the jacobian of the system nonlinear equation, F is the system nonlinear equation.

The parameters can be determined from Equation (2.27) by using Newton's method. This method can be called "Gauss-Newton algorithm" which used to solve nonlinear least squares problems. Moreover, this algorithm that is contained is a part of *lsqnonlin* which is a built-in function in MATLAB program.

2.5.2 Numerical Method of Lines

The numerical method of lines (Schiesser, 1991; Hamdi, et al., 2007; Schiesser and Griffiths, 2009) is a technique for solving partial differential equations (PDEs). This method proceeds by approximating the spatial derivative with finite difference while solving the resulted ordinary differential equations by initial value

methods. Table 2.1 lists the common finite difference formula mostly used. This numerical method of lines is often used to solve parabolic partial differential equations such as one-dimensional heat conduction equation.

The approximation of derivative term only one side (on spatial domain) is the strength of this method since it can reduce the truncations error. Thus, it is better than other methods that have the approximation of derivative term on both sides of differential equation such as finite difference method.

After obtaining the system of ordinary differential equation (ODEs), there are many commercial software for solving this equation such as POLYMATH, MATLAB.

Table 2.1 Finite difference formula.

Formula	Error terms	Comments
1. $f'(x_i) \approx \frac{f(x_{i-2}) - 4f(x_{i-1}) + 3f(x_i)}{2h}$	$O(h^2)$	Backward difference for 1 st derivative
2. $f'(x_i) \approx \frac{f(x_{i+1}) - f(x_{i-1}))}{2h}$	$O(h^2)$	Central difference for 1 st derivative
3. $f'(x_i) \approx \frac{-3f(x_i) + 4f(x_{i+1}) - f(x_{i+2}))}{2h}$	$O(h^2)$	Forward difference for 1 st derivative
4. $f''(x_i) \approx \frac{f(x_{i-1}) - 2f(x_i) + f(x_{i+1}))}{h^2}$	$O(h^2)$	Central difference for 2 nd derivative

CHAPTER III

RESEARCH METHODOLOGY

In this chapter, it begins with describing the derivation of mathematical model which is vital important section for a simulation. Then, the determining parameter of sorption isotherm GAB-T model was explained in the section of sorption isotherm equation - this inclusion of GAB-T model to model the water sorption isotherm on sugar grain is novel. Next, we illustrate how to solve the mathematical model and the validation of model appeared in this thesis. The model was then used to predict the moisture migration in the real shipping condition. The sensitivity analysis was also performed for investigating the impact of uncertain parameters. The details of those are as follows.

3.1 Derivation of Mathematical Model

The simulation for studying the moisture migration in a big bag of sugar during transportation by using mathematical model is the most convenient way comparing to the experimental method because the simulation can save the cost and time in studying.

3.1.1 Conceptual Model

During transportation by ships, sugar in a container has to face the high and low temperature fluctuation periodically until arriving at the final destination.

This fluctuation of temperature causes the moisture migration as described in the Section 2.3, and is regarded as “disturbance variable” of our system.

The main mechanisms that occur in system for our considering include;

- 1) Heat conduction in both solid and gas phases.
- 2) Moisture diffusion through gas phase.
- 3) Adsorption and Desorption phenomena of moisture between gas phase and solid phase.

3.1.2 System

System is a big bag of sugar as shown in Figure 3.1. Sugar is put in a big bag for keeping in a warehouse before distribution and shipping. The big bag is made from a polypropylene in which moisture cannot permeate through this packaging material. Generally, a size of big bag is 1 meter of diameter, 1.0 meter of height, and 1 ton of capacity



Figure 3.1 The big bag of sugar.

3.1.3 Assumptions

The following assumptions were applied in developing the mathematical model of moisture migration in big bag;

- i) Unsteady state system.
- ii) One-dimensional of heat and mass transport in r-direction of a cylinder.
- iii) Local thermal and moisture equilibriums between gas and solid phases.
- iv) Moisture diffusion in sugar crystal is negligible.
- v) Heat convection in gas phase is negligible.
- vi) Hysteresis is taken into account.
- vii) Excluding the heat conduction in the big bag.

The assumptions of local thermal and moisture equilibrium between gas and solid phases were also applied. Because gas phase in a big bag is stagnant, the transfers of heat and mass through the gas phase are slow; hence, the moisture diffusion in gas phase is the rate limiting step. This assumption allows us to calculate the relationship amount of moisture between gas and solid phases directly through the water sorption isotherm; this assumption was first proved and utilized by Billing and Paterson (2008). In addition, the effect of heat conduction in PE was not considered because of its higher heat conductivity when comparing to those of sugar grain and heat transfer coefficient due to convection in air-packaging interface.

3.1.4 Mathematical Model

The mathematical model was derived from mass and energy balances around shell as shown in Figure 3.2 based on the above assumptions.

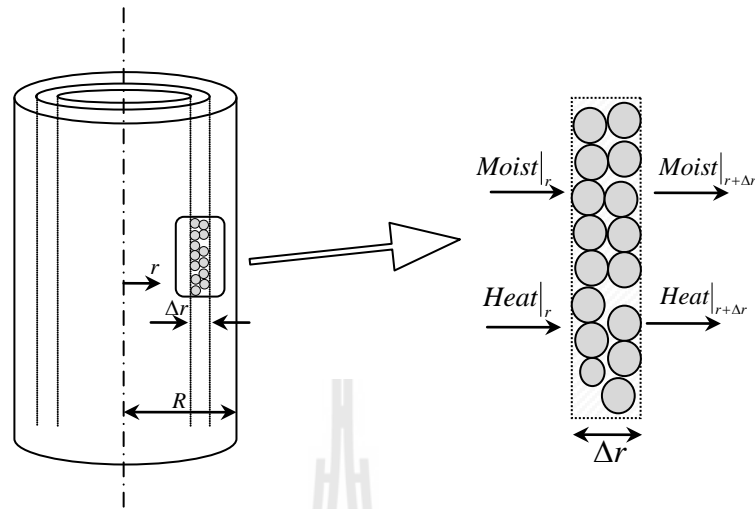


Figure 3.2 Schematic diagram of system for shell balance.

The mass transfer model can be written as;

$$\frac{\partial W}{\partial t} = \frac{1}{r} \frac{\partial}{\partial r} \left(r D_{eff} \frac{\partial}{\partial r} (\rho_{da} Y) \right) \quad (3.1)$$

$$W = \varepsilon Y \rho_{da} + (1 - \varepsilon) M \rho_s \quad (3.2)$$

The energy transfer model can be written as;

$$\frac{\partial H}{\partial t} = \frac{1}{r} \frac{\partial}{\partial r} \left(r D_{eff} \frac{\partial}{\partial r} (\rho_{da} Y) h_v \right) + \frac{k_{eff}}{r} \frac{\partial}{\partial r} \left(r \frac{\partial T}{\partial r} \right) \quad (3.3)$$

$$H = h_g \varepsilon \rho_{da} + h_s (1 - \varepsilon) \rho_s \quad (3.4)$$

3.1.5 Initial and Boundary Conditions

For initial condition, the temperature and moisture content in sugar are in local equilibrium with those of moist air;

$$T(r, t = 0) = T_0 \quad (3.5)$$

$$Y(r, t = 0) = Y_0 \quad (3.6)$$

For boundary conditions, the system is symmetry at $r = 0$; it can thus be written as Equations (3.7) and (3.8). At $r = R$, the mass flux of moisture is zero because of PE bag; however, heat transfer between a system and environment still exists. Therefore, Equations (3.9) and (3.10) are obtained.

$$-D_{eff} \left. \frac{\partial(Y\rho_{da})}{\partial r} \right|_{r=0} = 0 \quad (3.7)$$

$$-k_{eff} \left. \frac{\partial T}{\partial r} \right|_{r=0} = 0 \quad (3.8)$$

$$-D_{eff} \left. \frac{\partial(Y\rho_{da})}{\partial r} \right|_{r=R} = 0 \quad (3.9)$$

$$-k_{eff} \left. \frac{\partial T}{\partial r} \right|_{r=R} = h(T_{outside} - T_{r=R}) \quad (3.10)$$

where h is heat transfer coefficient and was calculated from the correction equation reported by Churchill and Chu (1975) which can use in the system occurring a heat transfer by nature flow between vertical wall and ambient condition as shown in

Equation (3.11); Nu is the Nusselt number, Ra is the Rayleigh number, and Pr is the Prandtl number.

$$Nu = \left(0.825 + \frac{0.387Ra^{1/6}}{\left[1 + (0.492 / Pr)^{9/16} \right]^{8/27}} \right)^2 \quad (3.11)$$

The Nusselt number, Rayleigh number, and Prandtl number can be defined as Equation (3.12), (3.13), and (3.14), respectively.

$$Nu = \frac{hL}{k} \quad (3.12)$$

where L is the length of the surface of heat transfer, k is thermal conductivity of air

$$Ra = \frac{\beta \Delta T g L^3}{\nu \alpha} \quad (3.13)$$

where β is the volumetric coefficient of expansion (K^{-1}); for the ideal gas is $\beta = 1/T$, ΔT is the temperature difference between surface and free stream (K or $^{\circ}C$), g is the acceleration of gravity (m/s^2), ν is the kinematic viscosity (m^2/s), and α is the thermal diffusivity (m^2/s).

$$Pr = \frac{\nu}{\alpha} \quad (3.14)$$

3.1.6 Constitutive Equations

The constitutive equations below were used with the mathematical model in solving to determine numerical solution.

3.1.6.1 Effective Diffusivity

The effective diffusivity can be defined from vapor diffuse through dry air in porous bed. It can be written as;

$$D_{eff} = \varepsilon D_a \quad (3.15)$$

where D_a is the diffusivity of vapor in dry air and is equal to

$1.7255 \times 10^{-7} (T + 273.15) - 2.552 \times 10^{-5}$, which is reported by Shah et al. (1984).

3.1.6.2 Effective Thermal Conductivity

The parallel model of effective thermal conductivity (Tsu-Ning Tsao, 1961) was applied to this work, which is the simplest model of heat transfer by heat conduction of heterogeneous materials, having two phases inside a material such as porous material. This model can also be applied to the packed bed system as the one developed in this work.

$$k_{eff} = \varepsilon k_a + (1 - \varepsilon) k_s \quad (3.16)$$

3.1.6.3 Density of Dry Air

The density of dry air is assumed to be the ideal gas because the range of pressure and temperature of interest are around ambient condition. Moreover, the density in void between particles should also consider an effect of moisture content on the density of moist air. However, the fraction of moisture in air is small; for example $Y = 0.024$ at 90%RH and 30°C. As a result, the effect of moisture was neglected. Therefore, it can be written as;

$$\rho_{da} = \frac{273.15}{22.4(273.15 + T)} \frac{1}{29} \quad (3.17)$$

3.1.6.4 Enthalpy

The enthalpy can be written as the following equations, in heat capacity form and the reference state of enthalpy is the saturated liquid at 0°C;

$$h_s = C_{ps}T + MC_{pw}T \quad (3.18)$$

$$h_v = C_{pv}T + h_{fg} \quad (3.19)$$

$$h_g = C_{pa}T + Yh_v \quad (3.20)$$

3.1.6.5 Absolute Humidity and Relative Humidity

The relationship between absolute humidity and relative humidity in equilibrium can be expressed as;

$$Y_{eq} = \frac{18}{29} \times \frac{ERH \times P_{sat}}{760 \times 100 - ERH \times P_{sat}} \quad (3.21)$$

$$\log_{10} P_{sat} = 7.96681 - \frac{1668.21}{228 + T} \quad (3.22)$$

$$ERH = a_w \times 100 \quad (3.23)$$

where P_{sat} is the vapor pressure of water.

3.1.6.6 Sorption Isotherm

The relationship of an amount of moisture content between gas and solid phases in equilibrium was expressed by sorption isotherm which will be mentioned for more detail in Section 3.2.

3.1.6.7 Model Parameters

The parameters and properties of materials used in the mathematical model were brought from the previous literatures and references as shown in Table 3.1. There is some properties of air that depended on temperature but is treated to be constant at 30C since the temperature change does not impact the properties significantly.

Table 3.1 Material properties

Material properties	Value	Unit	References
<u>Sugar</u>			
ρ_s	1660	kg/m ³	Chritakis et al., 2006
C_{ps}	2087.3	J/kg °C	Chritakis et al., 2006
k_s	0.208	J/m s °C	Chritakis et al., 2006
ε	0.365	[-]	Chritakis et al., 2006
<u>Air</u>			
C_{pw}	4.14	kJ/kg °C	McCabe (2004)
C_{pv}	1.863	kJ/kg °C	McCabe (2004)
C_{pa}	1.035	kJ/kg °C	McCabe (2004)
k_a	0.0187	W/m °C	McAdams, 1954
<u>Other</u>			
h_{fg}	2,272	kJ/kg	Chritakis et al., 2006
<u>Bag (PE)</u>			
ρ_{PE}	1192	Kg/m ³	Wang et al., 2004
k_{PE}	5	W/m °C	Wang et al., 2004
$C_{p,PE}$	4120	J/kg °C	Wang et al., 2004

3.2 Sorption Isotherm Equation

In this work, the new sorption isotherm is proposed by using GAB-T equation, as shown in Equations (2.4) to (2.7), to fit the sorption isotherm data of both adsorption and desorption lines of which is taken by Leaper et al. (2002) because the sorption isotherm equation used in previous works merely consider the effect of adsorption as shown in Equation (2.2) or did not consider the effect of temperature as listed in Equation (2.3).

Table 3.2 shows the data of adsorption and desorption isotherms which was plotted as curves illustrated in the Figure 2.7. Note that the data do not reach 100%RH because its range is only from 0 to 70 %RH.

Table 3.2 The moisture content data of adsorption and desorption isotherm from Figure 2.7

%RH	a_w	Adsorption			Desorption		
		T=10 °C	T=20 °C	T=40 °C	T=10 °C	T=20 °C	T=40 °C
0.00	0.0000	0.0000	0.0000	0.0000	0.0000	0.00000	0.00000
5.69	0.0569	0.00713	0.01696	0.02168	0.01067	0.02089	0.02639
10.36	0.1036	0.01106	0.02246	0.02993	0.01421	0.02796	0.03347
15.40	0.1540	0.01342	0.02600	0.03386	0.01696	0.03268	0.03858
20.44	0.2044	0.01578	0.02954	0.03779	0.01971	0.03740	0.04211
25.49	0.2549	0.01775	0.03268	0.04172	0.02168	0.04093	0.04683
30.34	0.3034	0.01971	0.03661	0.04526	0.02403	0.04447	0.05115
35.76	0.3576	0.02089	0.03897	0.04879	0.02679	0.04840	0.05469
40.61	0.4061	0.02286	0.04133	0.05194	0.02875	0.05115	0.05862
45.66	0.4566	0.02521	0.04447	0.05508	0.03111	0.05351	0.06294
50.70	0.5070	0.02679	0.04762	0.05941	0.03307	0.05587	0.06805
55.74	0.5574	0.02875	0.05194	0.06569	0.03504	0.05980	0.07434
60.60	0.6060	0.03189	0.05587	0.07198	0.03818	0.06255	0.08024
65.64	0.6564	0.03779	0.06058	0.08456	0.04133	0.06609	0.08770
70.12	0.7012	0.04565	0.07002	0.10140	0.04565	0.07002	0.10140

The objective function used in fitted the GAB-T equation for both adsorption and desorption by least square method was expressed as Equation (3.24).

$$S_{err} = \sum_i^N \left((X_i^{\text{exp}} - X_i^{\text{cal}})_{T=10^\circ\text{C}}^2 + (X_i^{\text{exp}} - X_i^{\text{cal}})_{T=20^\circ\text{C}}^2 + (X_i^{\text{exp}} - X_i^{\text{cal}})_{T=40^\circ\text{C}}^2 \right) \quad (3.24)$$

where SS_{err} is the sum of squares error or sum of squares residuals, X_i^{exp} is the experiment of moisture content of either from adsorption or desorption, X_i^{cal} is the moisture content that was calculated from Equations (2.4) to (2.7), and i is index of %RH.

As seen the Equations (2.4) to (2.7), those equations are nonlinear. Thus we can use the *lsqnonlin* (see Appendix C for details) which is built-in function in MATLAB program to solve this problem. However, the limitation of this method is that it yields the local optimum. Consequently, the good initial guess is necessary to determine before taking *lsqnonlin* in order to increase the probability to seek the correct answer and decrease the number of iteration of program.

The initial guess of this problem can be determined by following steps. Firstly, if considering Equation (2.4), we found that Equation can rearrange from the nonlinear equation into linear equation by grouping those variables, shown as Equations (3.25) to (3.28). As a result of this, we can directly use the linear regression to determine parameters α , β and γ for each temperature, and then use the Newton's method to solve parameter k , M_0 and C from Equations (3.26) to (3.28). Consequently, we now obtained the parameter k , M_0 and C for each temperature (10, 20 and 40 °C) at this step.

$$\frac{a_{w,eq}}{M} = \alpha a_{w,eq}^2 + \beta a_{w,eq} + \gamma \quad (3.25)$$

$$\text{where } \alpha = \frac{k}{M_0} \left(\frac{1}{C} - 1 \right) \quad (3.26)$$

$$\beta = \frac{1}{M_0} \left(1 - \frac{2}{C} \right) \quad (3.27)$$

$$\gamma = \frac{1}{M_0 C k} \quad (3.28)$$

Secondly, if looking at Equations (2.5) to (2.7), those equations are only a function of temperature and are in the exponential form. Hence, we can determine the parameters of those equations by taking logarithm on both sides for transforming into linear form, we obtained Equations (3.29) to (3.31), and then plotting $\log M'_0$, $\log C$ and $\log k$ against $1/T$.

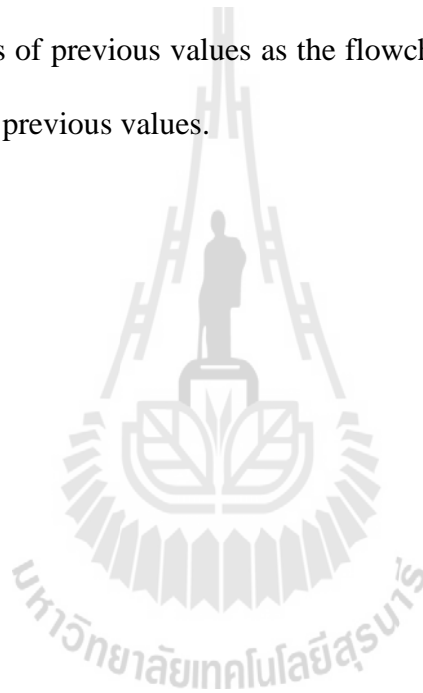
$$\log M_0(T) = \log M'_0 + \frac{\Delta H}{R} \frac{1}{T} \quad (3.29)$$

$$\log C(T) = \log C' + \frac{(H_l - H_m)}{R} \frac{1}{T} \quad (3.30)$$

$$\log k(T) = \log k' + \frac{(H_l - H_q)}{R} \frac{1}{T} \quad (3.31)$$

Having finished this procedure, we had parameters $M'_0, C', k', \Delta H/R, (H_l - H_m)/R$ and $(H_l - H_q)/R$, and these parameters were readily used to be initial guess for *lsqnonlin* program.

In order to make sure that those initial guess giving the correct answer, so we had to vary the initial guess around that point to search the lowest sum of squares residual. Consequently, the program for this propose was written over *lsqnonlin* either by decreasing 0.1times of previous values as the flowchart shown on Figure 3.3 or by increasing 0.1times of previous values.



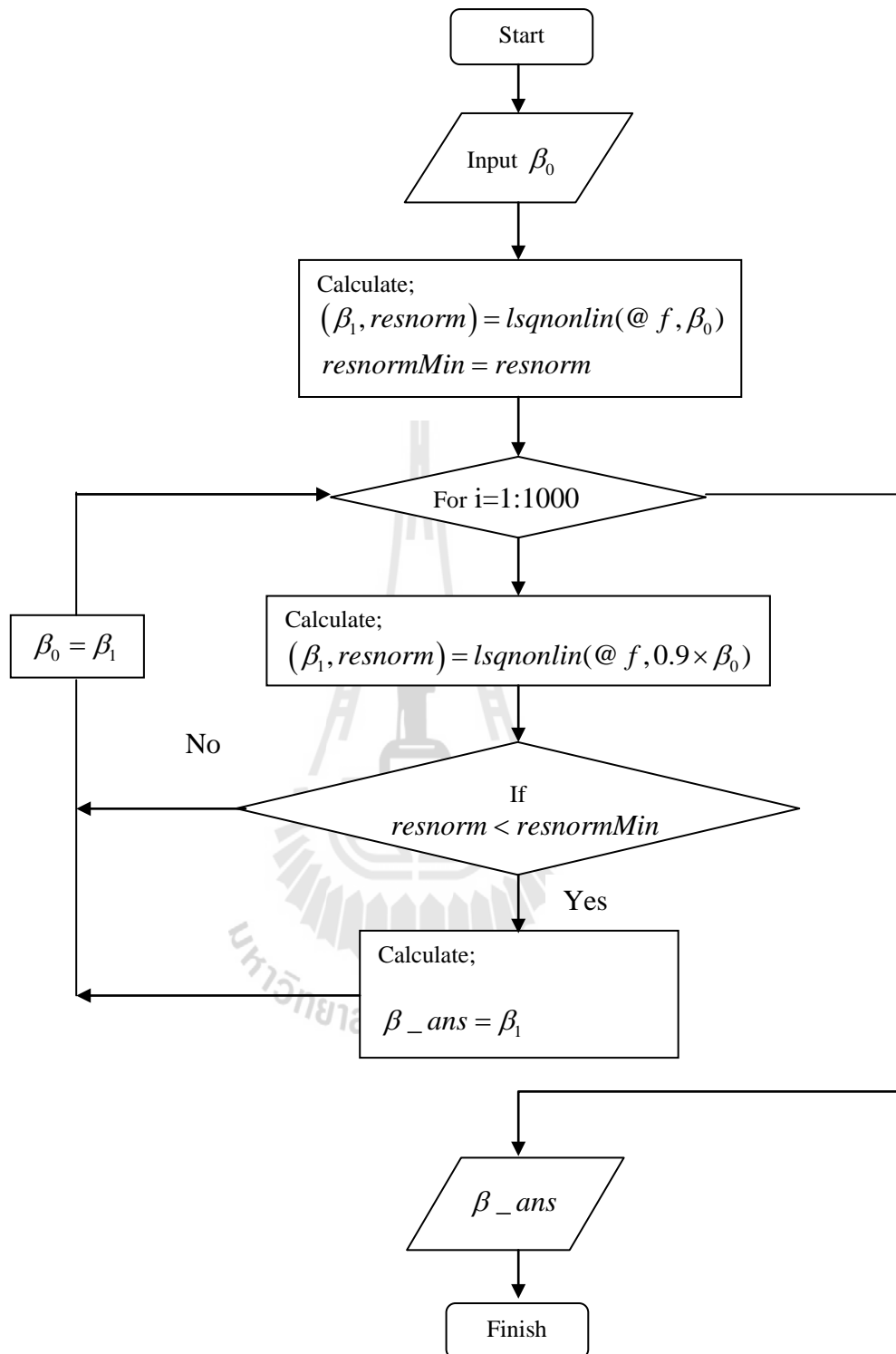


Figure 3.3 Flowchart for searching the lowest sum of squares error by decreasing evenly 0.1 of previous value.

3.3 Numerical Solution

The mathematical models were solved by numerical method of lines which is effective for solving the parabolic partial differential equations, and by using the *ode15s* (see Appendix C for details) to be tool in solving this problem. The numerical solution was carried out by the following steps;

3.3.1 Transforming the Modeling Equation to $M(t, y)y' = f$ form

In many engineering or physical problems, many mathematical models must be written the modeling equations in $M(t, y)y' = f(t, y)$ (Linear implicit DAEs) since it cannot be written in the form of $y' = f(t, y)$ form (a pure ODE system). Fortunately, a mathematical model equation in this form can be solved by MATLAB program which has many subroutines (build-in functions) that can solve the differential equation depending on that work or on the purpose of user, including *ode45*, *ode23*, *ode113*, *ode23s*, *ode23t*, *ode15s* and *ode23tb*. In this work, we used *ode15s* that can be used to solve the stiff differential equations since the stiffness may take place during solving the differential equations, especially on the case of nonlinear or the immediately changing state variable.

After substituting Equation (3.2) into Equation (3.1) and also substituting Equation (3.4) into Equation (3.3), we get;

$$\frac{\partial}{\partial t}(\varepsilon Y \rho_{da} + (1 - \varepsilon) M \rho_s) = \frac{1}{r} \frac{\partial}{\partial r} \left(r D_{eff} \frac{\partial}{\partial r} (\rho_{da} Y) \right) \quad (3.32)$$

$$\frac{\partial}{\partial t} (h_g \varepsilon \rho_{da} + h_s (1 - \varepsilon) \rho_s) = \frac{1}{r} \frac{\partial}{\partial r} \left(r D_{eff} \frac{\partial}{\partial r} (\rho_{da} Y) h_v \right) + \frac{k_{eff}}{r} \frac{\partial}{\partial r} \left(r \frac{\partial T}{\partial r} \right) \quad (3.33)$$

Again, substituted Equation (3.18), h_s , into Equation (3.33), we get;

$$\begin{aligned} \frac{\partial}{\partial t} \left(h_g \varepsilon \rho_{da} + (C_{ps} T + MC_{pw} T)(1 - \varepsilon) \rho_s \right) = \frac{1}{r} \frac{\partial}{\partial r} \left(r D_{eff} \frac{\partial}{\partial r} (\rho_{da} Y) h_v \right) \\ + \frac{k_{eff}}{r} \frac{\partial}{\partial r} \left(r \frac{\partial T}{\partial r} \right) \end{aligned} \quad (3.34)$$

As seen in Equations (3.32) and (3.34), we have three dependent variables, including T , Y and M . In addition, we have two differential equations (Equations (3.32) and (3.34)) and 1 algebraic equation (Equation (2.4)). In general, at this point, we have two choices that can solve this problem; first choice we can solve with two differential equations and one algebraic equation. But $M(t, y)$ in this way will be singular. Second choice we can eliminate the algebraic equation by substituting it in both differential equations. Hence, we will have only two differential equations. In this work, we chose the second choice because, normally, solving the system of differential equations in which $M(t, y)$ is non-singular is much easier solving the singular one even though the *ode15s* can solve both cases. Furthermore, we anticipated that the process of solving in the second approach is faster than the first one because, when there is singular $M(t, y)$, the process of finding consistent initial condition must be included. Moreover, the numerical method of lines must solve with many nodes depending on user's criteria.

Having finished this step, we obtained (see Appendix B for details);

$$M(t, y) = \begin{pmatrix} \varepsilon Y \frac{\partial \rho_{da}}{\partial T} + (1-\varepsilon) \rho_s \left(\frac{\partial M}{\partial T} \right)_Y & \varepsilon \rho_{da} + (1-\varepsilon) \rho_s \left(\frac{\partial M}{\partial Y} \right)_T \\ \varepsilon h_g \frac{\partial \rho_{da}}{\partial T} + \varepsilon \rho_{da} (C_{pa} T + Y C_{pv}) + (1-\varepsilon) \rho_s (C_{ps} + M C_{pw}) + (1-\varepsilon) \rho_s (C_{pw} T) \left(\frac{\partial M}{\partial T} \right)_Y & \varepsilon \rho_{da} (C_{pv} T + h_{fg}) + (1-\varepsilon) \rho_s (C_{pw} T) \left(\frac{\partial M}{\partial Y} \right)_T \end{pmatrix} \quad \dots(3.35)$$

$$y' = \begin{pmatrix} \frac{\partial T}{\partial t} \\ \frac{\partial Y}{\partial t} \end{pmatrix} \quad (3.36)$$

$$f(t, y) = \begin{pmatrix} \frac{1}{r} \left[r D_{eff} \left(\rho_{da} \frac{\partial^2 Y}{\partial r^2} + 2 \frac{\partial Y}{\partial r} \frac{\partial \rho_{da}}{\partial r} + Y \frac{\partial^2 \rho_{da}}{\partial r^2} \right) + \left(\rho_{da} \frac{\partial Y}{\partial r} + Y \frac{\partial \rho_{da}}{\partial r} \right) \left(r \frac{\partial D_{eff}}{\partial r} + D_{eff} \right) \right] \\ \frac{1}{r} \left[r D_{eff} \left(\left(\rho_{da} \frac{\partial Y}{\partial r} + Y \frac{\partial \rho_{da}}{\partial r} \right) \frac{\partial h_v}{\partial r} + h_v \left(\rho_{da} \frac{\partial^2 Y}{\partial r^2} + 2 \frac{\partial Y}{\partial r} \frac{\partial \rho_{da}}{\partial r} + Y \frac{\partial^2 \rho_{da}}{\partial r^2} \right) \right) + \left(\left(\rho_{da} \frac{\partial Y}{\partial r} + Y \frac{\partial \rho_{da}}{\partial r} \right) h_v \right) \left(r \frac{\partial D_{eff}}{\partial r} + D_{eff} \right) \right] + \frac{k_{eff}}{r} \left(r \frac{\partial^2 T}{\partial r^2} + \frac{\partial T}{\partial r} \right) \end{pmatrix} \quad \dots(3.37)$$

3.3.2 Discretizing the Derivative Terms

As seen in Equations (3.35) to (3.37), there are derivative terms in spatial direction which must be discretized in the numerical method of lines. The results are shown in Table 3.3. It should be noted that the first equation in Table 3.1 can easily be solved analytically but, in this work, we have already done with the discretizing. However, the error occurring from this approach was acceptable because we used the small temperature difference (10^{-6}) – the errors were finally checked with the numerical analysis of different step sizes. In the other terms such $(\partial M/\partial T)_Y$ or $(\partial M/\partial Y)_T$, it is not really easily to determine the analytical solution since M is highly nonlinear.

Besides of the derivative terms appearing in Equations (3.35) to (3.37), we also have the derivative terms in the boundary equations as shown in Equations (3.7) to (3.10) which would be discretized as well. The result of them has been shown in Table 3.4.

Table 3.3 The approximation of derivative terms in mathematical model.

Derivative terms	Approximation/discretion	Comments
1. in mass matrix, $M(t, y)$		
1.1 $\frac{\partial \rho_{da}}{\partial T}$	$\frac{\rho_{da}(T + dT) - \rho_{da}(T - dT)}{2dT}$	Terms no.1 to 3 were approximated by central difference of 1 st derivative.
1.2 $\left(\frac{\partial M}{\partial T}\right)_Y$	$\frac{M(T + dT, Y) - M(T - dT, Y)}{2dT}$	
1.3 $\left(\frac{\partial M}{\partial Y}\right)_T$	$\frac{M(T, Y + dY) - M(T, Y - dY)}{2dY}$	
2. in function, $f(t, y)$		
2.1 $\frac{\partial T}{\partial r}$	$\frac{T_{i+1} - T_{i-1}}{2dr}$	The subscript i appears in the equation which indicates the index of node.
2.2 $\frac{\partial Y}{\partial r}$	$\frac{Y_{i+1} - Y_{i-1}}{2dr}$	
2.3 $\frac{\partial h_v}{\partial r}$	$\frac{h_{v,i+1} - h_{v,i-1}}{2dr}$	The first 5 terms were approximated by central difference of 1 st derivative while the last 3 terms were approximated by central difference 2 nd derivative.
2.4 $\frac{\partial \rho_{da}}{\partial r}$	$\frac{\rho_{da,i+1} - \rho_{da,i-1}}{2dr}$	
2.5 $\frac{\partial D_{eff}}{\partial r}$	$\frac{D_{eff,i+1} - D_{eff,i-1}}{2dr}$	
2.6 $\frac{\partial^2 T}{\partial r^2}$	$\frac{T_{i+1} - 2T_i + T_{i-1}}{dr^2}$	
2.7 $\frac{\partial^2 Y}{\partial r^2}$	$\frac{Y_{i+1} - 2Y_i + Y_{i-1}}{dr^2}$	
2.8 $\frac{\partial^2 \rho_{da}}{\partial r^2}$	$\frac{\rho_{da,i+1} - 2\rho_{da,i} + \rho_{da,i-1}}{dr^2}$	

Table 3.4 The discretion of derivative terms in boundary condition

Boundary condition	Discretion
at $r = 0$	
1. $-D_{eff} \frac{\partial(Y\rho_{da})}{\partial r} \Big _{r=0} = 0$	$-D_{eff} \left[\frac{-3(Y\rho_{da})_0 + 4(Y\rho_{da})_{dR} - (Y\rho_{da})_{2dR}}{2dR} \right] = 0$
2. $-k_{eff} \frac{\partial T}{\partial r} \Big _{r=0} = 0$	$-k_{eff} \left[\frac{-3T_0 + 4T_{dR} - T_{2dR}}{2dR} \right] = 0$
at $r = R$	
3. $-D_{eff} \frac{\partial(Y\rho_{da})}{\partial r} \Big _{r=R} = 0$	$-D_{eff} \left[\frac{(Y\rho_{da})_{R-2dR} - 4(Y\rho_{da})_{R-dR} + 3(Y\rho_{da})_R}{2dR} \right] = 0$
4. $-k_{eff} \frac{\partial T}{\partial r} \Big _{r=R} = h(T_{outside} - T_{r=R})$	$-k_{eff} \left[\frac{T_{R-2dR} - 4T_{R-dR} + 3T_R}{2dR} \right] = h(T_{outside} - T_{r=R})$

3.3.3 Determining the Number of Node

By solving the PDEs using numerical method of lines, the spatial derivative (r-direction for this work) must be discretized into many nodes. The number of nodes has directly affected the numerical result via the truncation error; if we use the number of nodes not high enough, the large error would happen. In contrast, the large number of nodes it would load calculation on computer and require longer CPU time. Consequently, the suitable number of nodes is important in numerical analysis by numerical methods of lines. It was determined by comparing the numerical result with different number of nodes, including 10, 20 and 40 nodes ($\Delta r = 0.0454, 0.0238, 0.0122$ m.), and the experimental data available from Leaper and co-workers (2001).

3.4 Model Validation

The mathematical modeling was validated by comparing temperature distribution with the experimental data reported in Leaper et al. (2001) and Wang and coworkers' numerical results (Wang et al. 2004). Both works studied the moisture migration in a big bag by giving the initial temperature inside the big bag at 18°C and 0.068% of moisture content and then increasing and keeping the outside temperature to 40°C. These results show in Figure 3.4.

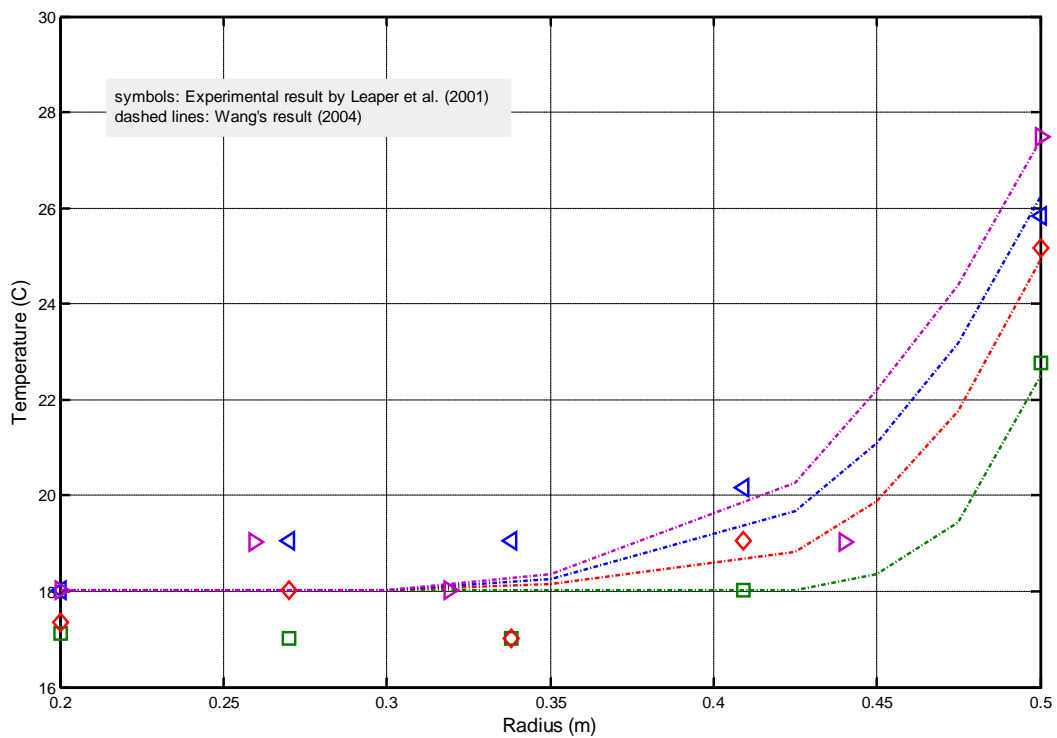


Figure 3.4 The results of temperature distribution by experimental data of Leaper et al (2001) and Wang and coworkers' numerical results (2004), (green: 1hrs, red: 2 hrs, blue: 3 hrs, purple: 4 hrs).

3.5 Conditions of Model Prediction

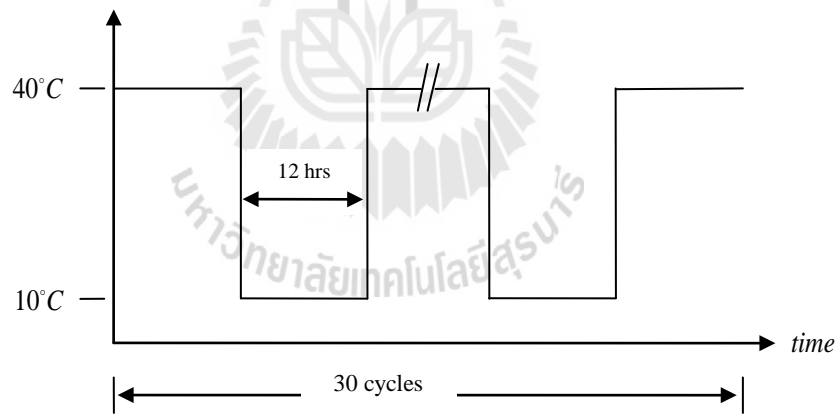
The condition of this study was divided into two major effects, including the effects of initial conditions and sorption isotherms. The outside temperature was assigned in square wave form which oscillates between 40 and 10°C as shown on Figure 3.5, which we used it to be an agent representing the temperature change during shipping; 40 and 10°C is a temperature average in daytime and nighttime, respectively,

In initial moisture content, it was divided two conditions coupled with temperature. They are the low and high initial moisture contents; $M_0=0.015\%$, $T_0=30^\circ\text{C}$ and $M_0=0.040\%$, $T_0=40^\circ\text{C}$. The both conditions based on the real observation by a Thai sugar factory, the first is condition after conditioning process and the second is condition before conditioning process (or after drying process), they found that the sugar caked would not occur in the first condition but would occur in the second condition. Therefore, both conditions were chosen in this study.

In sorption isotherm, all researchers who study moisture migration in the past only used the adsorption isotherm in calculating their mathematical model although Leaper and coworkers' research (2002) show that there is hysteresis of sugar in ranging 10 to 40°C. As a result, the hysteresis had been included in this study which would help us understand the underline mechanism better.

Table 3.5 Conditions of this study.

Effect of initial condition	Effect of sorption isotherm
1. $M_0=0.040\%$, $T_0=40^\circ\text{C}$ (High initial moisture content)	1. Adsorption isotherm (only)
	2. Desorption isotherm (only)
	3. Hysteresis
2. $M_0=0.015\%$, $T_0=30^\circ\text{C}$ (Low initial moisture content)	1. Adsorption isotherm (only)
	2. Desorption isotherm (only)
	3. Hysteresis

**Figure 3.5** Fluctuation of temperature in cyclic form.

3.6 Sensitivity Analysis

The parameters used in the mathematical model generally have the uncertainty which comes from either the error of measurement or estimated parameters from experimental data. There is the limit on our confidence of these parameters and their effects on the numerical results. Consequently, the investigation of impact of those parameters to the numerical results is necessary.

In this study, we have selected three parameters from Table 3.1, including k_s , ε and k_a because these three parameters have high uncertainties and the effect of moisture content of sugar on these three parameters are obvious. The sensitivity was performed on the high initial moisture content condition using adsorption isotherm line. Each parameter of those would be varied $\pm 10\%$ of normal value, while other parameters are kept constant.

Table 3.6 The values used to analyze the sensitivity

parameter	Value	-10%	+10%
k_s [J/m s °C]	0.208	0.1872	0.2288
ε [-]	0.365	0.3285	0.4015
k_a [W/m °C]	0.0187	0.0168	0.0206

It should be noted that the sensitivity analysis generally consists of two levels; local and global. The first level which we used in our work is normally fairly accurate in the case that expected uncertainty is small. In contrast, the latter will be used in the large uncertainty case.

CHAPTER IV

RESULTS AND DISCUSSIONS

4.1 Result of Sorption Isotherm Fitting

Table 4.1 shows the result of parameters fitting on both adsorption and desorption isotherm sorption by using GAB-T model. This model can describe the experimental data of both adsorption and desorption very well because SSE is lower than 3.2×10^{-4} . Considering at Figure 4.1, we saw that the GAB-T model is better than the model proposed by Leaper et al. (2002) in describing the experimental data. However, the result of this model still had its weakness at a_w is less than 0.05 and is greater than 0.70 and it can be seen that there are differences in results of model and experiment, particularly at $a_w < 0.05$ and 40°C . The reason of these differences is mainly the lack of reliable experimental data in this range. In addition, the adsorption and desorption isotherm should be convergent together in ranging $a_w = 0.7$ but it does not occur here because few reliable experimental results are not available.

Table 4.1 Parameters of sorption isotherm in GAB-T equation.

	M'_0	C'	k'	$\Delta H/(RT)$	$(H_i-H_m)/(RT)$	$(H_i-H_a)/(RT)$	SSE
Adsorption	9.16×10^{-2}	5.53×10^{22}	1.20×10^2	3.70×10^2	-1.51×10^4	-1.50×10^2	3.12×10^{-4}
Desorption	1.83×10^{-2}	1.07×10^{24}	8.26×10^2	9.20×10^2	-1.52×10^4	-2.12×10^2	2.93×10^{-4}

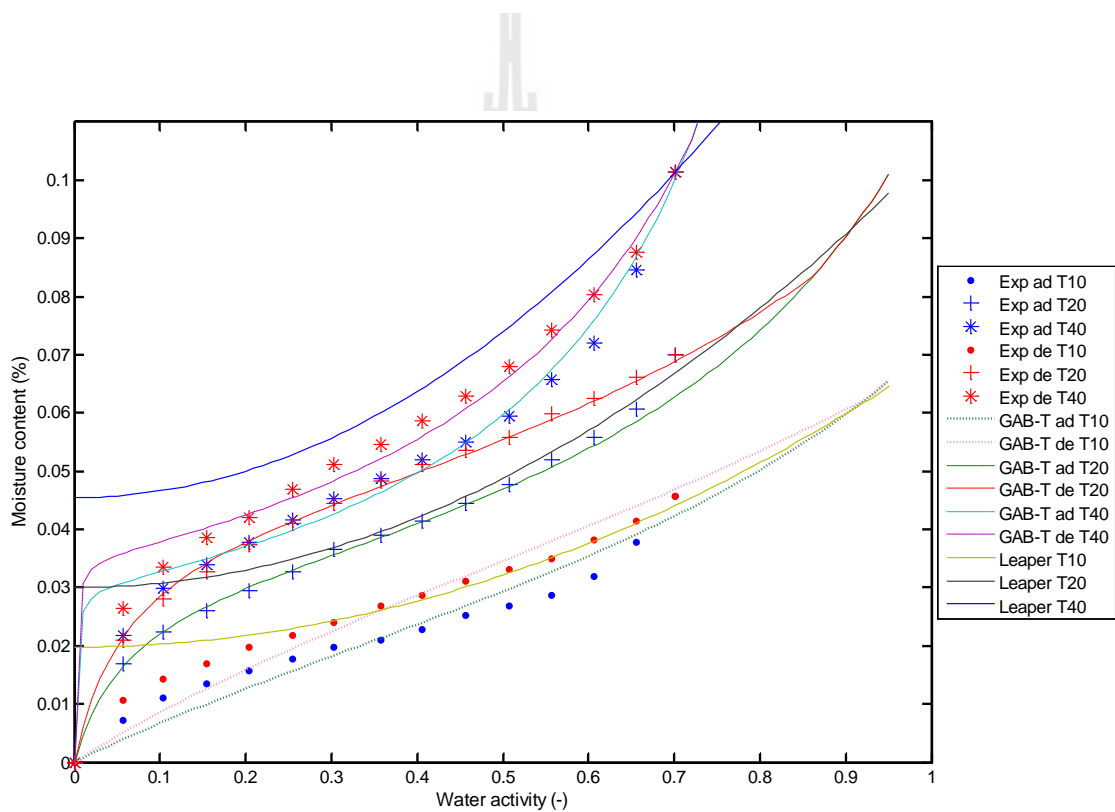


Figure 4.1 Comparison sorption isotherm of sucrose, including experimental data by Leaper et al. (2002), empirical equation by Leaper et al. (2002), and GAB-T equation.

4.2 Result of Determining the Number of Node

Figure 4.2 shows the comparison of numerical result with different number of nodes, including 10, 20, and 40 nodes ($\Delta r=0.0454, 0.0238, 0.0122$ m.), and the experimental data available from Leaper and co-workers (2001). We obviously found that the numerical results of 20 and 40 nodes are very close to each other while the numerical result of 10 nodes is far from those results as shown in Figure 4.2. Therefore, 20 nodes would be chosen and used throughout this thesis. The comparison of experimental data and numerical solution would be presented in the next section.



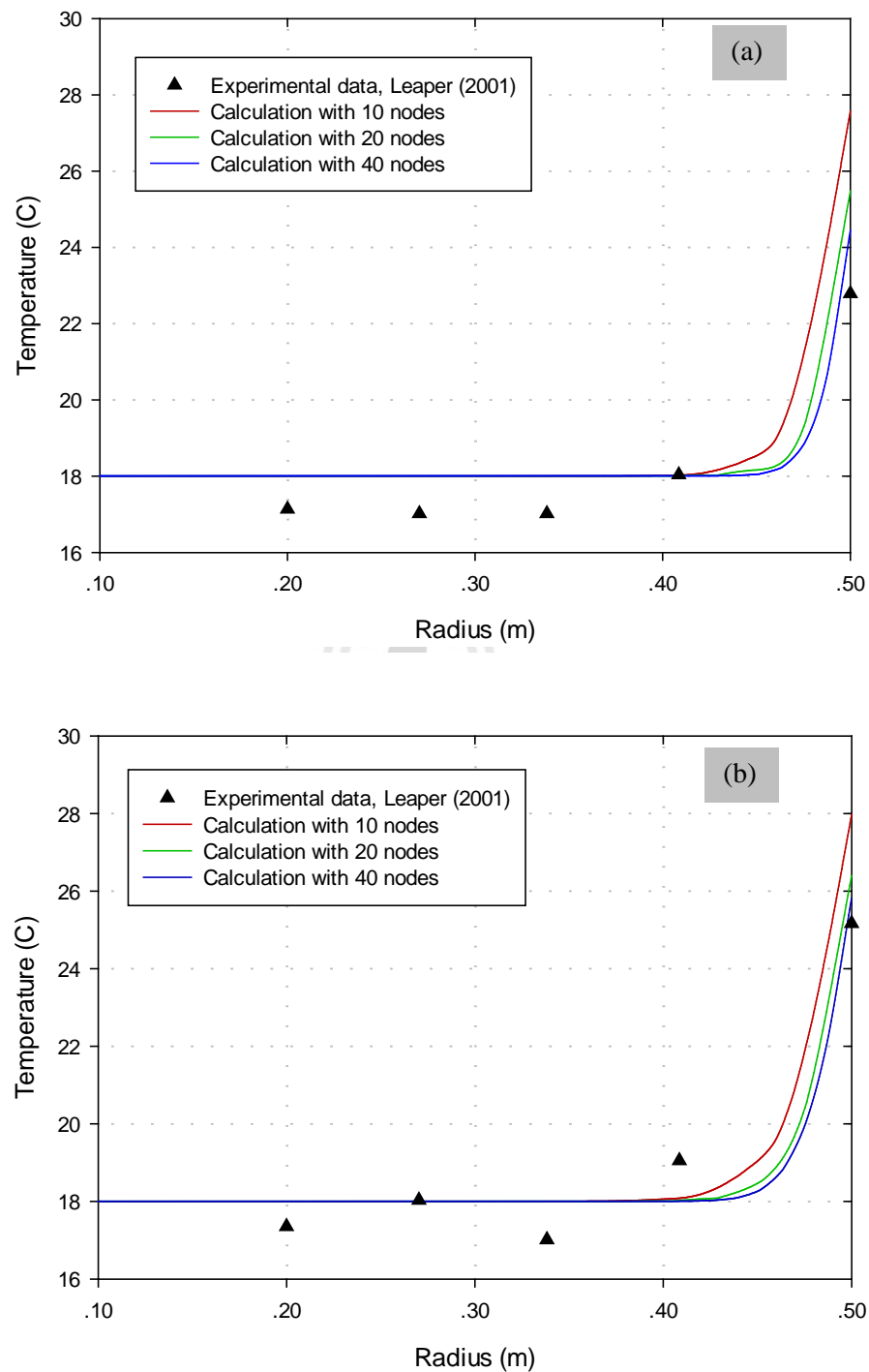


Figure 4.2 The comparison of temperature profiles in a big bag of each different number of node when $M_0=0.068\%$ and $T_0=18^\circ\text{C}$ and keeping $T_{\text{out}}=40^\circ\text{C}$, (a) is at 1 hour, (b) is at 2 hours.

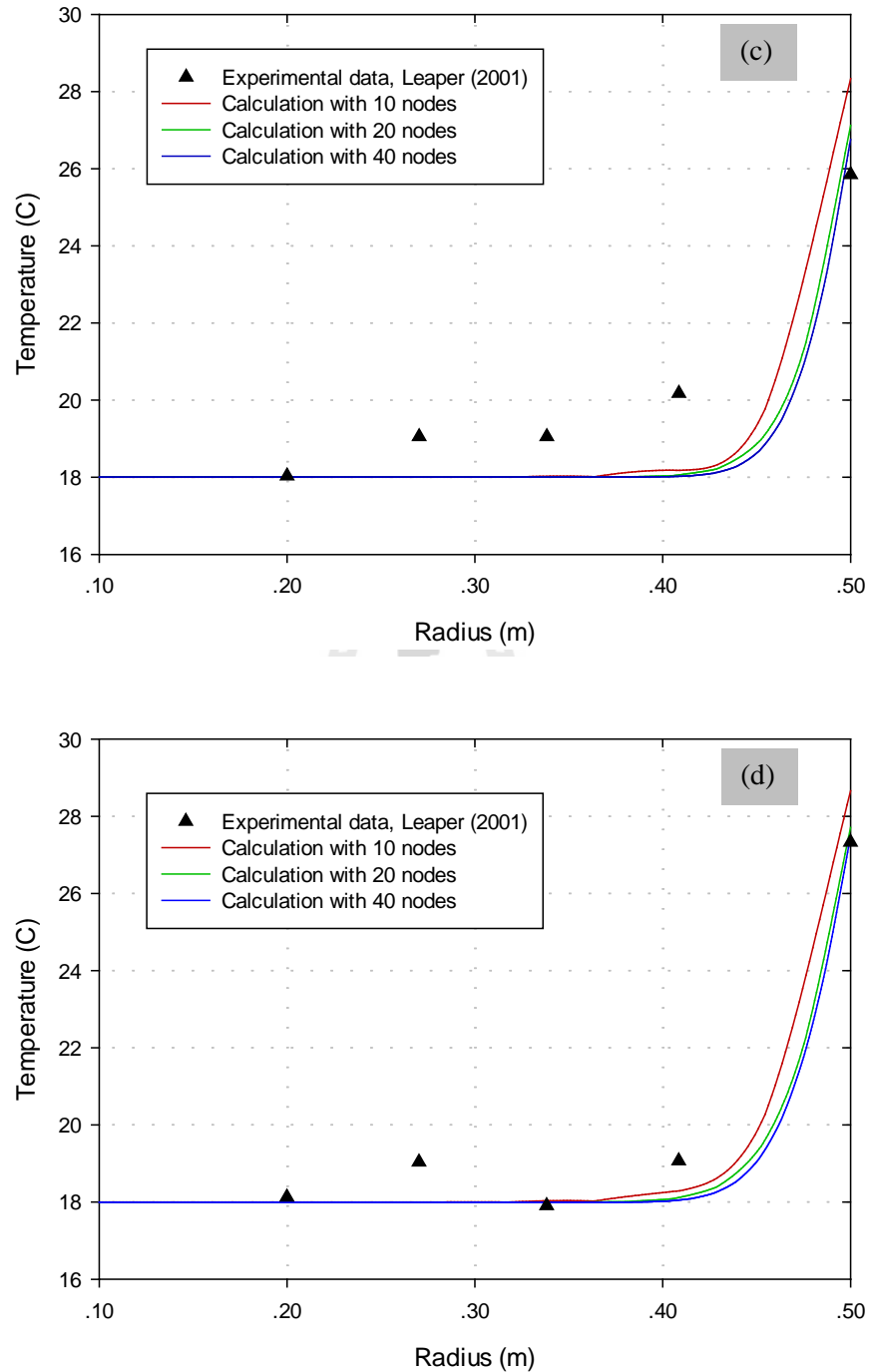


Figure 4.2 The comparison of temperature profiles in a big bag of each different number of node when $M_0=0.068\%$ and $T_0=18^\circ\text{C}$ and keeping $T_{\text{out}}=40^\circ\text{C}$, (c) is at 3 hour, (d) is at 4 hours (Continued).

4.3 Result of Model Validation

Figure 4.3a shows the comparison of temperature profiles from 1 to 4 hours. The numerical results performed in this article generally agreed with both the results of Leaper et al. (2001), especially at $r = 0.5$ m. At 1 hour, the predicted temperature in this article was quite different from the data of Wang et al (2004) and the experimental results; this difference was probably the cause from the steady state assumption of the polyethylene big bag of the mathematical model. For other cases, the deviations of the predicted temperature from the data of experiment were less than 2°C , which was within the experimental errors reported by Leaper et al. (2001).

Figure 4.3b shows the comparison of temperature profile at 4 hour as reported by Leaper et al. (2001). It obviously shows that the numerical results of this article agree with experiment data very well at this time and is better correlated with the experimental result than those of Wang and coworkers.

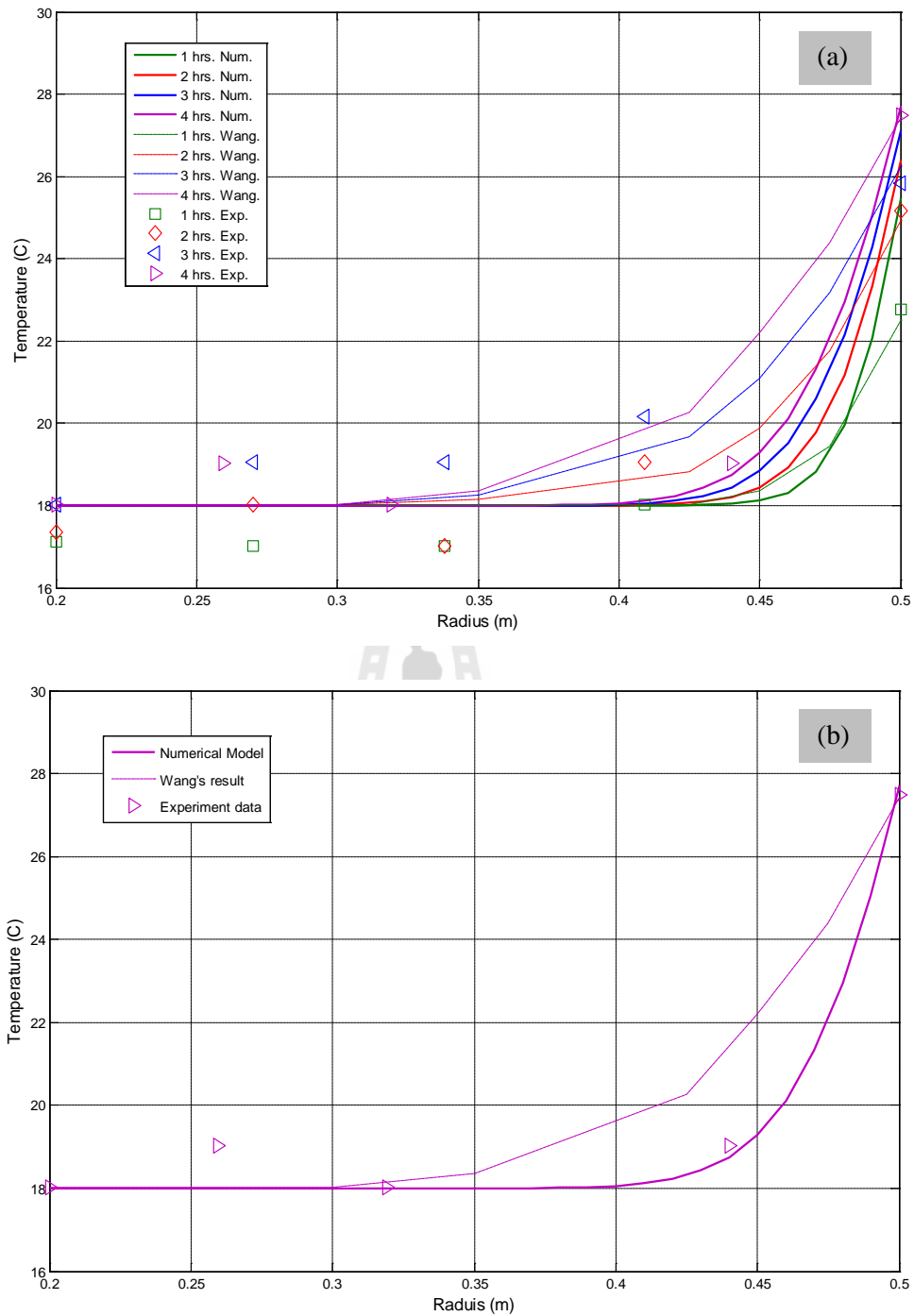


Figure 4.3 Comparison temperature profiles of between experimental data (Leaper et al., 2001), Wang et al. (2004)'s results, and numerical results at 18°C of initial temperature and increasing the outside temperature to 40°C (a) between 1 to 4 hours, (b) at 4 hours.

4.4 Model Prediction Results

The result of model prediction was considered in two views; short term and long term predictions because the view of short term prediction can tell us what happened when the outside temperature changes while the long term prediction can tell us what happened throughout thirty days. The variables monitored are the temperature, absolute humidity, and moisture content of sugar within the big bag.

The computer took 3 minutes for simulating time of 720 hours in the cases of Adsorption and Desorption by using 10 sec of time step, and 40 minutes in the case of Hysteresis by 1000 sec of time step.

4.4.1 Short Term View

For convenience in analyze, the diagram of moisture migration for the short term was prepared based on the data of temperature, absolute humidity, and moisture content profiles; thus, these profiles are not presented in this section but are presented in Appendix D.

4.4.1.1 Results of Calculation by Adsorption Isotherm

These figures below show the schematic diagram moisture migration calculated by adsorption isotherm curve for the cases of high initial moisture content (i.e. Figures 4.4 to 4.6) and low initial moisture content (i.e. Figures 4.7 to 4.9);

Figure 4.4 shows the case of high initial moisture content in period 0 to 12 hrs. The outside temperature is 40°C. It can be seen that there are no occurring adsorption, desorption, and moisture migration because the outside temperature which is disturbance variable is the same as the initial temperature.

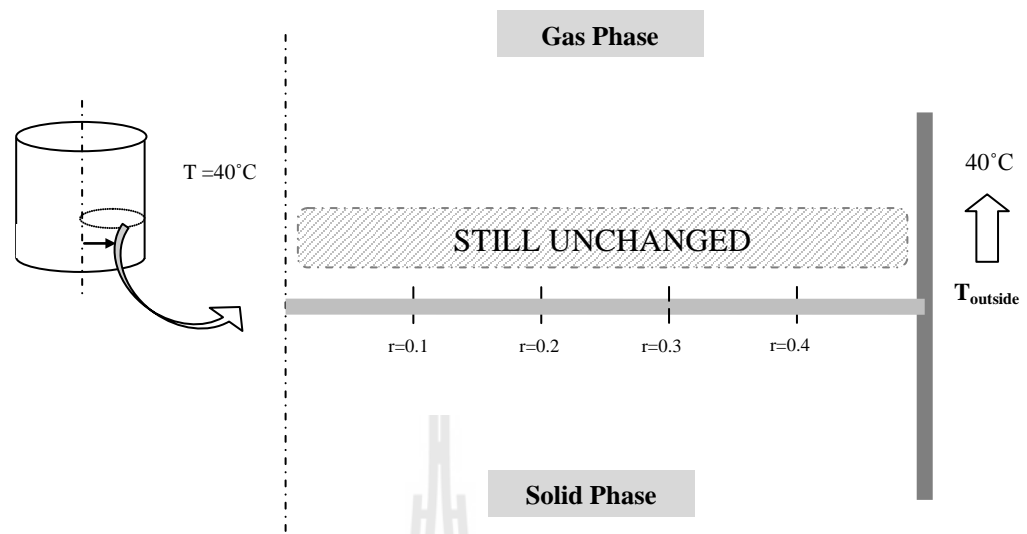


Figure 4.4 Schematic diagram of moisture migration for high initial moisture content using adsorption isotherm in period of 0-12 hrs.

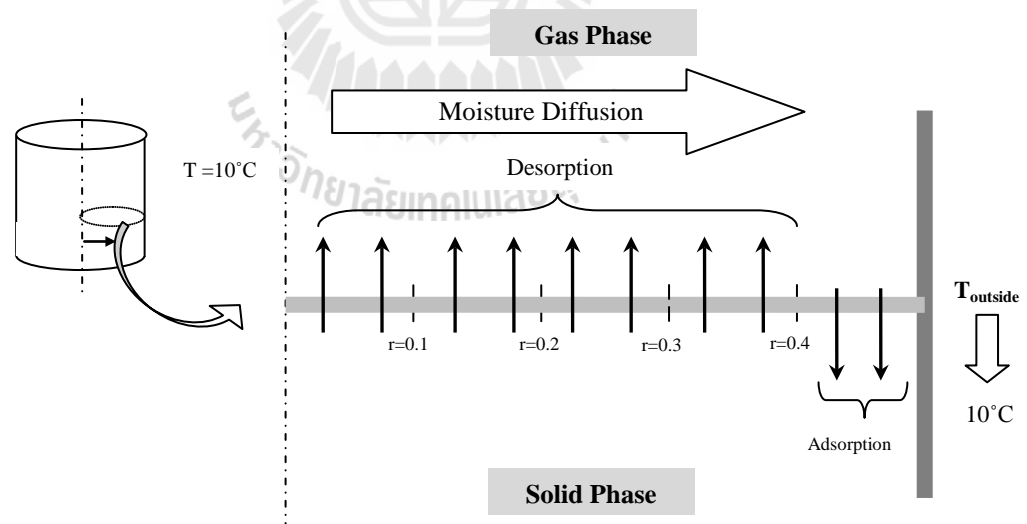


Figure 4.5 Schematic diagram of moisture migration for high initial moisture content using adsorption isotherm in period of 15-24 hrs.

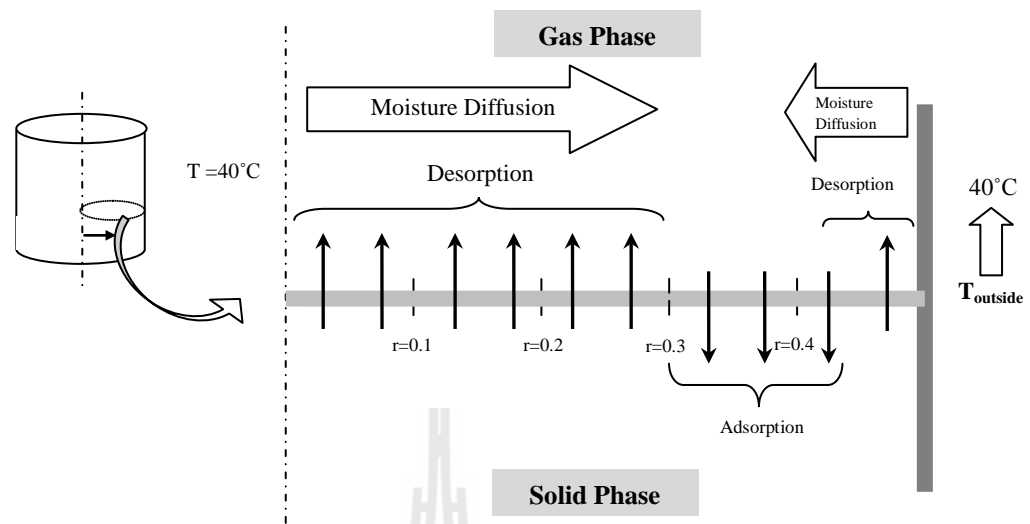


Figure 4.6 Schematic diagram of moisture migration for high initial moisture content using adsorption isotherm in period of 27-36 hrs.

Figure 4.5 shows the case of high initial moisture content in period of 15 to 24 hrs. The outside temperature immediately decreases and keeps constant at 1°C . It can be seen that there are moisture adsorption, moisture desorption, and moisture migration. The reason is the decreasing of outside temperature that leads to the decreasing of temperature near interface. This change leads to an increase in the relative humidity in that region (i.e. $r \approx 0.4$ to 0.5 m.) and moisture was then adsorbed onto surface of sugar grain. Subsequently, moisture gradient in gas phase will arise and moisture diffuses from core region towards interface region while moisture in gas and solid phases (i.e. $r \approx 0.0$ to 0.4 m.) has to retain the new equilibrium by desorbing moisture out to gas phase.

Figure 4.6 shows the case of high initial moisture content in period of 27 to 36 hrs. The outside temperature increases back and keeps at 40°C . It

can be seen as follows; there is the moisture desorption near interface (i.e. ≈ 0.45 to 0.5 m.) because temperature at that region increases which results in decreasing relative humidity. Thus, an amount of moisture in gas phase increased and moisture then diffused toward the core. After that, moisture was adsorbed onto surface of sugar grain in ranging from 0.3 to 0.45 meters of radius. Also, there are moisture diffusion from core toward interface along with moisture desorption in ranging from 0.0 to 0.30 meters of radius, this effect comes from previous period.

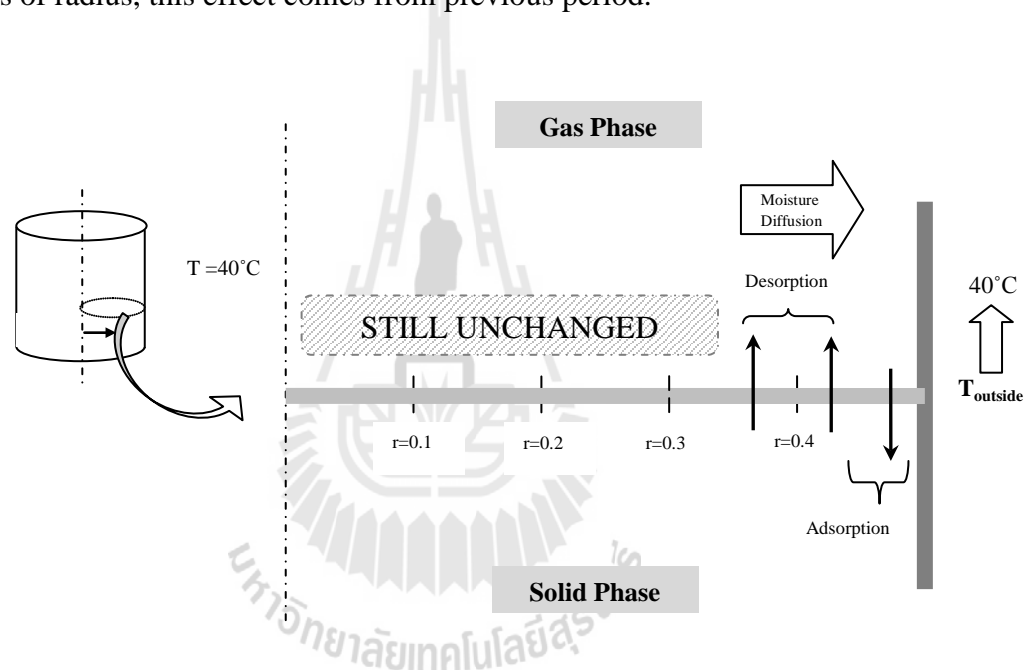


Figure 4.7 Schematic diagram of moisture migration for low initial moisture content using adsorption isotherm in period of 0-12 hrs.

Figure 4.7 shows the case of low initial moisture content in period from 0 to 12 hrs. The outside temperature increases and keeps constant at 40°C . It can be seen that there are moisture adsorption in approximately ranging from 0.45 to 0.50 meters of radius, moisture desorption in approximately ranging from 0.36 to 0.44 meters of radius, and moisture diffusion, over range of moisture desorption,

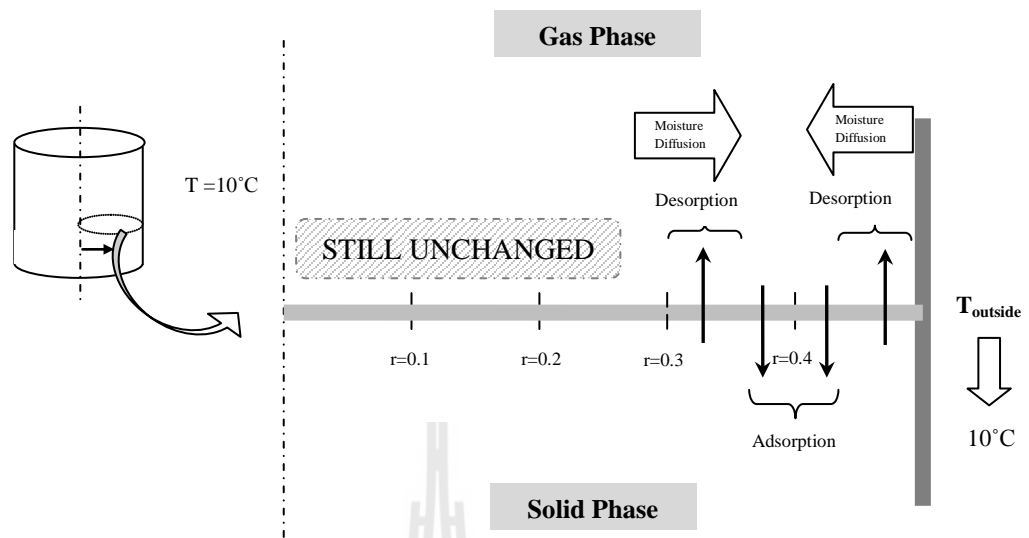


Figure 4.8 Schematic diagram of moisture migration for low initial moisture content using adsorption isotherm in period of 15-24 hrs.

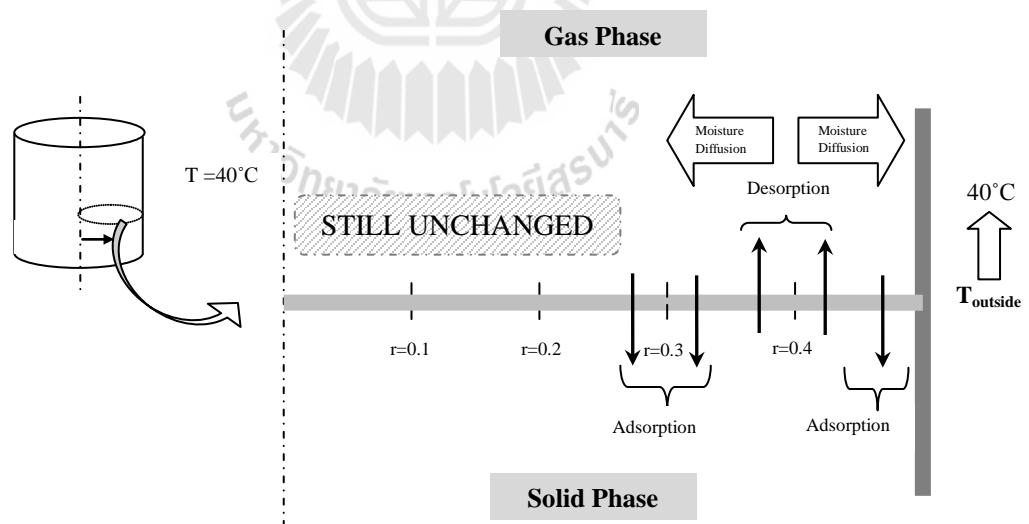


Figure 4.9 Schematic diagram of moisture migration for low initial moisture content using adsorption isotherm in period of 27-36 hrs.

toward interface. It should be noted that the moisture desorption near interface takes place when the outside temperature decreases, which is different from the case of high initial moisture content. This difference is caused by the characteristic of sorption isotherm that its derivative of moisture content by temperature gives negative number at a little amount of absolute humidity, and positive at a large amount of absolute humidity (see Appendix E).

Figure 4.8 shows the case of low initial moisture content in period of 15 to 24 hrs. The outside temperature increases and keeps constant at 10°C. It can be seen that there are moisture desorption near interface and in approximately ranging from 0.30 to 0.35 meters of radius, moisture adsorption in approximately ranging 0.35 to 0.45 meters of radius, moisture diffusion in gas phase from over both ranges of desorption into adsorption region.

Figure 4.9 shows the case of low initial moisture content in period 27 to 36 hrs. The outside temperature increases back and keeps constant at 40°C. It can be observed that the places of adsorption and desorption are swapped from the previous period. The other interesting observation is the range of disturbance increases with time; for example, 0.15 meters from interface in first 12 hours and 0.20 meters from interface in first 24 hours. Moreover, in comparison of the low initial moisture content and high initial moisture content, it can be found that the moisture in the case of high initial moisture was disturbed in the wider region.

4.4.1.2 Results of Calculation by Desorption Isotherm

The schematic diagram for the case calculated by using desorption isotherm is similar to the case calculated by using adsorption isotherm. However, if we consider the profiles of temperature, absolute humidity, and moisture content of this analysis, the following observations are found: (i) The initial absolute humidity calculated by adsorption isotherm line ($Y_0=0.0118$, 0.00023 kg/kg for high and low initial moisture content) is greater than the other ($Y_0=0.0067$, 0.000145 kg/kg for high and low initial moisture content) because the desorption sorption line, in fact, always gives the lower water activity (or absolute humidity) than adsorption isotherm line at the same temperature and moisture content. (ii) The amplitude calculated with adsorption isotherm line is higher than the other. It should be noted that the total amount of initial moisture content of between two cases are not significantly different a lot; namely, 0.4265 , 0.4244 kg/kg-node for the case of high initial moisture content that was calculated by adsorption and desorption isotherm lines respectively, while the case of low initial moisture is the same amount of moisture (i.e. 0.4244 kg/kg-node for both adsorption and desorption isotherm lines).

4.4.2 Long Term View

Figure 4.10 shows the numerical result throughout 720 hours of high initial moisture content with using adsorption isotherm. It can be seen that the profiles of temperature, absolute humidity, and moisture content near interface are highly oscillated as followed the outside temperature and gradually decreased away from interface. It is found that the shape of temperature profile decreases with time and also tends to the converged to 25°C which is the temperature average of outside temperature. For the absolute humidity, the shape of profile tends to decrease with

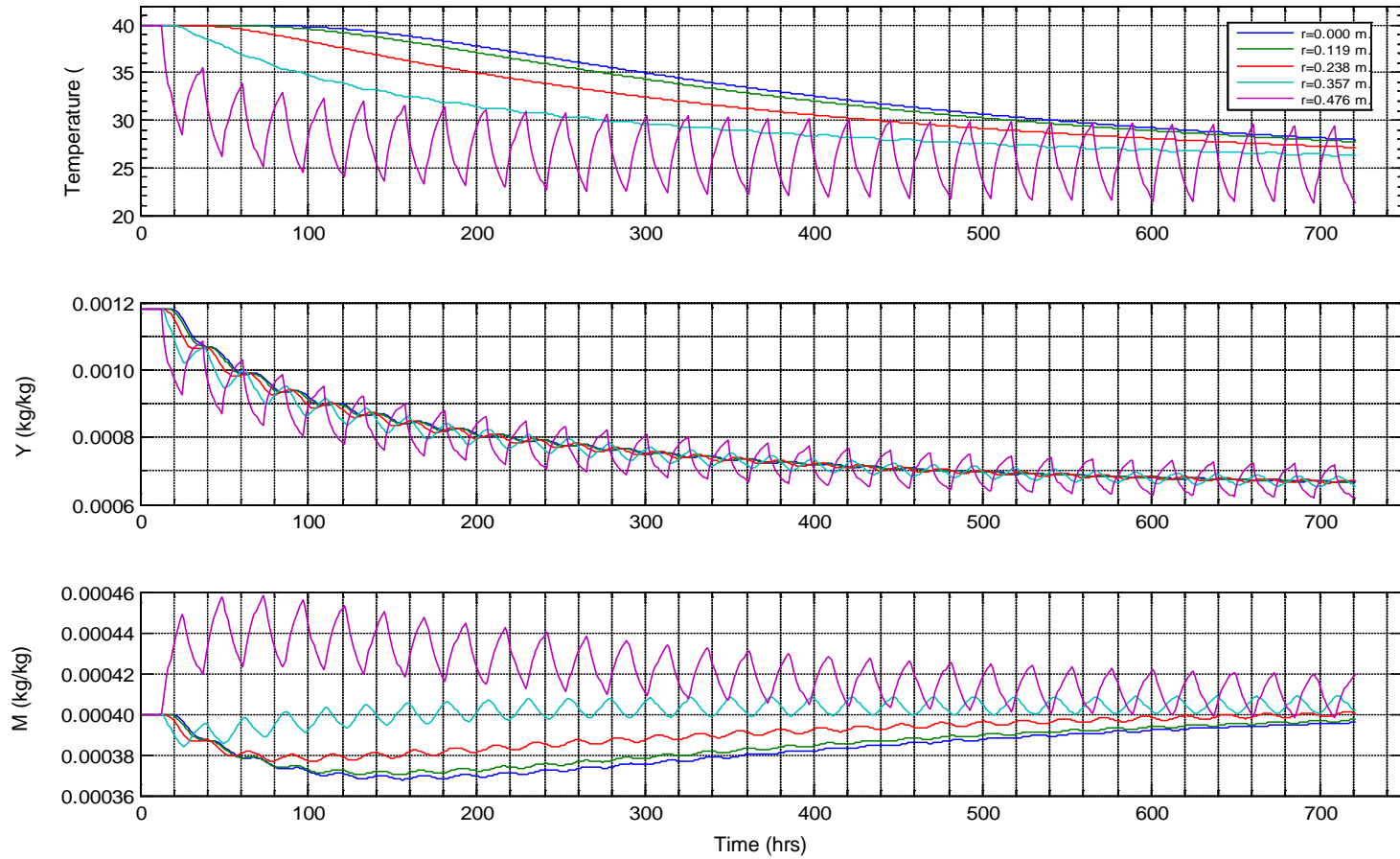


Figure 4.10 Numerical results throughout 720 hrs for *high* initial moisture content with *adsorption isotherm*.

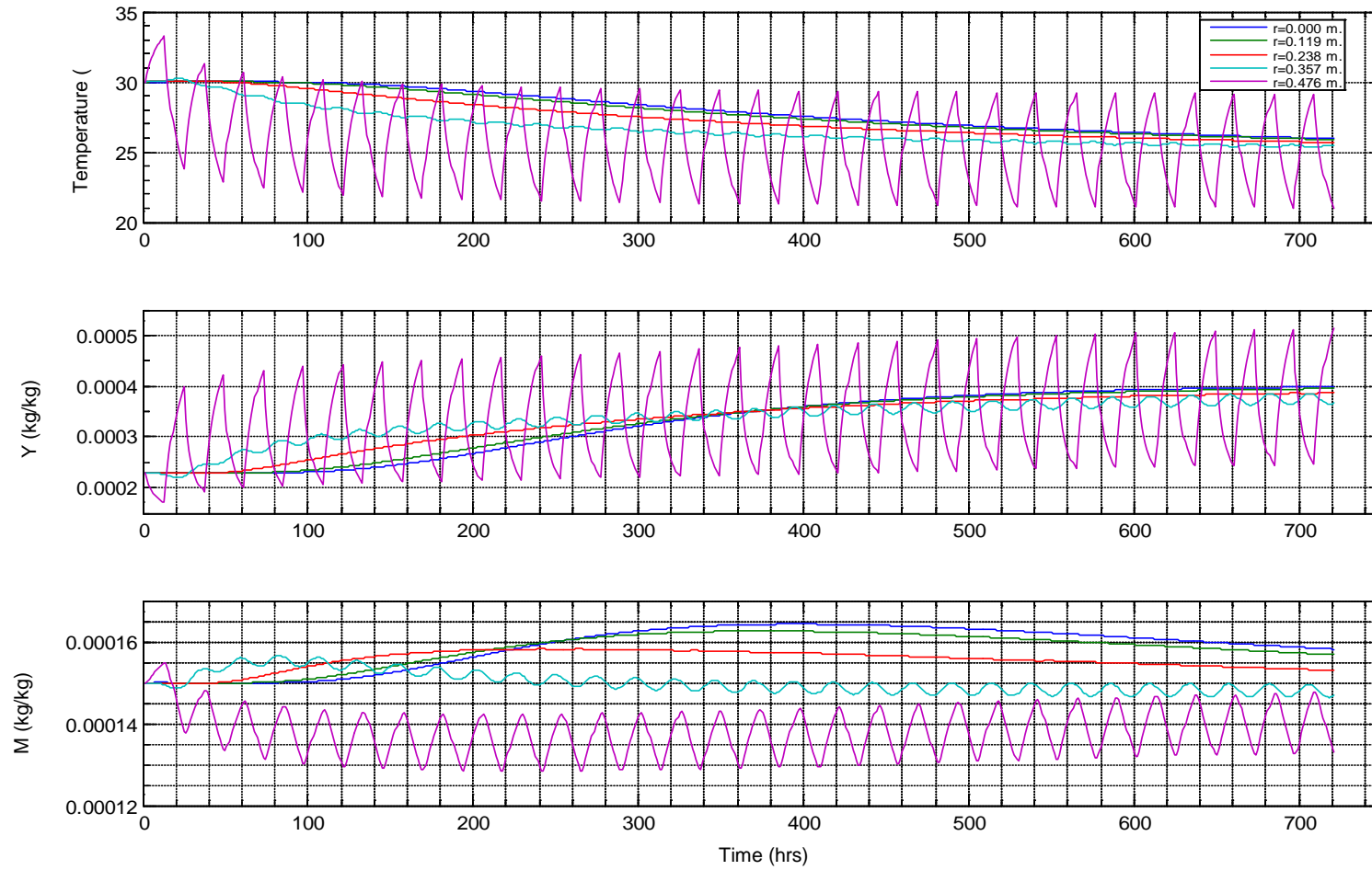


Figure 4.11 Numerical results throughout 720 hrs for *low* initial moisture content with *adsorption isotherm*.

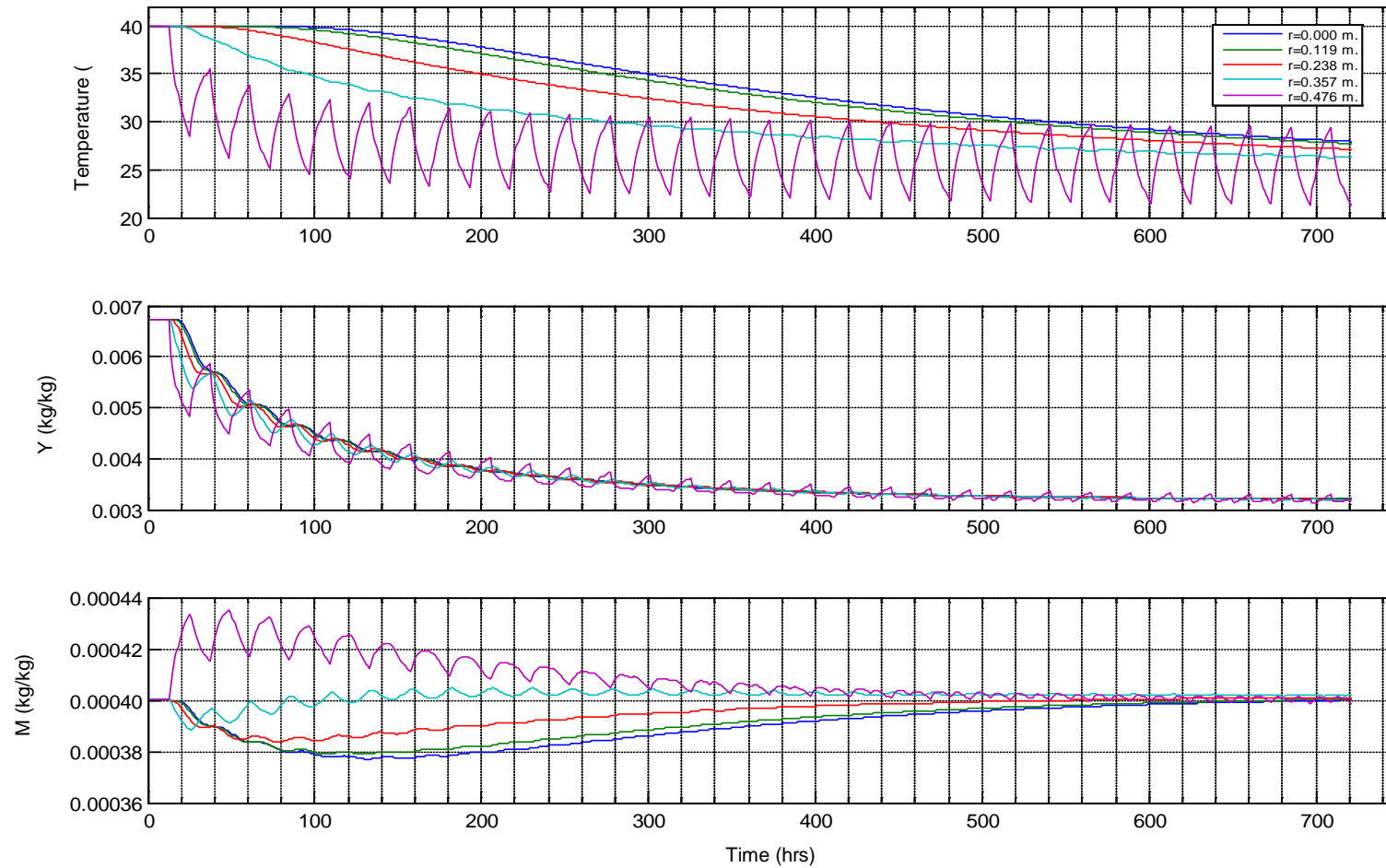


Figure 4.12 Dynamics of numerical result of first 36 hrs for *high* initial moisture content with *desorption isotherm*.

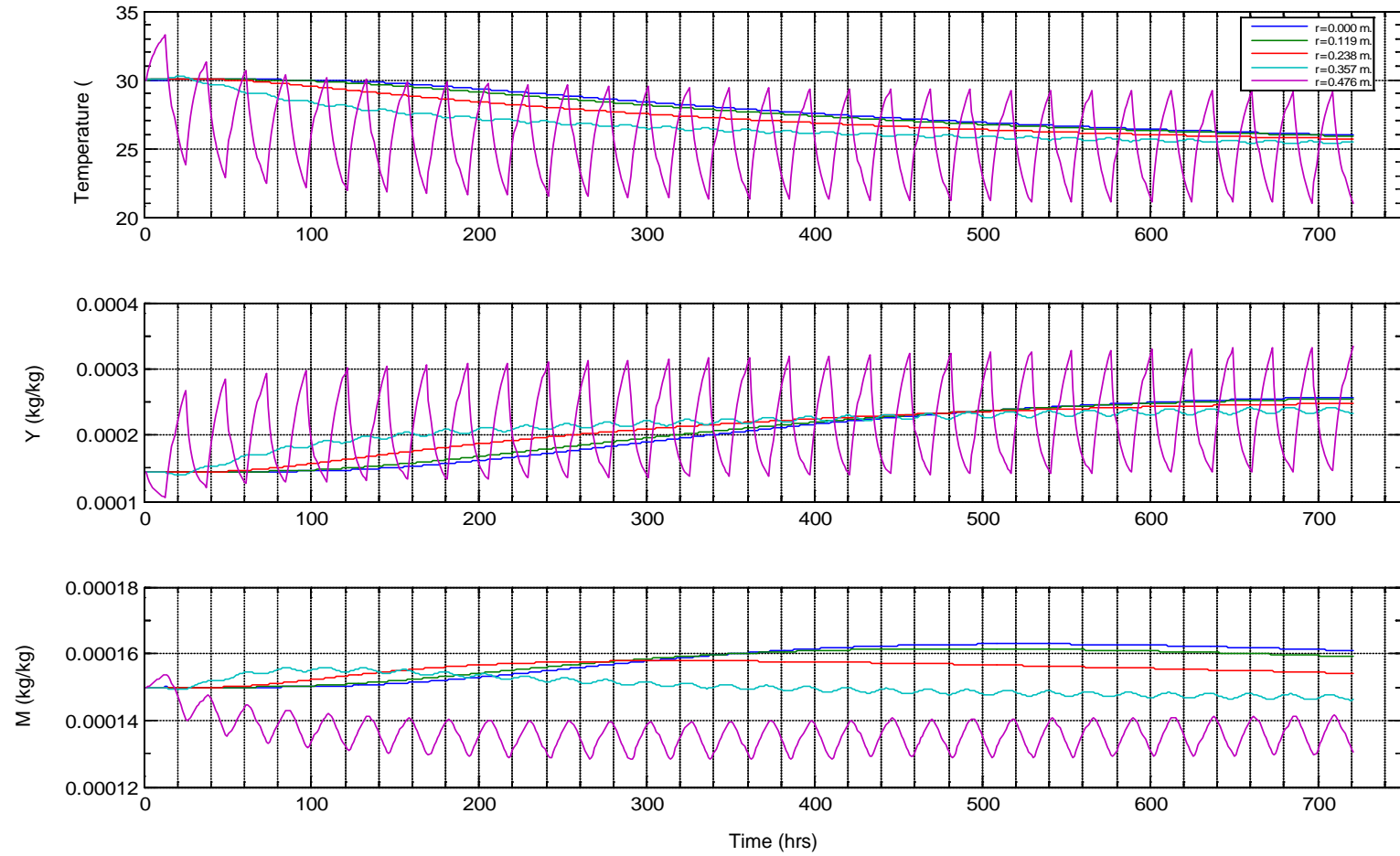


Figure 4.13 Numerical result throughout 720 hrs for *low* initial moisture content with *desorption isotherm*.

time as similar the temperature profile. It means that the amount of moisture in gas phase would decrease after 720 hours. Regarding on the moisture content, we have seen that the moisture content increases near the interface region but decreases at the core region in the first 100 hours. After that, the moisture content near interface decreases while the moisture content in the core region increases until 720 hours. The significance of this result is that the increasing of moisture content near the interface is the greatest throughout the big bag; hence, it implies that there would be the accumulation of moisture and; hence, the caking in this region.

Figure 4.11 shows the numerical result throughout 720 hours of low initial moisture content with using adsorption isotherm. The profiles of temperature, absolute humidity, and moisture content near interface are highly oscillated and gradually decreased with distance from interface as well as the case of high initial moisture content, especially on the temperature profile at the initial temperature of 30°C. For the absolute humidity, we observed that the absolute humidity profile of all of nodes increases with time. This indicates that there is increasing of amount of moisture in gas phase. Regarding on the moisture content, it can be seen that the moisture content near the core increases while the moisture content near interface decreases. However, the changing of moisture content of this case is insignificant because the increasing amount of moisture is quite small when compared to the high initial moisture content; hence, the risk of caking for this condition is less than the previous cases.

Figures 4.12 and 4.13 show the numerical result with using desorption isotherm for high and low initial moisture content. When comparing both cases with calculation of adsorption isotherm, it was found that the overall trend and shape of the

graph of these cases were similar to the case of adsorption isotherm, but the amplitudes of moisture content fluctuation calculated was smaller than those of adsorption isotherm.

4.4.3 Hysteresis

Figures 4.14 to 4.19 show the numerical result with hysteresis calculation for low and high initial moisture content. We observe that temperature profiles of both high and low initial moisture content of this case are not significantly different from the prediction by either adsorption isotherm line or desorption isotherm line. For absolute humidity, we have seen the black tab appearing on absolute humidity profile of all five positions in both low and high initial conditions. This tab occurs from the oscillation of absolute humidity that it was set to be the parameter shifting between curves of adsorption and desorption as in the scanning curve technique. It should be noted that this can also be seen in the profile of moisture content at the core. Consequently, it means that there is suddenly shifting or jumping moisture content around that region. As a result, this is the drawback of scanning curve technique used in this thesis. Furthermore, when comparing the results of this case with adsorption and desorption isotherm, we found that the shape and trend of the profiles of absolute humidity and moisture content is approximately equivalent from the average of adsorption and desorption isotherms.

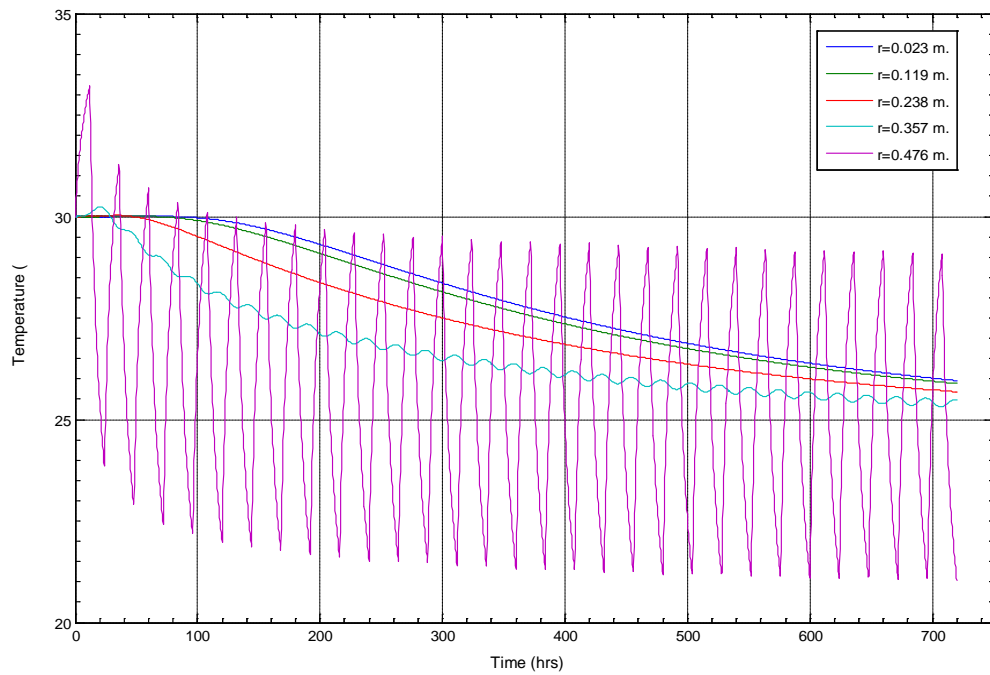


Figure 4.14 The temperature profile at different node which calculated using hysteresis isotherm for low initial moisture content

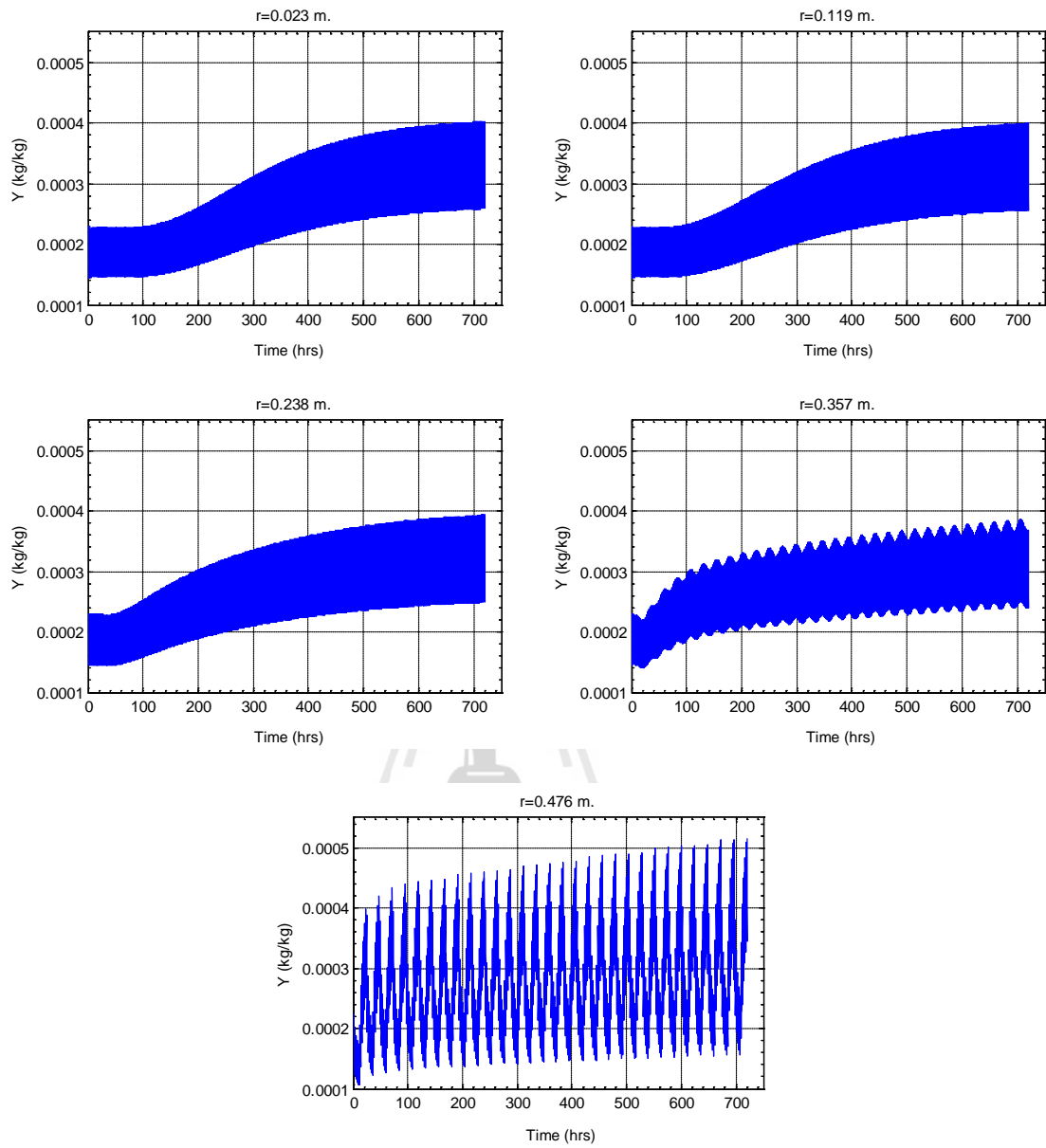


Figure 4.15 The absolute humidity profile of each node which calculated using hysteresis isotherm for low initial moisture content

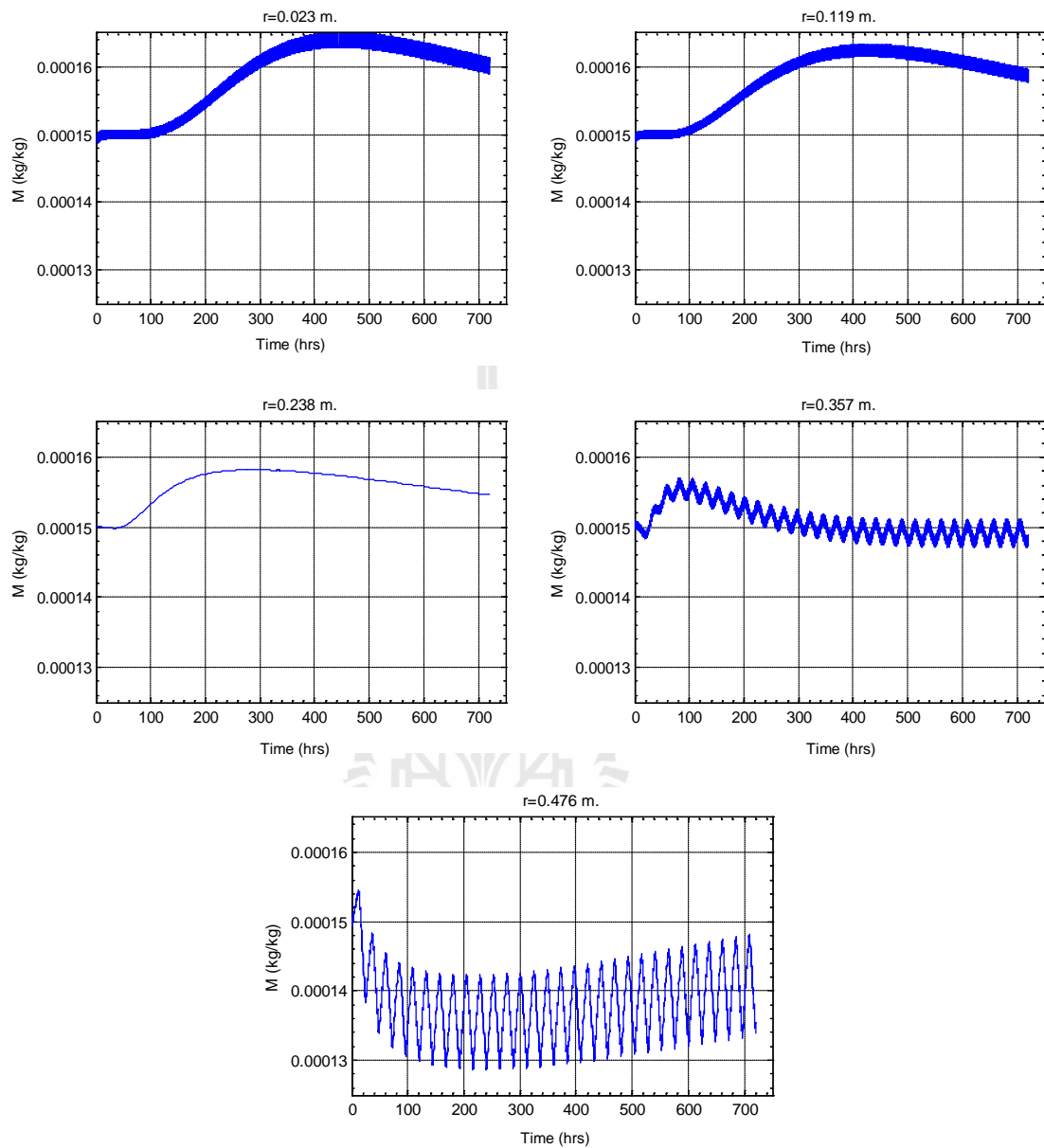


Figure 4.16 The moisture content profile of each node which calculated using hysteresis isotherm for low initial moisture content.

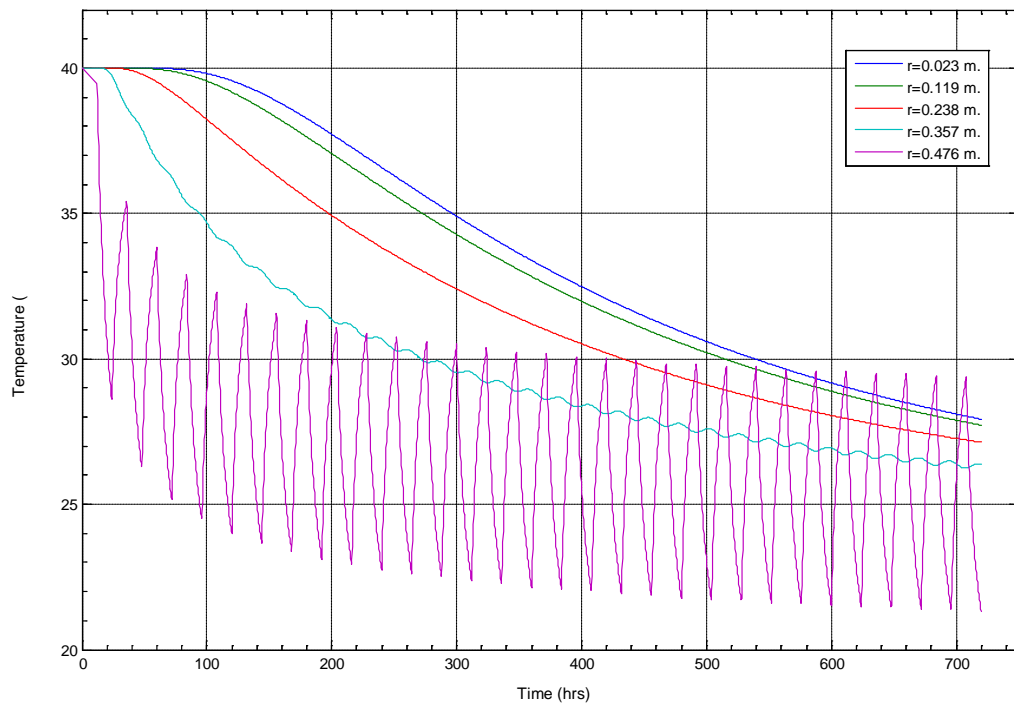


Figure 4.17 The temperature profile at different node which calculated using hysteresis isotherm for high initial moisture content.

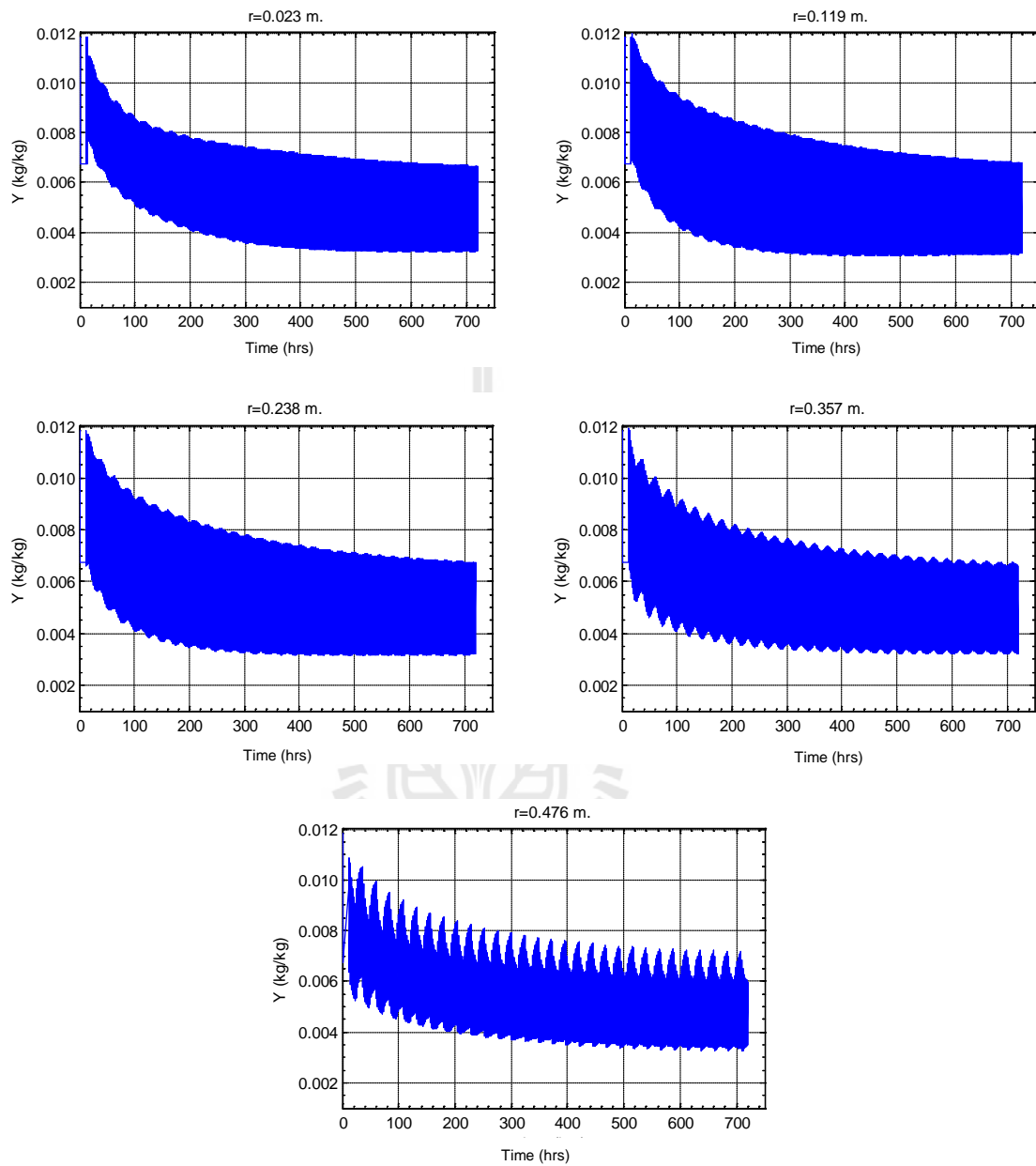


Figure 4.18 The absolute humidity profile of each node which calculated using hysteresis isotherm for high initial moisture content.

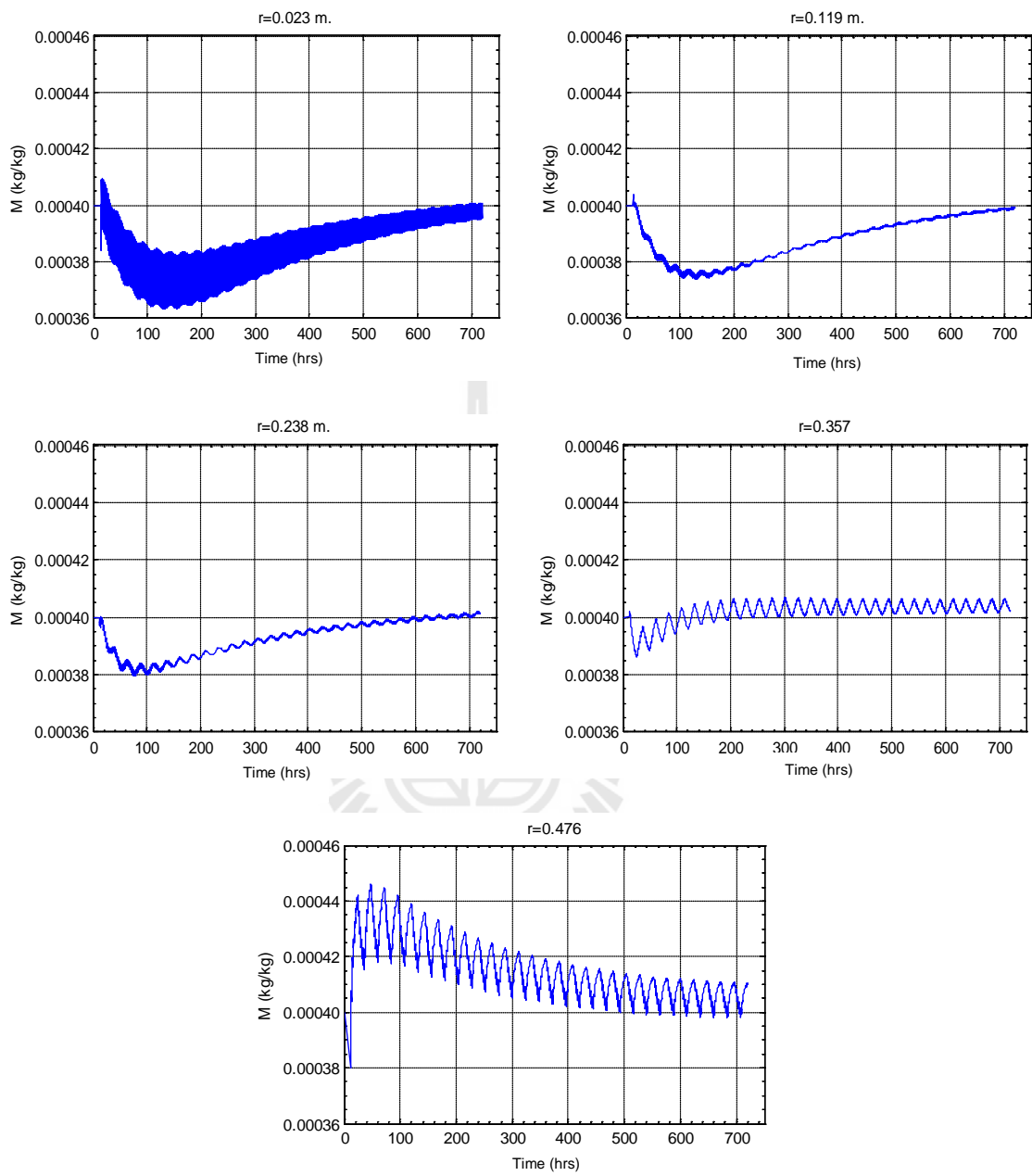


Figure 4.19 The moisture content profile of each node which calculated using hysteresis isotherm for high initial moisture content.

4.5 Sensitivity Analysis Result

Figure 4.20 shows the result of sensitivity analysis of the parameters of heat conductivity of sugar grain (k_s), porosity of bed (ε), and heat conductivity of air (k_a). This result consists of temperature and moisture content profiles in the first and second column, respectively. Three positions in the big bag were picked to illustrate the effect of parameter sensitivity; at $r=0.000$ meters, $r=0.238$ meters, and $r=0.476$ meters in order to represent core-, mid-, and interface-region inside the big bag. We found: (i) The heat conductivity of sugar grain has the most impact greater than other picked parameters; as seen the changing of parameter heat conductivity of sugar grain, both +10% and -10% lines shift most far than other parameter from the normal line. (ii) The changing of heat conductivity of air ($\pm 10\%$ of k_a) is not significant; they give the same line at all three position. (iii) Likewise, at the interface region, the changing $\pm 10\%$ of all parameters also gave the same line. (iv) As expected, the increasing heat conductivity of sugar and decreasing porosity of bed cause the increase heat transfer; because both lines stay under normal line. However, the changing $\pm 10\%$ of these parameter impacts the moisture content profile insignificantly.

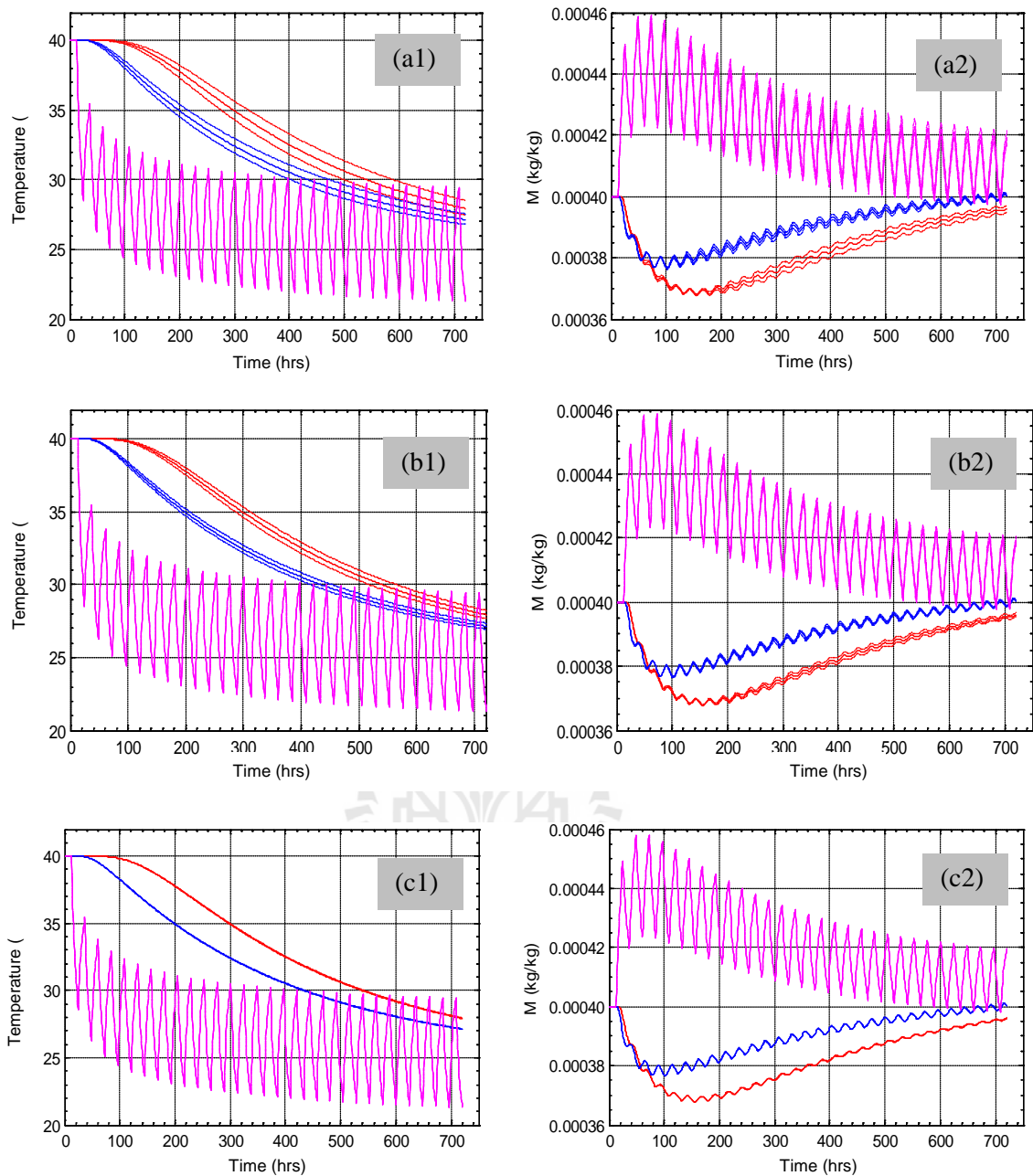


Figure 4.20 The profiles of temperature and moisture content from sensitivity analysis consisting of effects heat conductivity of sugar (a), porosity of bed (b), and heat conductivity of air (c); the red, blue, and pink lines represent position at $r=0.0$, 0.238 , and 0.476 meters, respectively, while the solid lines, dash lines, and short-long dash lines represent the results of deviation each parameter of 0%, -10%, and +10%, respectively.

CHAPTER V

CONCLUSIONS

5.1 Sorption Isotherm Fitting

This thesis work has shown that the GAB-T model can describe the experimental data of sorption isotherm very well, and is also better than the previous models in a past, especially the range 0.05 to 0.7 of a_w . However, the result of this result still has a weakness in ranging $a_w < 0.05$ and $a_w > 0.7$ because the experimental data of this range is not available.

5.2 Model Validation

This model was validated by comparing temperature distribution with the experimental data reported in Leaper et al. (2001) and Wang and coworkers' numerical results (Wang et al. 2004). It has been shown that the result of this model agree with both results.

5.3 Model Prediction

5.3.1 Effect of Initial Condition

This thesis work has found that the case of high initial moisture content has the significance that may induce the caking phenomenon. Since there is the maxi-

mum peak of the moisture content profile that may lead to occur the beginning of liquid bridging and it was also found the amount of moisture in gas phase tended to decrease after 30 days. Consequently, the moisture likely stays in the sugar grain rather than gas phase. While the case of low initial moisture content is no significance changes in moisture content of sugar because the changing moisture in the big bag is a very small when compared with the previous case.

5.3.2 Effect of Sorption Isotherm

This thesis work has found that the result by using the adsorption isotherm could cover the range of both desorption isotherm and hysteresis. In other word, the adsorption isotherm is enough to use when the desorption isotherm and hysteresis have not been included in the model of moisture migration. Although there is the appearance of hysteresis loop in the sugar sorption isotherm and occurring the period of adsorption and desorption of moisture during shipping, these effects do not significantly affect the numerical results of the model.

5.3.3 Sensitivity Analysis

This thesis work has found that the heat conductivity of sugar grain has the more impact to the numerical solution while the changing of heat conductivity of air is not significant. Moreover, changing of all parameters around interface region is not significant to numerical result as well.

CHAPTER IV

RECOMMENDATIONS

6.1 Mathematical Model

The mathematical modeling of this work has not yet answered the caking sugar during transportation; it just tells us the redistribution of moisture in the container which is the beginning of occurring caking. Hence the mathematical modeling involved the occurring caking should be studied further and will then be connected to mathematical model of this work.

6.2 Environmental Condition during Transport

Because this work used the changing of outside temperature in square-wave form which there is the jumping of temperature during transition between daytime and nighttime. In fact, the changing of temperature should be continuous. Thus, the study of changing temperature the way of shipping to apply in the model will reflect reality than using the square-wave form.

6.3 Sorption Isotherm

The experimental data of sorption isotherm that will be used to predict should be investigated because of the shape sorption isotherm of sugar depending on several factors.

REFERENCES

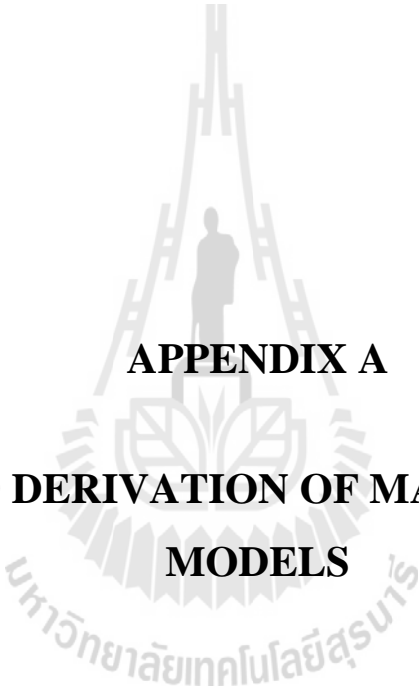
- Billings, S.W. and Paterson, A.H.J. (2008). Prediction of the onset of caking in sucrose from temperature induced moisture movement. **Journal of Food Engineering** 88: 466-473.
- Björck, Å. (1996). Numerical Methods for Least Squares Problems. SIAM.
- Bronlund, J.E. and Tony, P. (2008). Mathematical modelling of temperature induced moisture migration in bulk powders. **Chemical Engineering Science** 63: 2330-2340.
- Business Recorder. "Thailand aims to be sugar bowl of Asia." 17 June 2012. <http://www.brecorder.com/agriculture-a-allied/183/1201668/>. 2 October 2012.
- Chen, R.G. and Wang, H.R. (2006). Measurement and numerical simulation of moisture transport within potash beds as a prelude to moisture migration caking. **Advanced Powder Technol** 17, 29-47
- Christakis, N., Wang, J., Patel, M.K., Bradley, M.S.A., Leaper, M.C., Cross, M. (2006). Aggregation and caking processes of granular materials: continuum model and numerical simulation with application to sugar. **Advanced Powder Technology** 17: 543-565.
- Churchill and Chu. (1975). **Ind. J. Heat Mass Transfer** 18: 1323.
- Cloutier, A. and Forton, Y. (1994). Wood drying modeling based on the water potential concept: Hysteresis effects. **Drying Technology** 12: 1793-1814.

- Coleman, T.F. and Y. Li. (1994). On the Convergence of Reflective Newton Methods for Large-Scale Nonlinear Minimization Subject to Bounds. **Mathematical Programming** 67: 189-224.
- Coleman, T. F. and Y, Li. (1996). An Interior, Trust Region Approach for Nonlinear Minimization Subject to Bounds. **SIAM Journal on Optimization** 6: 418-445.
- Dennis, J.E., and Jr. (1997). **Nonlinear Least-Squares. State of the Art in Numerical Analysis**, ed. D. Jacobs. Academic Press, pp. 269-312.
- Excell, T.L., Stone, V.C. (1989). Moisture problems in the shipment of refined sugar in containers. **Proceedings of the south african sugar technologists' association.**
- Frandsen, H. L. (2007). "Selected constitutive models for simulating the hygro-mechanical response of wood". PhD thesis, Aalborg University, Aalborg, Denmark.
www.vbn.aau.dk/fbspretrieve/13648994 (Accessed March 16, 2010)
- Hamdi, S., Schiesser, W. E. and Griffiths, G. W. (2007), Method of lines, *Scholarpedia*, 2(7), 2859.
- Iglesias, H. A., and Chirife, J. (1982). **Handbook of Food Isotherm, Water Sorption Parameters for Food and Food Components**. Academic Press, New York: 262-263
- Leaper, M.C., Bradley, M.S.A., Sinclair, K., Barnes, A., Dean, E. (2001). **Investigating temperature fluctuation, moisture migration and cake formation in Big-Bags using heat transfer modelling and intermediate scale caking rig**. QPM Case study report. University of Greenwich, London.

- Leeper, M.C., Bradley, M.S.A., Cleaver, J.A.S., Bridle, I., Reed, A.R., Abou-chakra, H. and TüzüN, U. (2002). Constructing an engineering model for moisture migration in bulk solids as a prelude to predicting moisture migration caking. **Advanced Powder Technology** 13: 411-424.
- Levenberg, K. (1944). A Method for the Solution of Certain Problems in Least-Squares. **Quarterly Applied Math** 2: 164-168.
- Lievonen, S.M. and Roos, Y.H. (2002). Water sorption of food models for studies of glass transition and reaction kinetics. **Journal of Food Science** 65: Nr.5.
- Marquardt, D. (1963). An Algorithm for Least-Squares Estimation of Nonlinear Parameters. **SIAM Journal Applied Mat** 11: 431-441.
- Moré, J.J. (1977). The Levenberg-Marquardt Algorithm: Implementation and Theory. Numerical Analysis, ed. G. A. Watson, **Lecture Notes in Mathematics 630**, Springer Verlag, pp. 105-116.
- Mathlouhi, M and Rogé, B. (2003). Water vapour sorption isotherm and the caking of food powders. **Food Chemistry** 82: 61-71.
- Nie, X.D., Evitt, R.W., and Besant, R.W. (2008). Simulation of Moisture Uptake and Transport in a Bed of Urea Particles. **Ind. Eng. Chem. Res.** 47, 7888-7896
- Patakar, S. V. (1980). Numerical Heat Transfer and Fluid Flow. McGraw-Hill, New York.
- Peralta, P.N. (1995). Modelling wood moisture sorption hysteresis using the independent-domain theory. **Wood and Fiber Science** 27: 250-257.
- Rastikian, K., Capart, R., and Benchimol. (1999). Modelling of sugar drying in a countercurrent cascading rotary dryer from stationary profiles of temperature and moisture. **Journal of Food Engineering** 41: 93-201.

- Rodgers, T and Lewis, CL (1962-1963). The drying of white sugar and its effect on bulk handling. **Int. Sug. J.** 64: 359-362, 65: 12-16, 43-45, 80-83.
- Salin. (2011). Inclusion of the sorption hysteresis phenomenon in future drying models. some basic conditions. **Maderas: Ciencia y Tecnología** 13: 173-182.
- Schiesser, W. E. (1991). *The Numerical Method of Lines*. Academic Press.
- Schiesser, W. E. and Griffiths, G. W. (2009). *A Compendium of Partial Differential Equation Models: Method of Lines Analysis with Matlab*. Cambridge University Press.
- Scholz, E (1984). **Karl Fisher Titration: Determination of water**. Springer, Berlin.
- Shah, D.J., Ramsey, J.W., Wang, M. (1984). An experimental determination of the heat and mass transfer coefficients in moist unsaturated soils. **International Journal of Heat and Mass Transfer** 27: 1075-1085.
- Shampine, L.F., Reichelt, M.W. (1997). The MATLAB ODE Suite. **SIAM Journal on Scientific Computing** 18: 1-22.
- Shampine, L.F., Reichelt, M.W., Kierzenka, J.A. (1999). Solving Index-1 DAEs in MATLAB and Simulink. **SIAM Review** 41: 538-552.
- Time, B. (1998) "Hygroscopic moisture transport in wood". PhD thesis, Norwegian University of Science and Technology, Trondheim, Norway.
www.ivt.ntnu.no/docs/bat/bm/phd/AvhandlingBeritTime.pdf (Accessed March 16, 201
- Time, B. (2002). Studies on hygroscopic moisture transport in Norway spruce (*Picea abies*). Part 2: Modelling of transient moisture transport and hysteresis in wood. **Holz als Roh- und Werkstoff** 60: 405-410.

- Tsu-Ning Tsao, G. (1961). Thermal Conductivity of Two-Phase Materials. *Ind. Eng. Chem. 53* (5), 395–397
- van der Berg, C., Bruin, S. (1981). Water activity and its estimation in food system: theoretical aspects. **Water activity: influences on food quality (p 1-61)**. Academic Press, New York.
- Wang, J., Christakis, N., Patel, M.K., Cross, M., Leaper, M.C. (2004). A computational model of coupled heat and moisture transfer with phase change in granular sugar during varying environmental conditions. **Numerical Heat Transfer, Part A 45**: 751-776.
- Weisser, H. (1985). Influence of temperature on sorption equilibria. **Properties of water in foods (p. 95-118)**. Dordrecht: Martinus Nijhoff Publishers
- Whitaker, S. (1980). Heat and mass transfer in granular porous media. **Adv. Drying 1**, 23-61



APPENDIX A

**DETAILED DERIVATION OF MATHEMATICAL
MODELS**

DETAILED DERIVATION OF MATHEMATICAL MODELS

1. Mass (moisture) Transfer Model

Mass balance around shell;

$$(\text{Accumulation}) = (\text{In}) - (\text{Out}) + (\text{Generation}) - (\text{Consumption})$$

Description: in the system, there is the gas and solid phases in the shell and only moisture that transfers into and out of shell in void by diffusion as shown the diagram in Figure 3.2.

$$\frac{\partial}{\partial t}(2\pi r \Delta r L W) = 2\pi r L \varepsilon W_r \Big|_r - 2\pi r L \varepsilon W_r \Big|_{r+\Delta r} + 0 - 0 \quad (\text{A.1.1})$$

Divided throughout by $2\pi \Delta r L$;

$$\frac{2\pi r \Delta r L \frac{\partial}{\partial t} W}{2\pi \Delta r L} = \frac{2\pi r L \varepsilon W_r \Big|_r - 2\pi r L \varepsilon W_r \Big|_{r+\Delta r}}{2\pi \Delta r L} \quad (\text{A.1.2})$$

We obtained;

$$r \frac{\partial}{\partial t} W = \frac{r \varepsilon W_r \Big|_r - r \varepsilon W_r \Big|_{r+\Delta r}}{\Delta r} \quad (\text{A.1.3})$$

Take limit $\Delta r \rightarrow 0$;

$$r \frac{\partial}{\partial t} W = - \lim_{\Delta r \rightarrow 0} \left(\frac{r \varepsilon W_r \Big|_{r+\Delta r} - r \varepsilon W_r \Big|_r}{\Delta r} \right) \quad (\text{A.1.4})$$

From definition of derivative, we obtained;

$$r \frac{\partial}{\partial t} W = - \frac{\partial}{\partial r} (r \varepsilon W_r) \quad (\text{A.1.5})$$

No bulk motion but only moisture diffusion, so $W_r = J_r$ and $J_r = -D_a \frac{\partial(\rho_{da} Y)}{\partial r}$,

substitute into Equation (A.5);

$$r \frac{\partial}{\partial t} W = - \frac{\partial}{\partial r} \left(-r \varepsilon D_a \frac{\partial(\rho_{da} Y)}{\partial r} \right) \quad (\text{A.1.6})$$

$D_{eff} = \varepsilon D_a$, then the final equation is;

$$\frac{\partial}{\partial t} W = \frac{1}{r} \frac{\partial}{\partial r} \left(r D_{eff} \frac{\partial(\rho_{da} Y)}{\partial r} \right) \quad (\text{A.1.7})$$

2. Heat Transfer Model

Heat balance around shell;

$$(\text{Accumulation}) = (\text{In}) - (\text{Out}) + (\text{Generation}) - (\text{Consumption})$$

Description: the system is gas and solid phases in shell that mentioned in part of mass transfer model. Heat transfer through shell by heat conduction of both gas and solid phases and heat diffusion in the gas phase.

$$\begin{aligned} & \frac{\partial}{\partial t} \left\{ 2\pi r \Delta r L (\varepsilon \rho_{da} h_g + (1-\varepsilon) \rho_s h_s) \right\} \\ & = (2\pi r L q_r|_r + 2\pi r L \varepsilon W_r h_v|_r) - (2\pi r L q_r|_{r+\Delta r} + 2\pi r L \varepsilon W_r h_v|_{r+\Delta r}) + 0 - 0 \end{aligned} \quad (\text{A.2.1})$$

Substitute $H = \varepsilon \rho_{da} h_g + (1-\varepsilon) \rho_s h_s$ and take $2\pi r \Delta r L$ out the derivative term;

$$2\pi r \Delta r L \frac{\partial}{\partial t} H = (2\pi r L q_r|_r + 2\pi r L \varepsilon W_r h_v|_r) - (2\pi r L q_r|_{r+\Delta r} + 2\pi r L \varepsilon W_r h_v|_{r+\Delta r}) \quad (\text{A.2.2})$$

Divided throughout by $2\pi\Delta rL$;

$$\frac{2\pi r\Delta rL \frac{\partial}{\partial t} H}{2\pi\Delta rL} = \frac{(2\pi rLq_r|_r + 2\pi rL\varepsilon W_r h_v|_r) - (2\pi rLq_r|_{r+\Delta r} + 2\pi rL\varepsilon W_r h_v|_{r+\Delta r})}{2\pi\Delta rL} \quad (\text{A.2.3})$$

Become;

$$r \frac{\partial}{\partial t} H = \frac{rq_r|_r - rq_r|_{r+\Delta r}}{\Delta r} + \frac{r\varepsilon W_r h_v|_r - r\varepsilon W_r h_v|_{r+\Delta r}}{\Delta r} \quad (\text{A.2.4})$$

Take limit $\Delta r \rightarrow 0$;

$$r \frac{\partial}{\partial t} H = -\lim_{\Delta r \rightarrow 0} \left(\frac{rq_r|_{r+\Delta r} - rq_r|_r}{\Delta r} \right) - \lim_{\Delta r \rightarrow 0} \left(\frac{r\varepsilon W_r h_v|_{r+\Delta r} - r\varepsilon W_r h_v|_r}{\Delta r} \right) \quad (\text{A.2.5})$$

From definition of derivative, we obtained;

$$r \frac{\partial}{\partial t} H = -\frac{\partial}{\partial r} (rq_r) - \frac{\partial}{\partial r} (r\varepsilon W_r h_v) \quad (\text{A.2.6})$$

Substitute $q_r = -((1-\varepsilon)k_{solid} + \varepsilon k_{air}) \frac{\partial T}{\partial r}$ and $W_r = -D_a \frac{\partial(\rho_{da} Y)}{\partial r}$

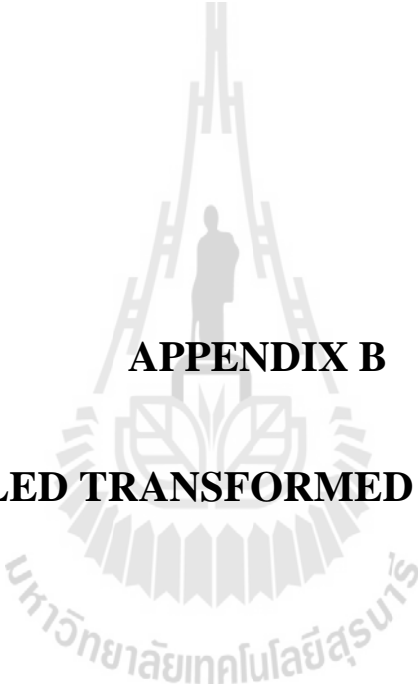
$$r \frac{\partial}{\partial t} H = -\frac{\partial}{\partial r} \left(-r((1-\varepsilon)k_{solid} + \varepsilon k_{air}) \frac{\partial T}{\partial r} \right) - \frac{\partial}{\partial r} \left(r\varepsilon \left(-D_a \frac{\partial(\rho_{da} Y)}{\partial r} \right) h_v \right) \quad (\text{A.2.7})$$

Substitute $k_{eff} = (1-\varepsilon)k_{solid} + \varepsilon k_{air}$ and $D_{eff} = \varepsilon D_a$, then;

$$r \frac{\partial}{\partial t} H = -\frac{\partial}{\partial r} \left(-rk_{eff} \frac{\partial T}{\partial r} \right) - \frac{\partial}{\partial r} \left(-rD_{eff} \frac{\partial(\rho_{da} Y)}{\partial r} h_v \right) \quad (\text{A.2.8})$$

Rearrange, the final equation is;

$$\frac{\partial H}{\partial t} = \frac{1}{r} \frac{\partial}{\partial r} \left(rk_{eff} \frac{\partial T}{\partial r} \right) + \frac{1}{r} \frac{\partial}{\partial r} \left(rD_{eff} \frac{\partial(\rho_{da} Y)}{\partial r} h_v \right) \quad (\text{A.2.9})$$



APPENDIX B
DETAILED TRANSFORMED EQUATIONS

DETAILED TRANSFORMED EQUATIONS

This Goal is to transform Equations (3.1) and (3.3) into the explicit dependent variables of T and Y with $M(t, y)y' = f(t, y)$ form by substituting the sorption isotherm equation. The detail is shown below;

1. Mass Transfer Model

Recall Equations (3.1) and (3.2);

$$\frac{\partial W}{\partial t} = \frac{1}{r} \frac{\partial}{\partial r} \left(r D_{eff} \frac{\partial}{\partial r} (\rho_{da} Y) \right)$$

$$W = \varepsilon Y \rho_{da} + (1 - \varepsilon) M \rho_s$$

Take derivative on Equation (3.2) respect with time;

$$\frac{\partial W}{\partial t} = \varepsilon \frac{\partial}{\partial t} (Y \rho_{da}) + (1 - \varepsilon) \rho_s \frac{\partial}{\partial t} M \tag{B.1}$$

$$\frac{\partial W}{\partial t} = \varepsilon \left(Y \frac{\partial}{\partial t} \rho_{da} + \rho_{da} \frac{\partial}{\partial t} Y \right) + (1 - \varepsilon) \rho_s \frac{\partial M}{\partial t} \tag{B.2}$$

From Equation (3.17), $\rho_{da} = \rho_{da}(T)$, so $\frac{\partial \rho_{da}}{\partial t} = \frac{\partial \rho_{da}}{\partial T} \frac{\partial T}{\partial t}$;

$$\frac{\partial W}{\partial t} = \varepsilon \left(Y \frac{\partial \rho_{da}}{\partial T} \frac{\partial T}{\partial t} + \rho_{da} \frac{\partial Y}{\partial t} \right) + (1 - \varepsilon) \rho_s \frac{\partial M}{\partial t} \tag{B.3}$$

From Equations (2.4), (3.21) to (3.23), tell us $M = M(T, Y)$

Take derivative respect with time;

$$\frac{\partial M}{\partial t} = \left(\frac{\partial M}{\partial T} \right)_Y \frac{\partial T}{\partial t} + \left(\frac{\partial M}{\partial Y} \right)_T \frac{\partial Y}{\partial t} \tag{B.4}$$

Substitute Equation (B.4) into Equation (B.3);

$$\frac{\partial W}{\partial t} = \varepsilon \left(Y \frac{\partial \rho_{da}}{\partial T} \frac{\partial T}{\partial t} + \rho_{da} \frac{\partial Y}{\partial t} \right) + (1 - \varepsilon) \rho_s \left(\left(\frac{\partial M}{\partial T} \right)_Y \frac{\partial T}{\partial t} + \left(\frac{\partial M}{\partial Y} \right)_T \frac{\partial Y}{\partial t} \right) \quad (\text{B.5})$$

Expand the derivative terms on RHS of Equation (3.1)

$$\begin{aligned} & \frac{1}{r} \frac{\partial}{\partial r} \left(r D_{eff} \frac{\partial}{\partial r} (\rho_{da} Y) \right) \\ &= \frac{1}{r} \frac{\partial}{\partial r} \left[r D_{eff} \left(\rho_{da} \frac{\partial Y}{\partial r} + Y \frac{\partial \rho_{da}}{\partial r} \right) \right] \\ &= \frac{1}{r} \left[r D_{eff} \frac{\partial}{\partial r} \left(\rho_{da} \frac{\partial Y}{\partial r} + Y \frac{\partial \rho_{da}}{\partial r} \right) + \left(\rho_{da} \frac{\partial Y}{\partial r} + Y \frac{\partial \rho_{da}}{\partial r} \right) \frac{\partial}{\partial r} (r D_{eff}) \right] \\ &= \frac{1}{r} \left[r D_{eff} \left(\rho_{da} \frac{\partial}{\partial r} \frac{\partial Y}{\partial r} + \frac{\partial Y}{\partial r} \frac{\partial \rho_{da}}{\partial r} + Y \frac{\partial}{\partial r} \frac{\partial \rho_{da}}{\partial r} + \frac{\partial \rho_{da}}{\partial r} \frac{\partial Y}{\partial r} \right) \right. \\ & \quad \left. + \left(\rho_{da} \frac{\partial Y}{\partial r} + Y \frac{\partial \rho_{da}}{\partial r} \right) \left(r \frac{\partial D_{eff}}{\partial r} + D_{eff} \frac{\partial}{\partial r} \right) \right] \\ &= \frac{1}{r} \left[r D_{eff} \left(\rho_{da} \frac{\partial^2 Y}{\partial r^2} + 2 \frac{\partial Y}{\partial r} \frac{\partial \rho_{da}}{\partial r} + Y \frac{\partial^2 \rho_{da}}{\partial r^2} \right) + \left(\rho_{da} \frac{\partial Y}{\partial r} + Y \frac{\partial \rho_{da}}{\partial r} \right) \left(r \frac{\partial D_{eff}}{\partial r} + D_{eff} \right) \right] \\ & \dots (\text{B.6}) \end{aligned}$$

Substitute Equation (B.5) and (B.6) back to Equation (3.1);

$$\begin{aligned} & \varepsilon \left(Y \frac{\partial \rho_{da}}{\partial T} \frac{\partial T}{\partial t} + \rho_{da} \frac{\partial Y}{\partial t} \right) + (1 - \varepsilon) \rho_s \left(\left(\frac{\partial M}{\partial T} \right)_Y \frac{\partial T}{\partial t} + \left(\frac{\partial M}{\partial Y} \right)_T \frac{\partial Y}{\partial t} \right) \\ &= \frac{1}{r} \left[r D_{eff} \left(\rho_{da} \frac{\partial^2 Y}{\partial r^2} + 2 \frac{\partial Y}{\partial r} \frac{\partial \rho_{da}}{\partial r} + Y \frac{\partial^2 \rho_{da}}{\partial r^2} \right) + \left(\rho_{da} \frac{\partial Y}{\partial r} + Y \frac{\partial \rho_{da}}{\partial r} \right) \left(r \frac{\partial D_{eff}}{\partial r} + D_{eff} \right) \right] \quad (\text{B.7}) \end{aligned}$$

The final equation;

$$\begin{aligned} & \left(\varepsilon Y \frac{\partial \rho_{da}}{\partial T} + (1 - \varepsilon) \rho_s \left(\frac{\partial M}{\partial T} \right)_Y \right) \frac{\partial T}{\partial t} + \left(\varepsilon \rho_{da} + (1 - \varepsilon) \rho_s \left(\frac{\partial M}{\partial Y} \right)_T \right) \frac{\partial Y}{\partial t} \\ &= \frac{1}{r} \left[r D_{eff} \left(\rho_{da} \frac{\partial^2 Y}{\partial r^2} + 2 \frac{\partial Y}{\partial r} \frac{\partial \rho_{da}}{\partial r} + Y \frac{\partial^2 \rho_{da}}{\partial r^2} \right) + \left(\rho_{da} \frac{\partial Y}{\partial r} + Y \frac{\partial \rho_{da}}{\partial r} \right) \left(r \frac{\partial D_{eff}}{\partial r} + D_{eff} \right) \right] \quad (\text{B.8}) \end{aligned}$$

2. Heat Transfer Model

Recall Equations (3.3) and (3.4);

$$\frac{\partial H}{\partial t} = \frac{1}{r} \frac{\partial}{\partial r} \left(r D_{\text{eff}} \frac{\partial}{\partial r} (\rho_{da} Y) h_v \right) + \frac{k_{\text{eff}}}{r} \frac{\partial}{\partial r} \left(r \frac{\partial T}{\partial r} \right)$$

$$H = h_g \varepsilon \rho_{da} + h_s (1 - \varepsilon) \rho_s$$

Take derivative on Equation (3.4) respect with time;

$$\frac{\partial}{\partial t} H = \varepsilon \frac{\partial}{\partial t} (h_g \rho_{da}) + (1 - \varepsilon) \rho_s \frac{\partial}{\partial t} h_s \quad (\text{B.9})$$

$$\frac{\partial H}{\partial t} = \varepsilon \left(h_g \frac{\partial \rho_{da}}{\partial t} + \rho_{da} \frac{\partial h_g}{\partial t} \right) + (1 - \varepsilon) \rho_s \frac{\partial h_s}{\partial t} \quad (\text{B.10})$$

We have already known; $\frac{\partial \rho_{da}}{\partial t} = \frac{\partial \rho_{da}}{\partial T} \frac{\partial T}{\partial t}$

From Equation (3.20), $h_g = h_g(T, Y)$, so $\frac{\partial h_g}{\partial t} = \left(\frac{\partial h_g}{\partial T} \right)_Y \frac{\partial T}{\partial t} + \left(\frac{\partial h_g}{\partial Y} \right)_T \frac{\partial Y}{\partial t}$

From Equation (3.18), $h_s = h_s(T, M)$, so $\frac{\partial h_s}{\partial t} = \left(\frac{\partial h_s}{\partial T} \right)_M \frac{\partial T}{\partial t} + \left(\frac{\partial h_s}{\partial M} \right)_T \frac{\partial M}{\partial t}$

Substitute them into Equation (B.10);

$$\begin{aligned} \frac{\partial H}{\partial t} = & \varepsilon \left[h_g \left(\frac{\partial \rho_{da}}{\partial T} \frac{\partial T}{\partial t} \right) + \rho_{da} \left(\left(\frac{\partial h_g}{\partial T} \right)_Y \frac{\partial T}{\partial t} + \left(\frac{\partial h_g}{\partial Y} \right)_T \frac{\partial Y}{\partial t} \right) \right] \\ & + (1 - \varepsilon) \rho_s \left(\left(\frac{\partial h_s}{\partial T} \right)_M \frac{\partial T}{\partial t} + \left(\frac{\partial h_s}{\partial M} \right)_T \frac{\partial M}{\partial t} \right) \end{aligned} \quad (\text{B.11})$$

Substitute Equation (B.4) into Equation (B.11)

$$\begin{aligned} \frac{\partial H}{\partial t} = & \varepsilon \left[h_g \left(\frac{\partial \rho_{da}}{\partial T} \frac{\partial T}{\partial t} \right) + \rho_{da} \left(\left(\frac{\partial h_g}{\partial T} \right)_Y \frac{\partial T}{\partial t} + \left(\frac{\partial h_g}{\partial Y} \right)_T \frac{\partial Y}{\partial t} \right) \right] \\ & + (1 - \varepsilon) \rho_s \left(\left(\frac{\partial h_s}{\partial T} \right)_M \frac{\partial T}{\partial t} + \left(\frac{\partial h_s}{\partial M} \right)_T \left(\left(\frac{\partial M}{\partial T} \right)_Y \frac{\partial T}{\partial t} + \left(\frac{\partial M}{\partial Y} \right)_T \frac{\partial Y}{\partial t} \right) \right) \end{aligned} \quad (\text{B.12})$$

Recall Equation (3.20);

$$h_g = C_{pa}T + Yh_v$$

Substitute Equation (3.19) into Equation (3.20);

$$h_g = C_{pa}T + Y(C_{pv}T + h_{fg}) \quad (\text{B.13})$$

Take derivative Equation (B.13) respect with T;

$$\left(\frac{\partial h_g}{\partial T}\right)_Y = C_{pa} + YC_{pv} \quad (\text{B.14})$$

Take derivative Equation (B.13) respect with Y;

$$\left(\frac{\partial h_g}{\partial Y}\right)_T = C_{pv}T + h_{fg} \quad (\text{B.15})$$

Recall Equation (3.18);

$$h_s = C_{ps}T + MC_{pw}T$$

Take derivative Equation (3.18) respect with T;

$$\left(\frac{\partial h_s}{\partial T}\right)_M = C_{ps} + MC_{pw} \quad (\text{B.16})$$

Take derivative Equation (3.18) respect with M;

$$\left(\frac{\partial h_s}{\partial M}\right)_T = C_{pw}T \quad (\text{B.17})$$

Then, substitute Equations (B.14) to (B.17) into Equation (B.12);

$$\begin{aligned} \frac{\partial H}{\partial t} = \varepsilon \left[h_g \left(\frac{\partial \rho_{da}}{\partial T} \frac{\partial T}{\partial t} \right) + \rho_{da} \left((C_{pa}T + YC_{pv}) \frac{\partial T}{\partial t} + (C_{pv}T + h_{fg}) \frac{\partial Y}{\partial t} \right) \right] \\ + (1 - \varepsilon) \rho_s \left((C_{ps} + MC_{pw}) \frac{\partial T}{\partial t} + (C_{pw}T) \left(\left(\frac{\partial M}{\partial T} \right)_Y \frac{\partial T}{\partial t} + \left(\frac{\partial M}{\partial Y} \right)_T \frac{\partial Y}{\partial t} \right) \right) \end{aligned}$$

...(B.18)

Rearrange Equation (B.18);

$$\begin{aligned} \frac{\partial H}{\partial t} = & \left(\varepsilon h_g \frac{\partial \rho_{da}}{\partial T} + \varepsilon \rho_{da} (C_{pa} T + Y C_{pv}) + (1-\varepsilon) \rho_s (C_{ps} + M C_{pw}) + (1-\varepsilon) \rho_s (C_{pw} T) \left(\frac{\partial M}{\partial T} \right)_Y \right) \frac{\partial T}{\partial t} \\ & + \left(\varepsilon \rho_{da} (C_{pv} T + h_{fg}) + (1-\varepsilon) \rho_s (C_{pw} T) \left(\frac{\partial M}{\partial Y} \right)_T \right) \frac{\partial Y}{\partial t} \end{aligned} \quad \dots(\text{B.19})$$

Expand the derivative terms on RHS of Equation (3.3)

$$\begin{aligned} & \frac{1}{r} \frac{\partial}{\partial r} \left(r D_{eff} \frac{\partial}{\partial r} (\rho_{da} Y) h_v \right) + \frac{k_{eff}}{r} \frac{\partial}{\partial r} \left(r \frac{\partial T}{\partial r} \right) \\ & = \frac{1}{r} \frac{\partial}{\partial r} \left(r D_{eff} \left(\rho_{da} \frac{\partial}{\partial r} Y + Y \frac{\partial}{\partial r} \rho_{da} \right) h_v \right) + \frac{k_{eff}}{r} \left(r \frac{\partial}{\partial r} \frac{\partial T}{\partial r} + \frac{\partial T}{\partial r} \frac{\partial}{\partial r} r \right) \\ & = \frac{1}{r} \left[r D_{eff} \frac{\partial}{\partial r} \left(\left(\rho_{da} \frac{\partial Y}{\partial r} + Y \frac{\partial \rho_{da}}{\partial r} \right) h_v \right) + \left(\left(\rho_{da} \frac{\partial Y}{\partial r} + Y \frac{\partial \rho_{da}}{\partial r} \right) h_v \right) \frac{\partial}{\partial r} (r D_{eff}) \right] \\ & + \frac{k_{eff}}{r} \left(r \frac{\partial^2 T}{\partial r^2} + \frac{\partial T}{\partial r} \right) \\ & = \frac{1}{r} \left[r D_{eff} \left(\left(\rho_{da} \frac{\partial Y}{\partial r} + Y \frac{\partial \rho_{da}}{\partial r} \right) \frac{\partial}{\partial r} h_v + h_v \frac{\partial}{\partial r} \left(\rho_{da} \frac{\partial Y}{\partial r} + Y \frac{\partial \rho_{da}}{\partial r} \right) \right) \right. \\ & \quad \left. + \left(\left(\rho_{da} \frac{\partial Y}{\partial r} + Y \frac{\partial \rho_{da}}{\partial r} \right) h_v \right) \left(r \frac{\partial}{\partial r} D_{eff} + D_{eff} \frac{\partial}{\partial r} r \right) \right] + \frac{k_{eff}}{r} \left(r \frac{\partial^2 T}{\partial r^2} + \frac{\partial T}{\partial r} \right) \\ & = \frac{1}{r} \left[r D_{eff} \left(\left(\rho_{da} \frac{\partial Y}{\partial r} + Y \frac{\partial \rho_{da}}{\partial r} \right) \frac{\partial h_v}{\partial r} + h_v \left(\rho_{da} \frac{\partial}{\partial r} \frac{\partial Y}{\partial r} + \frac{\partial Y}{\partial r} \frac{\partial}{\partial r} \rho_{da} + Y \frac{\partial}{\partial r} \frac{\partial \rho_{da}}{\partial r} + \frac{\partial \rho_{da}}{\partial r} \frac{\partial}{\partial r} Y \right) \right) \right. \\ & \quad \left. + \left(\left(\rho_{da} \frac{\partial Y}{\partial r} + Y \frac{\partial \rho_{da}}{\partial r} \right) h_v \right) \left(r \frac{\partial D_{eff}}{\partial r} + D_{eff} \right) \right] \\ & + \frac{k_{eff}}{r} \left(r \frac{\partial^2 T}{\partial r^2} + \frac{\partial T}{\partial r} \right) \end{aligned} \quad \dots (\text{B.20})$$

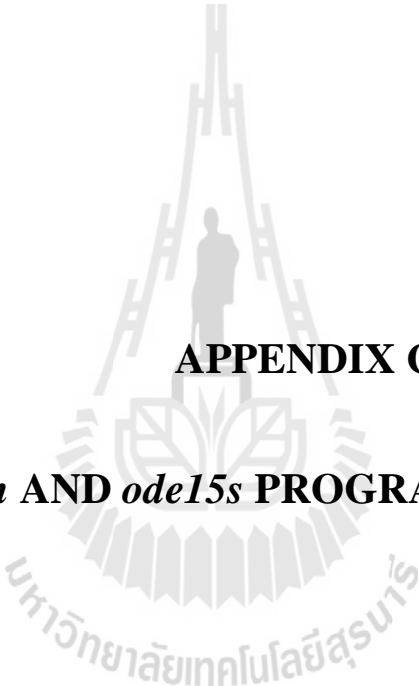
Therefore,

$$\begin{aligned}
& \frac{1}{r} \frac{\partial}{\partial r} \left(r D_{eff} \frac{\partial}{\partial r} (\rho_{da} Y) h_v \right) + \frac{k_{eff}}{r} \frac{\partial}{\partial r} \left(r \frac{\partial T}{\partial r} \right) \\
&= \frac{1}{r} \left[r D_{eff} \left(\left(\rho_{da} \frac{\partial Y}{\partial r} + Y \frac{\partial \rho_{da}}{\partial r} \right) \frac{\partial h_v}{\partial r} + h_v \left(\rho_{da} \frac{\partial^2 Y}{\partial r^2} + 2 \frac{\partial Y}{\partial r} \frac{\partial \rho_{da}}{\partial r} + Y \frac{\partial^2 \rho_{da}}{\partial r^2} \right) \right) \right. \\
&\quad \left. + \left(\left(\rho_{da} \frac{\partial Y}{\partial r} + Y \frac{\partial \rho_{da}}{\partial r} \right) h_v \right) \left(r \frac{\partial D_{eff}}{\partial r} + D_{eff} \right) \right] \\
&\quad + \frac{k_{eff}}{r} \left(r \frac{\partial^2 T}{\partial r^2} + \frac{\partial T}{\partial r} \right)
\end{aligned} \tag{B.21}$$

Substitute Equations (B.19) and (B.21) into Equation (3.3), we will obtain the final equation;

$$\begin{aligned}
& \left(\varepsilon h_g \frac{\partial \rho_{da}}{\partial T} + \varepsilon \rho_{da} (C_{pa} T + Y C_{pv}) + (1 - \varepsilon) \rho_s (C_{ps} + M C_{pw}) + (1 - \varepsilon) \rho_s (C_{pw} T) \left(\frac{\partial M}{\partial T} \right)_Y \right) \frac{\partial T}{\partial t} \\
&+ \left(\varepsilon \rho_{da} (C_{pv} T + h_{fg}) + (1 - \varepsilon) \rho_s (C_{pw} T) \left(\frac{\partial M}{\partial Y} \right)_T \right) \frac{\partial Y}{\partial t} \\
&= \frac{1}{r} \left[r D_{eff} \left(\left(\rho_{da} \frac{\partial Y}{\partial r} + Y \frac{\partial \rho_{da}}{\partial r} \right) \frac{\partial h_v}{\partial r} + h_v \left(\rho_{da} \frac{\partial^2 Y}{\partial r^2} + 2 \frac{\partial Y}{\partial r} \frac{\partial \rho_{da}}{\partial r} + Y \frac{\partial^2 \rho_{da}}{\partial r^2} \right) \right) \right. \\
&\quad \left. + \left(\left(\rho_{da} \frac{\partial Y}{\partial r} + Y \frac{\partial \rho_{da}}{\partial r} \right) h_v \right) \left(r \frac{\partial D_{eff}}{\partial r} + D_{eff} \right) \right] \\
&\quad + \frac{k_{eff}}{r} \left(r \frac{\partial^2 T}{\partial r^2} + \frac{\partial T}{\partial r} \right)
\end{aligned}$$

... (B.22)



APPENDIX C

***lsqnonlin* AND *ode15s* PROGRAMS in MATLAB®**

***lsqnonlin* AND *ode15s* PROGRAMS in MATLAB[®]**

1. *lsqnonlin* Function (Program)

lsqnonlin is one of built-in functions in the MATLAB program for solving the nonlinear least-squares problems. The *lsqnonlin* is based on many algorithms such as interior-reflective Newton method (Coleman, and Li,1996, 1994), Gauss-Newton method (Dennis, 1997), Levenberg-Marquardt Method (Levenberg, 1944,. Marquardt, 1963., Moré, 1977).

The form of problem to be solved is;

$$\min \sum \{FUN(x).^2\}$$

where x and the values of returned by FUN can be vectors or matrices.

1.1 Syntax

There are many manners which can be used depending on the purpose of user or level complex problem (see more information in MATLAB help or MATLAB[®] Central). This below is just some typical manner;

$$x = lsqnonlin(FUN,x0)$$

$$[x,resnorm] = lsqnonlin(FUN,x0,...)$$

1.2 Description

`x=lsqnonlin(FUN,x0)` starts at the matrix `x0` and finds a minimum `x` to the sum of squares of the functions in `FUN`. `FUN` accepts input `x` and returns a vector (or matrix) of function values `F` evaluated at `x`. Note: `FUN` should return `FUN(X)` and not the sum-of-squares `sum(FUN(X).^2)`. (`FUN(X)` is summed and squared implicitly in the algorithm).

`[x,resnorm]=lsqnonlin(FUN,x0,...)` returns the value of the squared 2-norm of the residual at `x`: `sum(FUN(X).^2)`.

1.3 Example

Find `x` that minimizes (from MATLAB help);

$$\sum_{k=1}^{10} \left(2 + 2k - e^{kx_1} - e^{kx_2} \right)^2$$

First, write an M-file to compute the `k`-component vector `F`.

```
function F = myfun(x)
k = 1:10;
F = 2 + 2*k-exp(k*x(1))-exp(k*x(2));
```

Next, invoke an optimization routine.

```
x0 = [0.3 0.4] % Starting guess
[x,resnorm] = lsqnonlin(@myfun,x0) % Invoke optimizer
```

This example gives the solution

```
x = % results of x1 and x2
    0.2578  0.2578
resnorm = % Residual or sum of squares
    124.3622
```

2. *ode15s* Function (Program)

ode15s is one of built-in functions for solving the Ordinary Differential Equations, especially the stiff differential equations or Differential-Algebraic Equations (DAEs). This is based on Backward Differentiation Formulas (BDFs) which is also known as Gear's method.

2.1 Syntax

$$[t, Y] = \text{ode15s}(\text{odefun}, \text{tspan}, \text{y0}, \text{options})$$

where *odefun* is a function that evaluates the right side of the differential equations.

tspan is a vector specifying the interval of integration, [t0,tf].

y0 is a vector of initial conditions.

options is structure of optional parameters that change the default integration properties via *odeset.m* file.

2.2 Examples

2.2.1 Example of stiff differential equation.

The problem (come from MATLAB help) is;

$$y_1' = y_2 \qquad y_1(0) = 2$$

$$y_2' = 1000(1 - y_1^2)y_2 - y_1 \qquad y_2(0) = 0$$

Then, creates a function *vdp1000* containing the equations above;

```
function dy = vdp1000(t,y)
dy = zeros(2,1); % a column vector
dy(1) = y(2);
dy(2) = 1000*(1 - y(1)^2)*y(2) - y(1);
```

For this problem, we will use the default relative and absolute tolerances ($1e-3$ and $1e-6$, respectively) and solve on a time interval of $[0 \ 3000]$ with initial condition vector $[2 \ 0]$ at time 0.

```
[t,y] = ode15s(@vdp1000,[0 3000],[2 0]);
```

Plotting the first column of the returned matrix y versus t shows the solution;

```
plot(t,y(:,1),'-o')
```

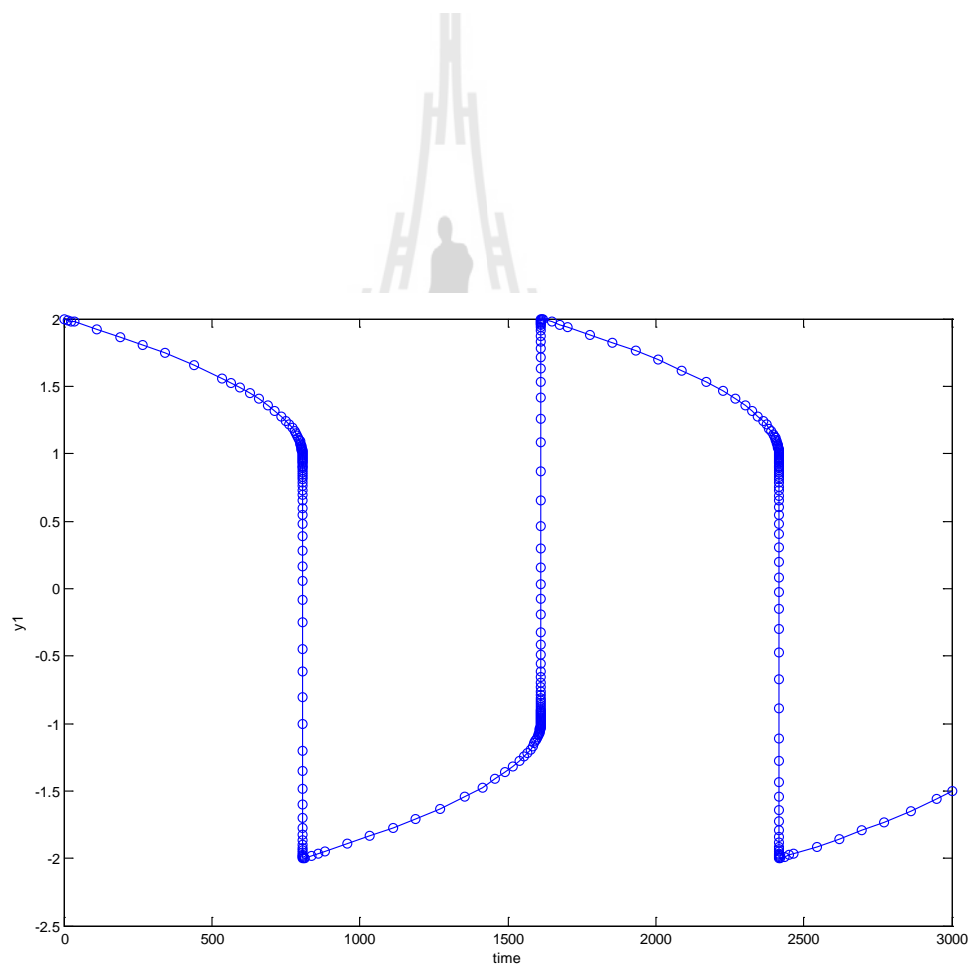


Figure C.1 The relationship between y_1 and time (Example of stiff differential Equation)

2.2.2 Example of DAEs

The problem (come from MATLAB central) is;

$$\begin{aligned} y_1' &= -0.04y_1 + 10000y_2y_3 & y_1(0) &= 1 \\ y_2' &= 0.04y_1 - 10000y_2y_3 - 3 \times 10^7 y_2^2 & y_2(0) &= 0 \\ 0 &= y_1 + y_2 + y_3 - 1 \end{aligned}$$

This differential-algebraic equation (DAE) system expressed as a problem with a singular mass matrix, $M \cdot y' = f(t, y)$.

First, creates a function f containing the equations above (only RHS);

```
function out = f(t,y)
out = [ -0.04*y(1) + 1e4*y(2)*y(3)
        0.04*y(1) - 1e4*y(2)*y(3) - 3e7*y(2)^2
        y(1) + y(2) + y(3) - 1 ];
```

Then, types the following on Command Window;

```
% A constant, singular mass matrix
```

```
M = [1 0 0
      0 1 0
      0 0 0];
```

```
y0 = [1; 0; 0];
```

```
tspan = [0 4*logspace(-6,6)];
```

```
%The 'MassSingular' property is left at its default 'maybe' to test the automatic
%detection of a DAE.
```

```
options = odeset('Mass',M,'RelTol',1e-7,'AbsTol',1e-7,'InitialStep',1e-7);
```

```
[t,y] = ode15s(@f,tspan,y0,options);
```

```
y(:,2) = 1e4*y(:,2);
```

```
figure;
```

```
semilogx(t,y);  
ylim([0,1])  
ylabel('1e4 * y(:,2)');
```

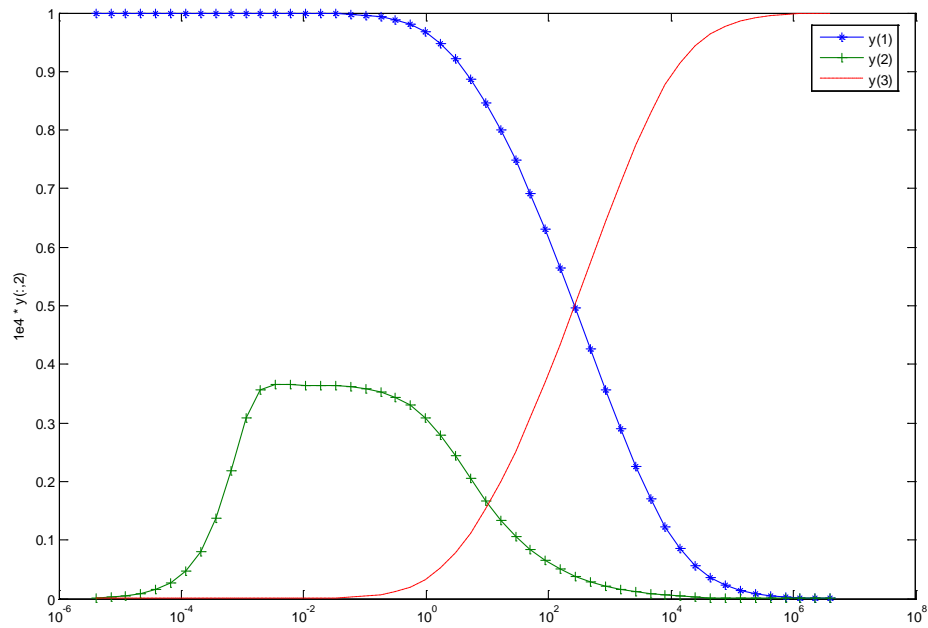
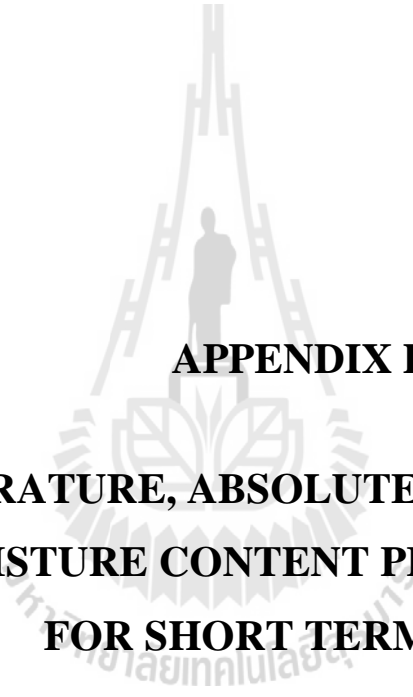


Figure C.2 The result of Example of DAEs

Note that the more details and information of the using two functions above is available in the MATLAB help and MATLAB central.



APPENDIX D

**TEMPERATURE, ABSOLUTE HUMIDITY, AND
MOISTURE CONTENT PROFILES
FOR SHORT TERM VIEW**

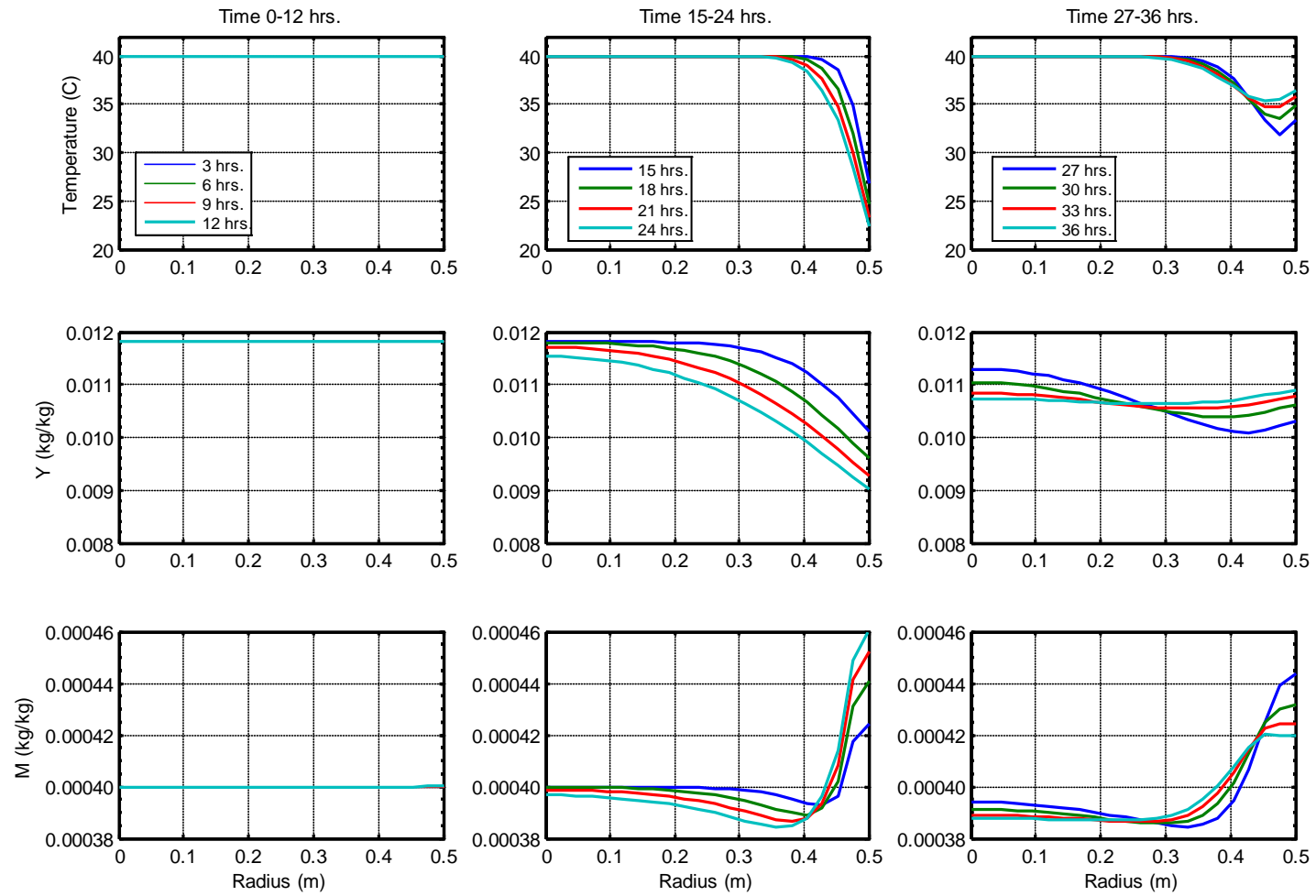


Figure D.1 Dynamics of numerical result of first 36 hrs for *high* initial moisture content with *adsorption isotherm*.

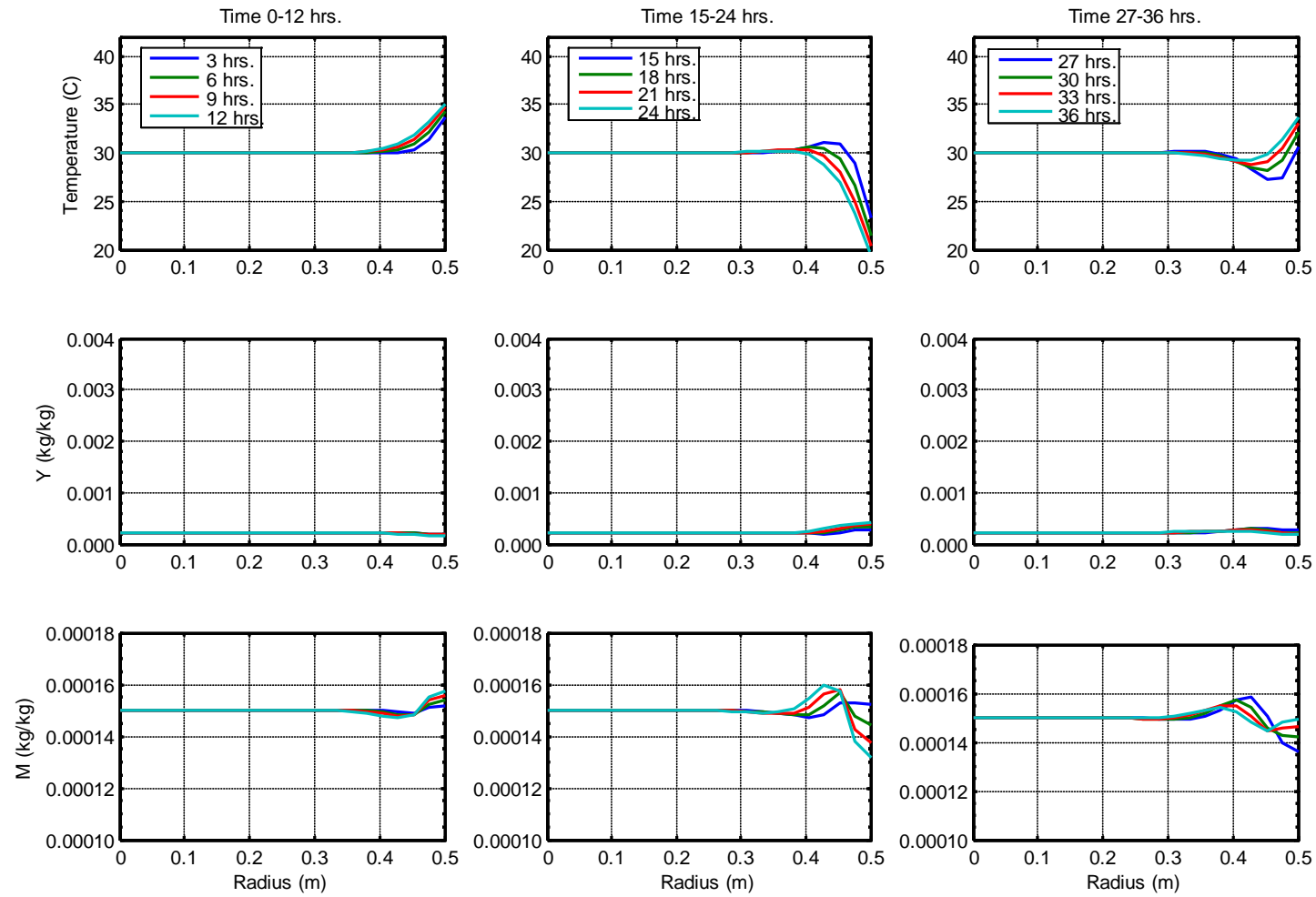


Figure D.2 Dynamics of numerical result of first 36 hrs for *low* initial moisture content with *adsorption isotherm*.

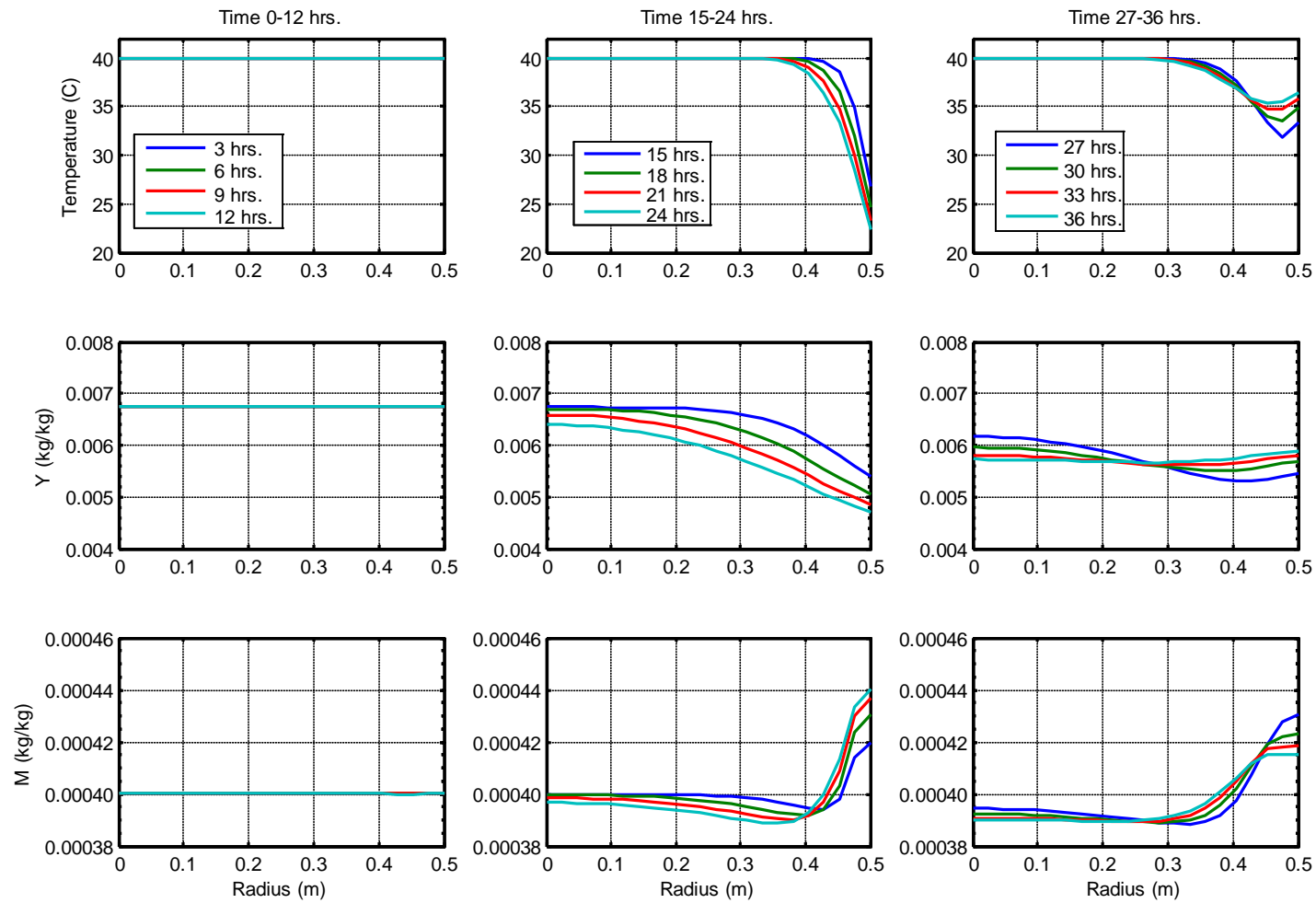


Figure D.3 Dynamics of numerical result of first 36 hrs for *high* initial moisture content with *desorption isotherm*.

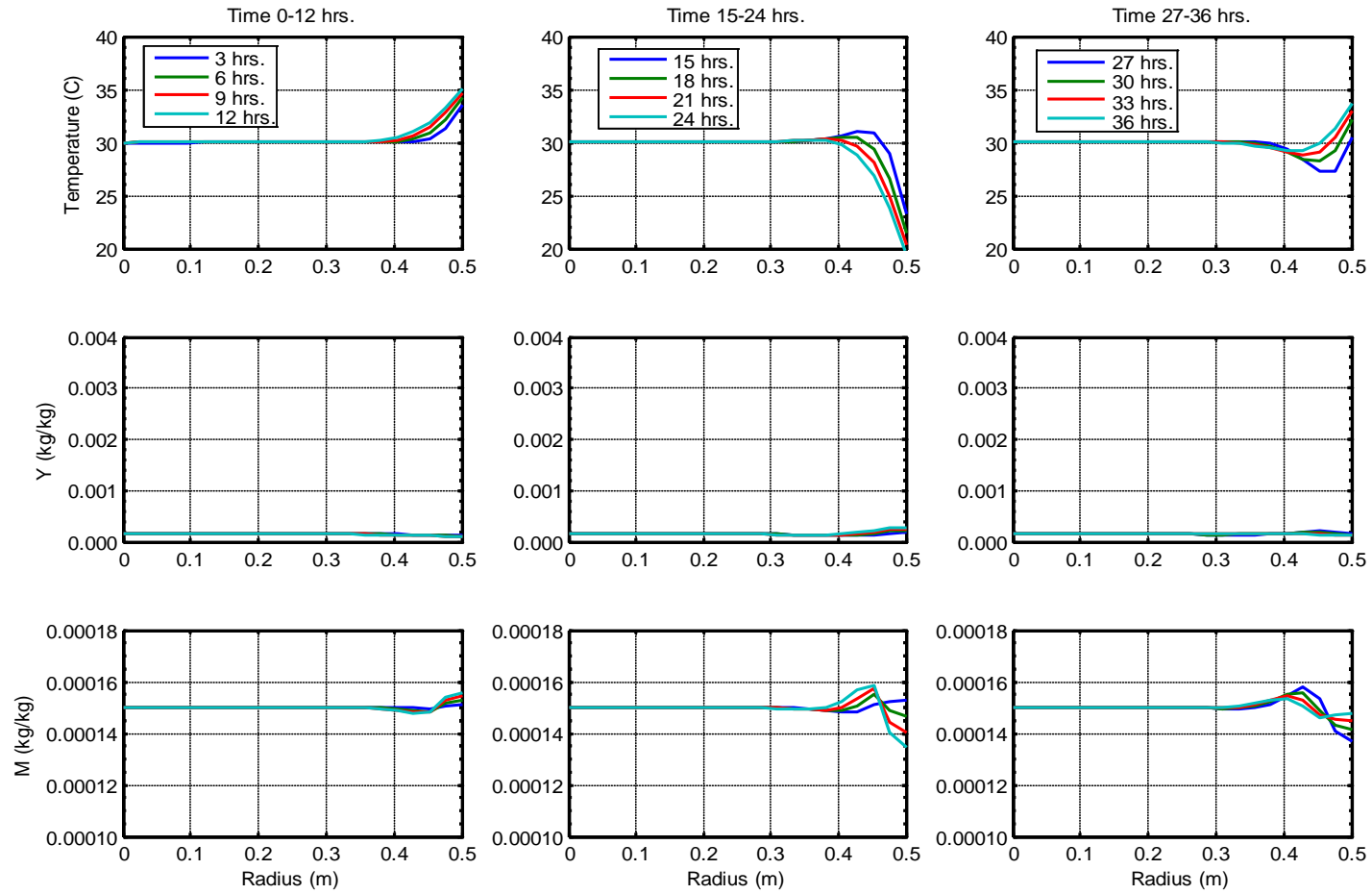
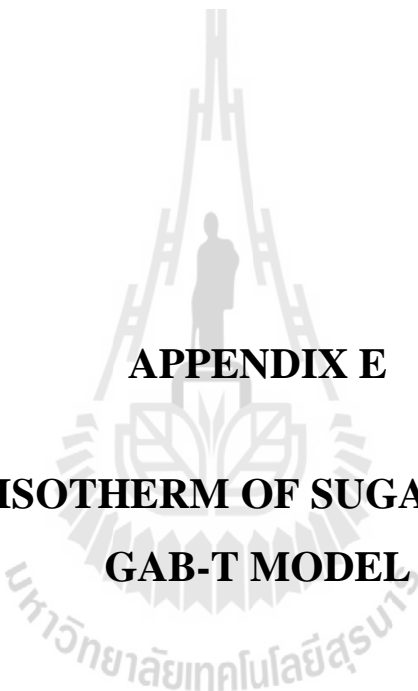


Figure D.4 Dynamics of numerical result of first 36 hrs for *low* initial moisture content with *desorption isotherm*.



APPENDIX E

**SORPTION ISOTHERM OF SUGAR GRAIN FROM
GAB-T MODEL**

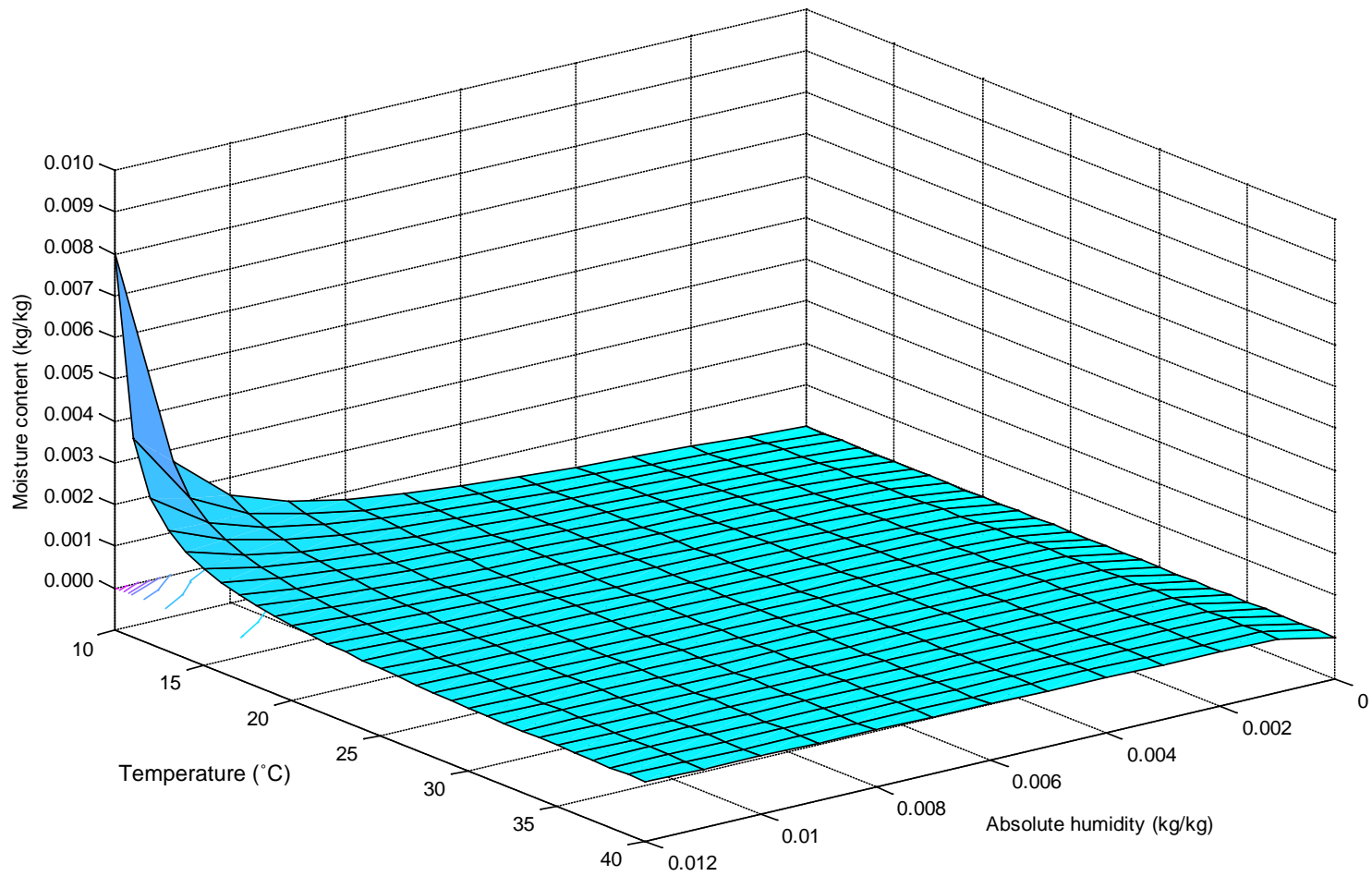


Figure E.1 GAB-T Model of adsorption isotherm of sugar grain in 3Dimensional view

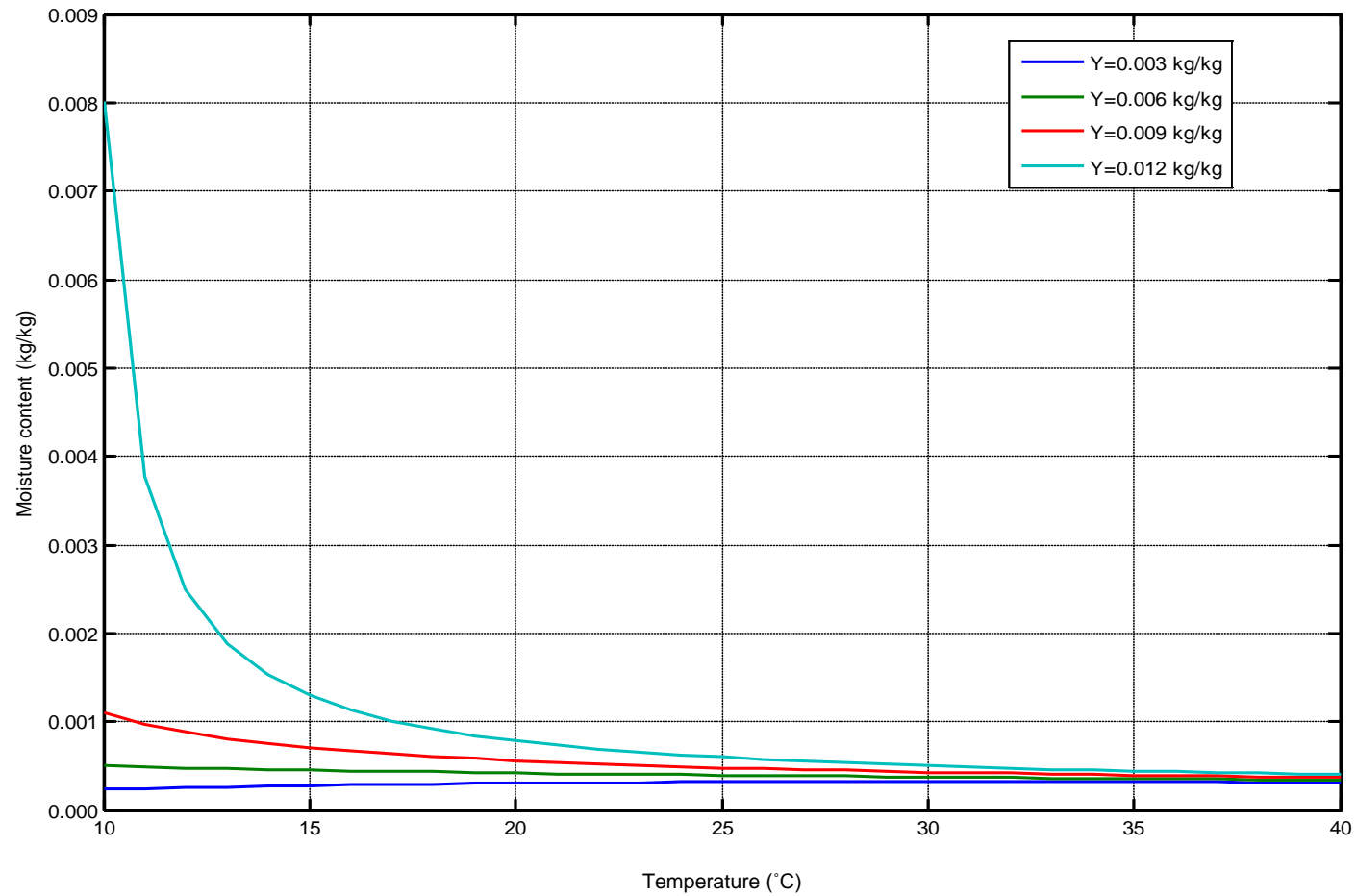


Figure E.2 The relationship between moisture content and temperature at constant absolute humidity (or left view from Figure E.1).

BIOGRAPHY

Mr. Chalawut Suwannatri was born on August 27th, 1985 in Khamcha-E Sub-District, Khamcha-E District, Mukdaharn Province of Thailand. After completing his high school at his home town, he moved to Nakhon Ratchasima Province to study Chemical Engineering in Bachelor's degree. At last semester of his undergraduate, he joined Mitr Phol Company, which is the Thailand's and Asia's biggest sugar producer, at Phu-Khieo plant as internship program (or Cooperative Education program). He was assigned to study the undetermined loss of sugar and to investigate the efficiency of C-Reheater which is one kind of heat exchangers in the sugar plant, during his internship program. Additionally, the topic of his senior project is mathematical modeling of mass and heat transfer of sugar in moving-bed dryer. After his graduation, he had been the research assistant under Dr. Terasut Sookkunerd in studying the topic of development UV-Resistant Insect Glue for UV Lamp Insect Traps. Then, he has studied the Master's degree of Chemical Engineering since 2009.